

รายงานวิจัยฉบับสมบูรณ์

โครงการ

"การเตรียมและตรวจสอบตัวรอ<mark>งรับค</mark>ะตะลิสต์ที่สังเคราะห์ จากสารประกอบอลูมาเทรนและไซลาเทรนโดยวิธีโชล-เจล"

โดย หางสุจิตรา วงศ์เกษมจิตต์

พฤศจิกายน 2545

สัญญาเลขที่ BGJ4380014

รายงานวิจัยฉบับสมบูรณ์

โครงการ

"การเตรียมและตรวจสอบตัวรองรับคะตะลิสต์ที่สังเคราะห์จากสารประกอบอลูมา เทรนและไซลาเทรนโดยวิธีโชล-เจล"

โดย นางสุจิตรา วงศ์เกษมจิตต์

วิทยาลัยปิโตรเลียมและปิโตรเคมี จุฬาลงกรณ์มหาวิทยาลัย

สนับสนุนโดยสำนักงานกองทุนสนับสนุนการวิจัย

(ความเห็นในรายงานนี้เป็นของผู้วิจัย สกว.ไม่จำเป็นต้องเห็นด้วยเสมอไป)

กิตติกรรมประกาศ

ผู้วิจัยขอขอบพระคุณสำนักงานกองทุนสนับสนุนการวิจัย ที่ใต้ให้การสนับสนุนโครงการวิจัยนี้ตลอดทั้ง โครงการ

บทคัดย่อ

รหัสโครงการ: BGJ4380014

ชื่อโครงการ: "การเตรียมและตรวจสอบตัวรองรับคะตะลิสต์ที่สังเคราะห์จากสาร

ประกอบอลูมาเทรนและไชลาเทรนโดยวิธีโชล-เจล"

ชื่อนักวิจัย: นางสุจิตรา วงศ์เกษมจิตต์

วิทยาลัยปิโดรเลียมและปิโตรเคมี จุฬาลงกรณ์มหาวิทยาลัย

E-mail Address : dsujitra@chula.ac.th

ระยะเวลาโครงการ : 2 ปี

วัดถุประสงค์ของงานวิจัยนี้ คือ เพื่อศึกษาวิธีการเดรียมตัวรองรับอลูมินาและซิลิกาจากสาร ประกอบอลูมาเทรนและไซลาเทรน ตามลำดับ โดยวิธีโซล-เจล และตรวจสอบพื้นที่ผิว ปริมาตรรู พรุน และความว่องไวในการทำปฏิกิริยาของตัวรองรับคะตะลิสต์ที่เดรียมได้ เพื่อหวังว่าจะสามารถ นำคะตะลิสต์ที่เหมาะสมมาใช้กับตัวรองรับที่เตรียมได้ และนำไปใช้ในอุตสาหกรรมปิโตรเคมี โดย ศึกษาปฏิกิริยารีดักชั่นของก๊าซในตริกออกไซด์ หรือปฏิกิริยาออกซิเดชั่นของก๊าซคาร์บอนออกไซด์ ดังนั้น งานวิจัยนี้ จึงเริ่มจากการสังเคราะห์ประกอบอลูมาเทรนและไชลาเทรน หลังจากตรวจสอบ โครงสร้างของประกอบอลูมาเทรนและไชลาเทรนที่สังเคราะห์ได้ ขั้นตอนต่อไป คือ การสังเคราะห์ตัว รองรับอลูมินาและซิลิกาจากสารประกอบอลูมาเทรนและไชลาเทรน ตามลำดับ โดยผ่านกระบวน การโซล-เจล ซึ่งพบว่า อลูมินาและซิลิกาที่ได้จากการผ่านกระบวนการโซล-เจลมีสมบัติของความ เป็นรูพรุนในกลุ่มของเมโซพอรัส และมีพื้นที่ผิวค่อนข้างสูงสมบัติเหล่านี้สามารถนำไปศึกษาต่อโดย ใช้เป็นตัวรองรับคะตะลิสต์ให้กับคะตะลิสต์ที่เหมาะสมได้

คำหลัก: ดัวรองรับคะตะลิสต์ สารประกอบไซลาเทรน สารประกอบอลูมาเทรน อลูมินา ซิลิกา และ โซล-เจล Abstract

Project Code: BGJ4380014

Project Title: "Preparation and Characterization of Catalyst Supports Synthesized from

Silatrane and Alumatrane via Sol-Gel Method"

Investigator: Ms. Sujitra Wongkasemjit

The Petroleum and Petrochemical College, Chulalongkorn University

E-mail Address : dsujitra@chula.ac.th

Project Period:

2 Years

The objectives of this research work is to study the synthetic method and properties of catalyst support alumina and silica from alumatrane and silatrane, respectively, via the sol-gel method to hopefully be able to be used with a suitable catalyst needed in petrochemical industries. Therefore, this work was started with the synthesis of alumatrane and silatrane compounds followed by their structural identification. Next step is to synthesize alumina and silica via the sol-gel process. It was found that those synthesized alumina and silica gave homogeneous mesoporous property with high surface area. These properties catalytically are attractive and should be further studied.

Key words: Catalyst support, Silatrane, Alumatrane, Silica, Alumina and Sol-gel process

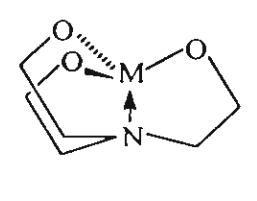
Table Content

		Page
Title page		::
Title page		ii
Acknowledgement		iii
Abstract (Thai)		iv
Abstract (English)		V
Table Content		vi
Chapter I		1
	1.1 Alumatrane	1
	1.2 Spirosilicates	3
	1.3 Sol-Gel Process	5
	- References	7
Chapter II	Synthesis of Silatrane	10
	- Abstract	10
	- Introduction	10
	- Experimental	11
	- Results and Discussion	12
	- Conclusions	20
	- References	20
Chapter III	Synthesis of Alumatrane	22
	- Abstract	22
	- Introduction	22
	- Experimental	24
	- Results and Discussion	25
	- Conclusions	36
	- References	36
Chapter IV	Sol-gel Processing of Silatranes	37
	- Abstract	37
	- Introduction	37
	- Experimental	37

	- Results and Discussion	41
\	- Conclusions	48
	- References	48
Chapter V	Sol-gel Processing of Alumatrane	50
	- Abstract	50
	- Introduction	50
	- Experimental	51
	- Results and Discussion	53
	- Conclusions	64
	- References	65
Chapter VI	Project Output	67
Appendix	A. Reprint of Formation and Structure of Tris(alumatranyloxy	68
	-i-propyl)amine Directly from Alumina and Triiospropanolamine	
	B. Reprint of Sol-Gel Processing of Silatranes	78
	C. Manuscript of Sol-Gel Transition Study and Pyrolysis	87
	of Alumina Based Gels Prepared from Alumatrane Precursor	

CHAPTER I

Metallatranes, or simply atranes, are intramolecular complex cyclic ester or alkoxides of tris(2-hydroxyalkyl)amines having a skeleton of general structure I,



where M is an n-valent element having inorganic or organic substituents when n>3. The term metallatranes, proposed by VORONKOV and ZELCHAN in 1965, is an abbreviation used for aminotrialkoxy

derivatives of different elements that contain the above skeleton (j). For example, amino-

trialkoxyphosphoranes, aminotrialkoxyboranes and aminotrialkoxysilanes give phosphatranes, boratranes and silatranes, respectively. Atrane structures are generally characterized by the tricyclic model having a

transannular M←N bond assumed to be present.

Metallatranes with M = B, Al, Si, Ge, Sn, Pb, P, Ti, V, Mo, etc. have been synthesized and studied during the last three decades [VORONKOV et al., (1968); BRADLEY et al., (1978)]. These compounds are of interest because of their cage structure, physical/chemical properties, and especially biological activity.

1.1 Alumatrane

The behavior of monomer A and oligomeric alumatrane has been described previously [HEIN and ALBERT (1952); MEHROTRA (1962); SHKLOVER et al., (1984); BRADLEY et al., (1978); VORONKOV and BARYSHOK (1982); MEHROTRA and RAI (1991)]. In benzene solution, cryoscopy [HEIN and ALBERT (1952)] and ebullioscopy [MEHROTRA (1962)] indicate octameric and hexameric behaviors. A mass spectroscopic (EI 70 eV) study [MEHROTRA (1962)] showed the stability of the dimer B in the gas phase.

There are several methods to prepare alumatranes. The simplest alumatrane was prepared in high yield by the reaction of aluminum alkoxide with triethanolamine in an aromatic solvent (benzene [MEHROTRA (1962)], toluene [THOMAS et al., (1961)]) or with no solvent [HEIN et al., (1952); ICKEN et al., (1964); STANLEY (1968); ELBING et al., (1964)] according to eq 1.1

$$n \text{ Al(OR)}_3 + (\text{HOCH}_2\text{CH}_2)_3\text{N} \longrightarrow \left[\begin{array}{c} \checkmark \\ \text{Al(OCH}_2\text{CH}_2)_3\text{N} \end{array} \right]_n^+ \quad 3n \text{ ROH}$$
 (1.1)

Triethylaluminum also reacts with triethanolamine in toluene or hexane at -78°C to form alumatrane [HIGASHI et al., (1968)] see eq. 1.2

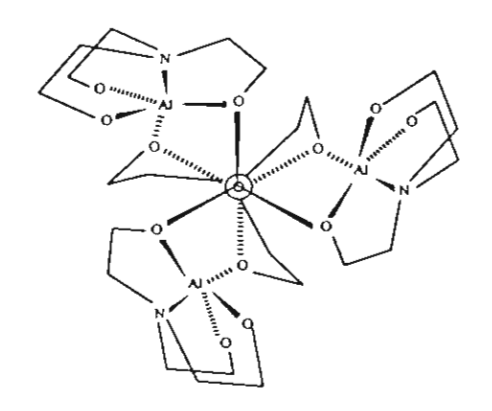
$$n \operatorname{Al(C_2H_5)_3} + n \left(\operatorname{HOCH_2CH_2} \right) \operatorname{3N} \longrightarrow \left[\begin{array}{c} \checkmark \\ \operatorname{Al(OCH_2CH_2)_3N} \end{array} \right]_{n}^{+} + 3n \operatorname{C_2H_6} \quad (1.2)$$

VERKADE et al., (1993) used the alcoholysis of tris-(dimethylamido) aluminum with triethanolamine (eq 1.3) and also the transligation of monomeric and dimeric alumaazatranes with triethanolamine (Scheme 1.1)

$$AI(NMe_2)_3 + (HOCH_2CH_2)_3N \longrightarrow \left[AI(OCH_2CH_2)_3N \right]_n^+ 3MeNH \qquad (1.3)$$

Scheme 1.1

According to ²⁷Al-, ¹H-, and ¹³C-NMR data, they found tetramers in solution and mass spectra revealed the stable tetramer (Scheme 1.2) in the gas phase.



Scheme 1.2

1.2 Silatrane

The first silatranes complexes, \underline{C} (with $X = C_6H_5$ and C_2H_5O), were patented by Finestone in 1960, who at that time suggested the existence of the Si \leftarrow N transannular dative bond in the silatrane molecule synthesized (Finestone A. B., 1960). In 1961, Frye, Vogel, and Hall reported a number of new, 1-substituted silatrane, \underline{C} [X = H, CH₃, n-C₁₈H₃₇, C₆H₅(CH₃)CH and etc.].

They described the 1-ethoxy and 1-phenylsilatranes (melting points = 100°-102°C and 208°-209°C, respectively) and reported some data in support of intramolecular transannular dative bonds in silatrane complexes.

Rosenheim et. al. (Rosenheim A., 1931) reported that silica, sand, and quartz powder could also be employed to react with alkali catecholates to give hexacoordinate silicate complexes. However, Corriu's group demonstrated that these catechol silicate complexes were quite unstable. They could only be modified usefully by reacting with strong nucleophile to obtain tri- and tetrasubstituted products, which were necessary in industry primarily for polymer synthesis, as shown in scheme 1.3 (Corriu R. J. P., 1988).

$$SiO_2 + 2KOH + 3$$

$$\begin{bmatrix} 1.2-C_6H_4(OH)_2 \end{bmatrix} \xrightarrow{-4H_2O} K_2 \begin{bmatrix} O & Si \\ RMgBr/HCl & RLi/H_2O \end{bmatrix}$$

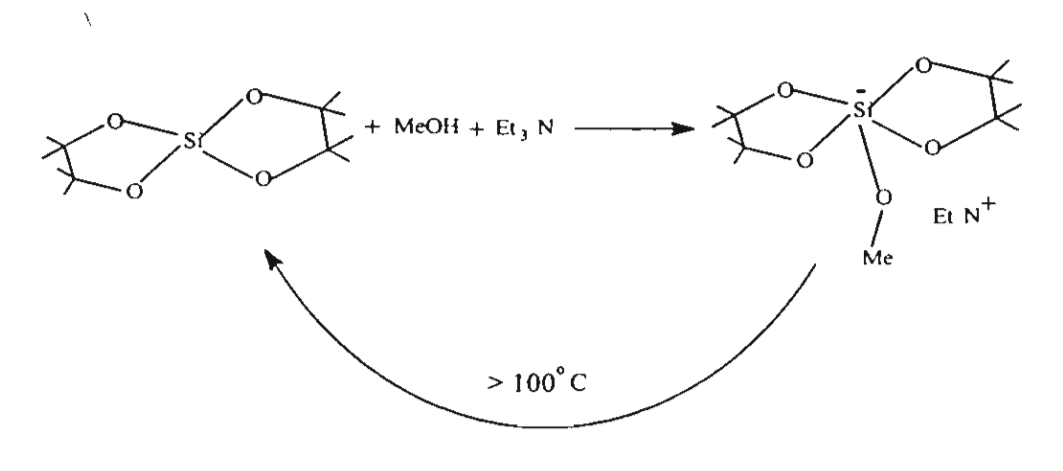
$$SiH_4$$

$$R_4Si + R_3SiCl & R_4Si + R_3SiOH$$

M = Li, Na, K or Cs

Scheme 1.3

Frye's obervation (Frye C. L., 1970: 1971) indicated that spirosilicates could react with MeOH and amine base (e.g. Et₃N) to form pentacoordinate, anionic silicate—with ammonium counterion at ambient temperature. These species were not stable above 100°C, reverting to the tetracoordinate spirosilicate, as shown in scheme 1.4.



Scheme 1.4

1.3 Sol-gel Process

Basically the sol-gel process means the synthesis of an inorganic network by a chemical reaction in solution at low temperature. The most obvious feature of this reaction is the transition from a liquid (solution or colloidal solution) into a solid (di-or multiphasic gel) led to the expression of "sol-gel process".

Sof-gel chemistry is based on inorganic polymerization reactions starting from molecular precursors, such as metal alkoxides, an oxide network is obtained via inorganic polymerization reactions. Initiation is performed through the hydroxylation of metal alkoxides which occurs upon the hydrolysis of alkoxy groups, as followed in equation 1.4.

$$M-OR + H_2O \longrightarrow M-OH + ROH$$
 (1.4)

As soon as hydroxyl groups are generated, propagation occurs through a polycondensation process. Depending on experimental conditions, two competitive mechanisms have to be considered. They can be described as follows:

1. Olation: formation of hydroxo bridges through the elimination of solvent molecules, see equation 1.5.

$$X$$
 M -OH $+$ M-O-H
 M -O-M + X-OH (1.5)

(X = H or alkyl group)

2. Oxolation : formation of oxygen bridges through the elimination of $\rm H_2O$ or XOH, as shown in equation 1.6.

These three reactions (hydrolysis, olation and oxolation) can be involved in the transformation a metal alkoxide precursor into an oxide network. The structure and the morphology of the resulting network strongly depend on the relative contribution of them. These reactions can be described as nucleophilic substitutions which depend on the nucleophilic group (H₂O, OH-, HO-M), the leaving group (ROH, H₂O) and the metal atom (Si, Ti, Zr, etc.).

One property of the sol-gel process is the ability to control the process all the way, from the molecular precursor to the product. Sol-gel chemistry offers many advantages, such as a lower processing temperature allowing the synthesis of metastable oxides phases and opening a field of opportunity for the synthesis of new materials including both organic and inorganic components. The rheological properties of sols and gels allow fibers or films to be processed by techniques, such as spin-drawing, dip-coating or screen-printing.

Generally, sol-gel process relatively involves 4 following steps:

- Solution chemistry (gel formation)
- Aging
- Drying
- Calcination/Sintering

Solution chemistry step: Starting materials (metal salt or metal alkoxides) are dissolved in an appropriate solvent to form a solution. The gel is hereafter formed in the gelation process, involving simultaneous hydrolysis and polycondensation of metal alkoxide precursor. At this step, the most important parameters are types of precursor, solvent, precursor concentration and temperature.

Aging step:. This step represents the time between the formation of a gel and the removal of solvent. As long as the pore liquid remains in the matrix, a gel can undergo many transformations. For alkoxide derived gels, concentration between surface functional group continues to occur after the gel point. This step can actually be desirable because it leads to a more cross-linked network that is mechanically stronger and easier to handle.

Drying step: It is a process of evaporating solvent from a gel network. Similarly to aging, a gel is not static during drying and, for that reason, drying can be viewed as part of the overall aging process. The properties of product are thus dependent on the drying method and condition.

Calcination/Sintering: It often is done in the presence of a reactive gas (e.g. flowing air, oxygen) in order to burn off any residue organics or to oxidize the sample. Exposing the sample to a high temperature over an extended period of time leads to sintering and consequently a decrease in surface area. The process also causes the material to crystallize into different structure forms. Thus, the physical

characteristics of the product depend on parameters, such as temperature, heating rate and gaseous environment.

Fundamentally, the uses of metal alkoxides depend on their chemical reactivity coupled with their volatility and solubility in common organic solvents. The chemical reactivity is manifest in a variety of catalytic applications of the alkoxides, ranging from redox catalyst (aluminium alkoxides in Meerwein-Ponndorf-Verly reactions with those used to synthesize primary alcohol from aldehyde), olefin polymerization catalysts (titanium and vanadium alkoxides as components of Ziegler-Natta catalysts) to accelerators for drying paints and inks. Ultimately, the alkoxides are valuable precursors to the metal oxides through hydrolysis, pyrolysis or combustion. Where high purity is at stake and the metal alkoxides offer considerable advantages as starting materials for the preparation of high purity oxides.

The starting materials to synthesize silicon or aluminium alkoxides are expensive and the syntheses are multistep. LAINE et al. have developed an inexpensive way to convert metal oxides, namely, alumina and silica, into novel materials ranging from ion conducting, liquid crystalline polymers (RAY et al., 1992), to oligomeric and polymeric precursors.

LAINE et al. found that higher boiling point amine bases (b.p.>200°C), such as triethanolamine and triethylenetetramine can be used either in catalytic or stoichiometric quantities to dissolve SiO₂. Moreover, they also found that approximately stoichiometric quantities of TEA will effectively dissolve Al(OH)₃. The "Oxide One Pot Synthesis Process (OOPS)" for alkoxyalanes was developed after it was discovered that stoichiometric amounts of TEA would dissolve aluminum hydroxide, the source material for most pure alumina [KIRK-OTHEMER (1979); COTTON and WILKINSON (1967)].

This research work was aimed at the synthesis and characterization of silica and alumina directly from silatrane and alumatrane complexes via the sol-gel process.

References

Alberty R. A. and Silbey R. J., Physical Chemistry, John Wiley & sons, Inc., Singapore, 547-710, 1955

Bradley, D. C., Mehrotra, R. C., Gaur, D. P., Metal Alkoxides; Academic Press: N. Y., 1978, 266.

Cotton, F. A. and Wilkinson, G. F., *Advanced Inorganic Chemistry*, John Wiley&sons, Interscience Pulb., N.Y., 1981.

Corriu R. J. P., Pure and Appl. Chem., 60, 99-160, 1988

Elbing, I. N. and Finestone, A. B., German offen 1., 1964, 1,162,439; Chem. Abstr., 1964, 60, 17/4705.

Finestone A. B., US 2, 953, 545, 1960

Frye C. L., Ibid 93, 6805-6810, 1971

Frye C. L., J. Am. Chem. Soc., 92, 1205-1210, 1970

Frye C. L., Vogel G. E., Hall J. A., J.Am. Chem. Soc., 83, 996, 1961

Hein, F. and Albert, P. W. Z., Anorg. Allg. Chem., 1952, 269, 67.

Higashi, H. and Namikawa, S., Kogyo Kagaku Zasshi, 1967, 70,97.

Icken, J. M. and Jahren, E. J., Belg. Patent 619, 1963, 940; Chem. Abstr., 1963, 60, 2768.

Kirk-Othemer, *Encyclopedia of Chemical Technology*, third edition, Wiley-Interscience Publ., N.Y., 1979, 2, 129-262.

Laine R. M., NATURE, 353, 1991

Mehrontra, R. C. and Mehrotra, R. K., J. Indian Chem. Soc., 1962, 39, 677.

Mehrotra and Rai, A. K., Polyhedron, 1991, 10, 1967.

Ray, D. G., Laine, R. M., Robinson, T. R., Viney, C., Mol. Crys. Liq. Crystal, 1992, 225,153.

Rosenheim A., Raibmann B and Schendel, G.Z., Anorg. Allg. Chem, 160, 196, 1931

Shklover, V. E., Struchkov, Yu. T., Voronkov, M. G., Ovchinnikova, Z. A. and Baryshok, V. P., *Dokl. Akas. Nauk (Engl. Transl)*, 1984, 227, 723.

Stanley, R. H., British Patent 1, 1968, 123,559; Chem. Abstr., 1968, 69, 78532.

Thomas, W. M., Groszos, S. J and Day, N. E., *U.S. Patent 2*, 1961, 985, 685; *Chem. Abstr.*, 1961, 55, 20966.

Verkade, J. K., Acc. Chem. Res., 1993, 26, 483.

Voronkov, M. G., Vestnik Akad. Nauk SSSR, 1968, 38, 48

Voronkov, M. G. and Baryshok, V. P., Organomet. Chem., 1982, 239, 199.

Voronkov, M. G. and Zelchan, G. I., Khim. geterotsikl. soed., 1965, 51.

CHAPTER II SYNTHESIS OF SILATRANE

ABSTRACT

New convenient and inexpensive method of tris(silatranyloxy-*i*-propyl)amine synthesis directly from silica and triisopropanolamine (TIS) has been elaborated using ethylene glycol solvent. The silatrane product is obtained in one step via the "Oxide One Pot Synthesis (OOPS)" process. In the presence of catalytic amounts of triethylenetetramine (TETA), the reaction easily takes place. The product is characterized using DSC, TGA, ¹H-, ¹³C-, ²⁹Si-NMR and FAB*-MS. The FTIR result indicates the presence of N—>Si transannular bonding. The chemical and physical properties of these compounds are described specially with respect to their polymeric properties.

INTRODUCTION

The limited number of simple silicon-containing starting materials restricts the potential role of inorganic and organometallic silicon compounds in the development of new chemical reagents, polymeric glasses and ceramics. The reason is that silicon-containing chemicals are almost exclusively prepared from elemental silicon, obtained from the carbothermal reduction of silica at around 1200 °C¹. The utilization of crude silica to form silicon-containing compounds directly, in order to circumvent this energy-intensive step, has been the aim of a number of research groups by a variety of strategies.

Silatranes, for example, as a class of pentacoordinated silicon compounds are known for more than three decades, and their specific biological²⁻³, physico-chemical⁴⁻⁵ and structural⁶⁻⁷ properties still attract research interests. Although the investigation results were published in many papers⁸⁻¹⁰, most of them deal solely with the intriguing property study of these compounds.

The most popular methods for the silatrane synthesis are the reactions of halo-, hydro- and alkoxysilanes with triethanolamine or its derivatives¹¹(see eq.2.1). The original way of silatrane synthesis from ethoxysilanes and boratrane in the presence of $AI(O_i-Pr)_3$ or AI_2CI_6 has also been described¹²⁻¹³.

$$XSi(OC_2H_5)_3 + (HOCH_2CH_2)_3N \longrightarrow XSi(HOCH_2CH_2)_3N + 3C_2H_5OH (2.1)$$

$$X = C_2H_5O, C_6H_5$$

Recently, Laine and colleagues have found a way to synthesize organosilicon compounds directly from inexpensively starting material, silica (SiO₂), and ethylene glycol in only one step¹⁴⁻¹⁶. They also found a way to synthesize tris(silatranyloxyethyl)amine from silica and triethanolamine¹⁷ via the "OOPS" process, as shown in eq.2.2.

SiO₂ + N(CH₂CH₂OH)₃
$$\xrightarrow{\text{Ethylene}}$$
 $\xrightarrow{\text{Olycol}}$ $\xrightarrow{\text{Olycol}}$ OH (2.2)

We have been further investigating this reaction with different kind of trialkoxylamine, namely TIS, to determine whether similar silatrane product can be obtained. This paper describes the production and characterization of tris(silatranyloxy-i-propyl)amine via the "OOPS" process directly from silica, which is a widespread and inexpensive starting material, as compared to triethoxysilanes which are far more expensive, and TIS.

EXPERIMENT

Materials

All reactions were carried out under a N₂ atmosphere with careful exclusion of extraneous moisture and air since the product is slightly sensitive to moisture and air. The glassware used for these experiments was oven dried. Amorphous, precipitated silicon dioxide, SiO₂, with a multi-point BET surface area of 182 m²/g, was donated by PPG Siam Silica Co., Ltd. and used as received. It was stored in a dry environment prior to use to prevent moisture adsorption. Ethylene glycol, EG, (99.5% Farmitalia Carlo Erba) used as solvent in the reaction was distilled before used by fractional distillations at 200 °C. Triethylenetetramine, TETA, (Union Carbide, Thailand, Ltd.) used as a base catalyst was distilled under vacuum prior to use. TIS was obtained from Fluka Chemika Company and used as received. Anhydrous diethyl ether and dichloromethane (J.T. Baker Inc.) used as purification solvents were purified by standard techniques under N₂ atmosphere. Dichloromethane was distilled from anhydrous calcium chloride, and anhydrous diethyl ether was dried by adding anhydrous calcium chloride and kept in a clear dry Winchester bottle.

Characterization

FTIR spectra were obtained using a Bio-Rad FT-45A spectrometer with a resolution of 4 cm⁻¹. A solid sample was thoroughly ground using 1% of sample to 99% by weight of pure and dry crystalline KBr, followed by mixing and pressing hydraulically into pellet. ¹H-, ¹³C-, ²⁹Si-NMR spectra were obtained using a 500 MHz JEOL spectrometer at room temperature in DMSO-d₆ as solvent and TMS as

internal reference. Mass spectra were obtained on a Fison Instrument (VG Autospec-ultima 707E) with VG data system using a direct probe of the positive fast atom bombardment technique (FAB* mode) and cesium lodide (CsI) as a standard for peak calibration.

Thermal transition properties were determined using a Netzsch DSC 200 at a heating rate of 10°C /min under nitrogen atmosphere. The thermal stability of the synthesized products was obtained using Netzsch TGA 209 at a heating rate and flow rate of 20°C and 10 mL per min., respectively. Synthetic Method

Synthesis of silatrane complex was carried out with and without catalyst TETA by placing 6.09g. (100 mmol) of silica, 19.12 g. (100 mmol) of TIS, and 100 mL of ethylene glycol into a 250 mL two-neck reaction flask. In case of running the reaction with catalyst, then 0.15 g. (1 mmol) of TETA was also added into the mixture. The solution mixture was magnetically stirred and heated to the boiling point of EG under N₂ atmosphere to distill off EG and by-product, water. During the course of reaction, the same amount of fresh EG as distillate was added. This process of EG distillation and addition was repeated until the mixture turned clear, indicating that the reaction was complete which took approximately 5 and 10 h for the reaction containing with and without TETA, respectively. The remaining EG was removed by vacuum distillation (10° torr) using an oil-bath temperature of 100± 5°C. The resulting product turned very viscously at this point. It was then purified by precipitating with dried 10% dichloromethane in diethyl ether. The powder product was filtered off, dried in vacuum oven at 50°C for 10 h., and finally characterized by TGA, DSC, FAB*-MS, FTIR and NMR.

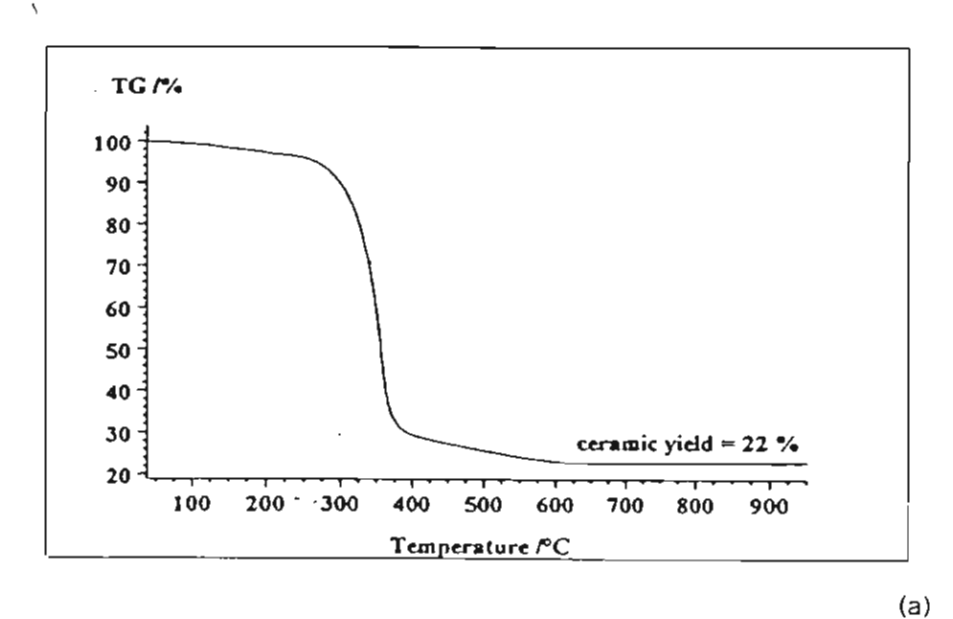
RESULTS AND DISCUSSION

Silatrane complex, tris(silatranyloxy-*i*-propyl)amine, (J), was synthesized via the "Oxide One Pot Synthesis (OOPS)" process using widely available SiO₂ in the presence and absence of TETA catalyst under identical conditions. The reaction without TETA took twice longer than the one with TETA. Characterization of isolated products from both reactions indicated that their structures were almost identical, except that the product obtained from the reaction with TETA was bis(silatranyloxy-*i*-propyl)-hydroxyl-*i*-propyl amine, (II), as discussed in detail below.

Thermogravimetric Analysis (TGA)

The silatrane product without TETA show three regions of mass loss, 150°-250°C, 290°-370°C and 390°-620°C, see Figure 2.1(a). The first one corresponds to the loss of traces of residual EG and TIS. The second and the last mass loss correspond to organic ligand decomposition and the oxidation of residual carbon char, respectively. The final %ceramic yield is 22%, as compared to 21.5% for the theoretical ceramic yield.

In case of the product obtained with TETA (Fig. 2.1(b)), it show similar mass losses to that from the reaction without TETA, except the mass loss between 260°-320°C. This region is likely belong to the TETA mixed in the product which is supported by NMR data indicating that approximately 15% TETA is present in the product. As a result, the % ceramic yield was only 16%, which is lower than the theoretical ceramic yield, 19.2%.



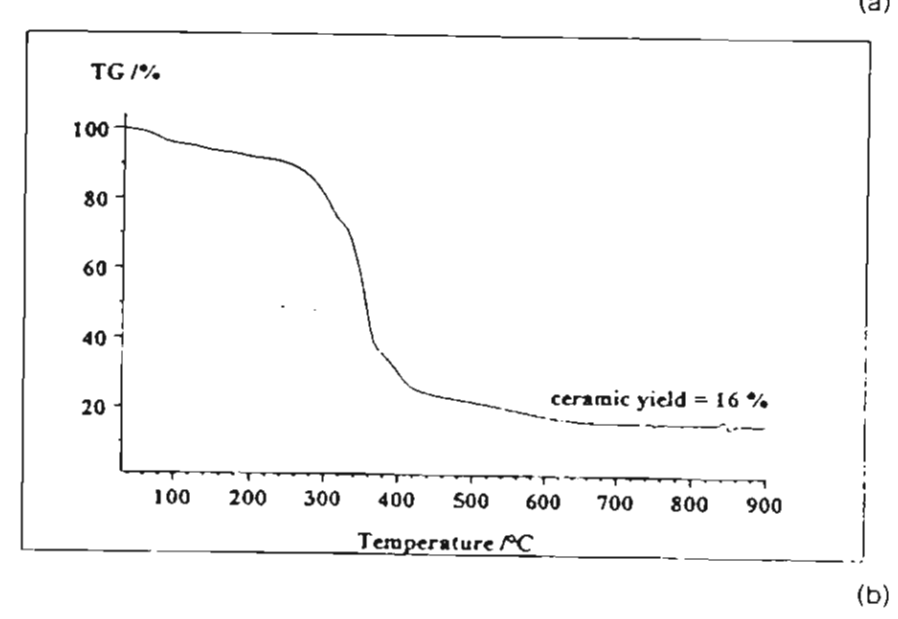


Figure 2.1: TGA of Precipitated Silatrane Complexes, (a) without TETA and (b) with TETA

Differential Scanning Calorimeter (DSC)

DSC data of both products (Figure 2.2) show similar results to the TGA profiles. Both exotherms at about 140 °C correspond to decomposition of EG, TIS and TETA. The peaks at 220° and 180 °C in Figures 2.2(a) and 2.2(b), respectively, corresponding to the melting point of silatrane complexes, confirm that using catalyst in a reaction always results in shorter oligomers, as supported by FAB*-MS, than the product obtained from the one without TETA.

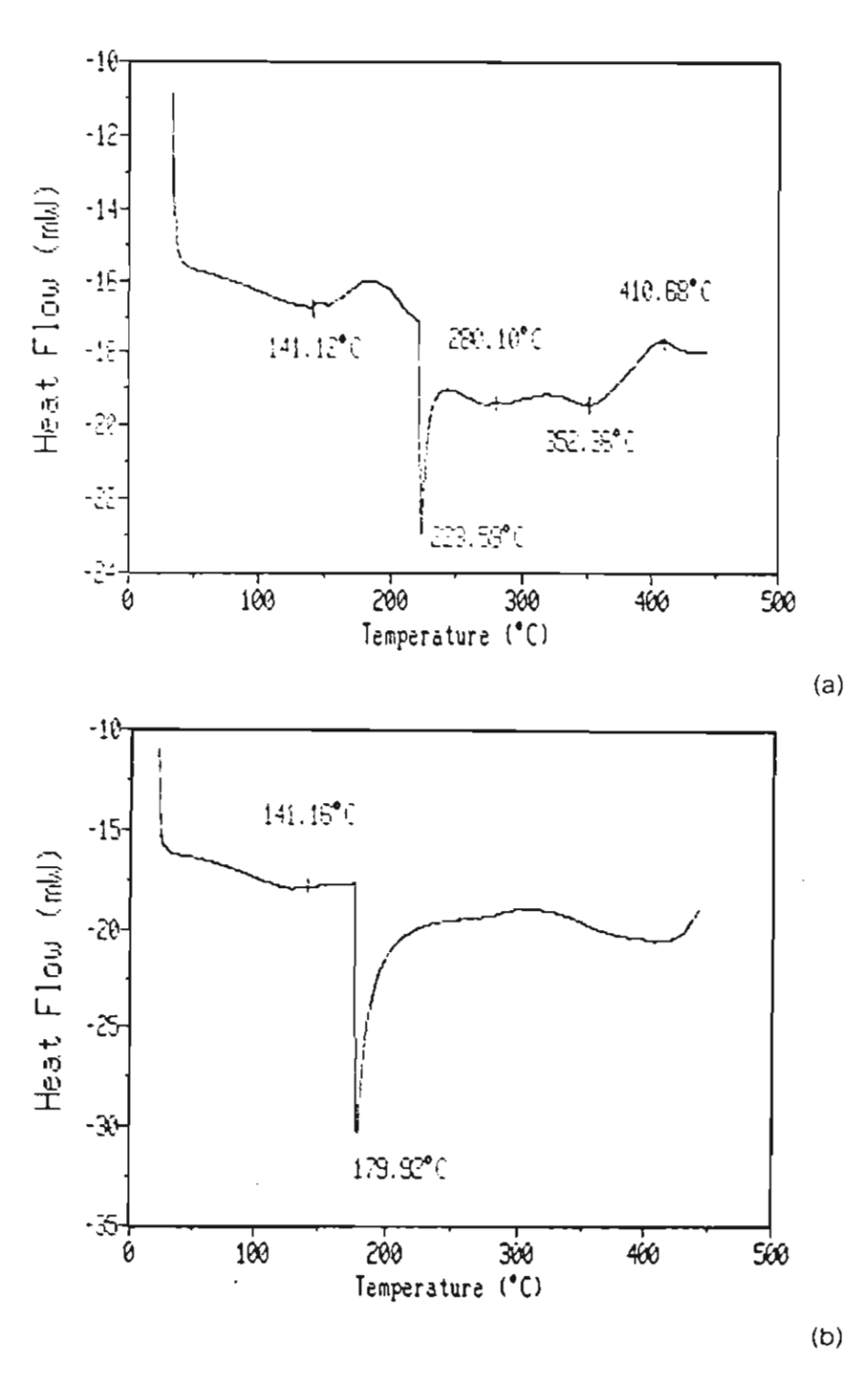


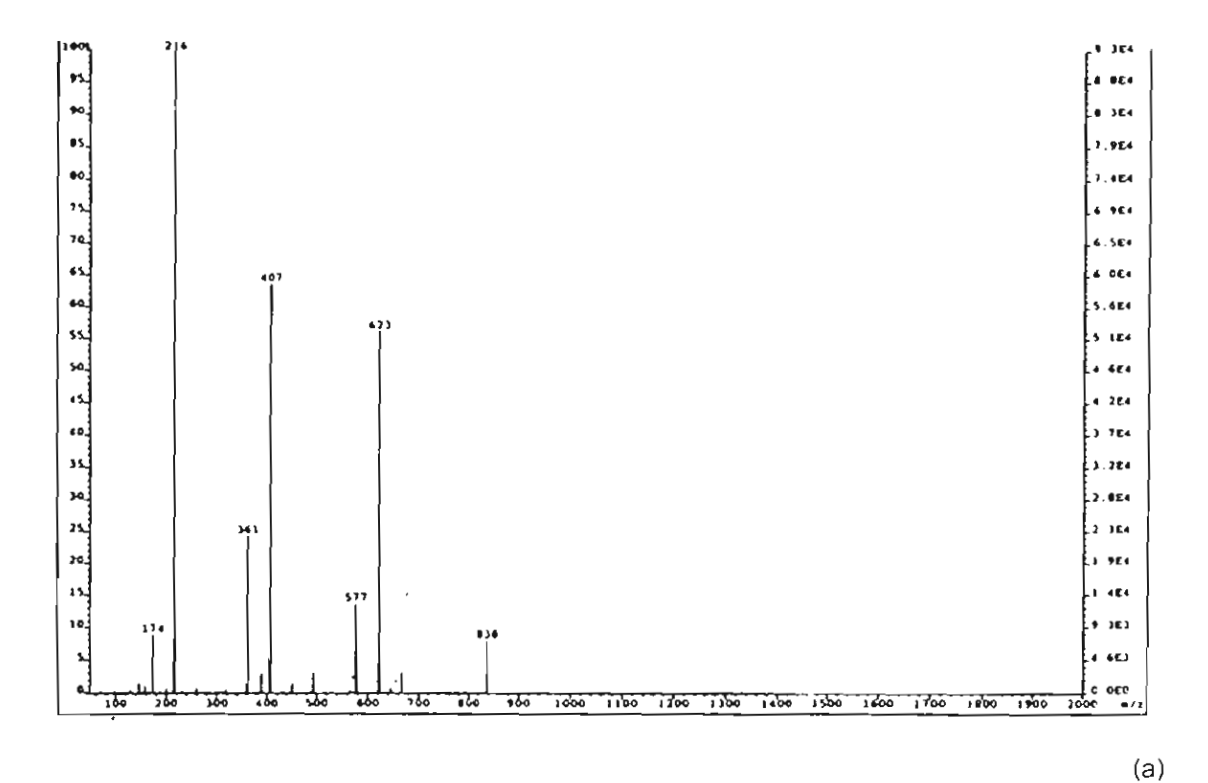
Figure 2.2: DSC of Precipitated Silatrane Complexes, (a) without TETA and (b) with TETA

Positive Fast Atom Bombardment Mass Spectroscopy (FAB*-MS)

The FAB*-MS spectrum fragmentation pattern can be employed to confirm the silatrane structures, as can be seen in Table 2.1 showing the proposed structures of the complexes obtained from the reaction without and with TETA. These structures support the fragmentation patterns in Figure 2.3.

Table 2.1: The proposed structures and the pattern of fragmentation of the products octained from the reactions w/o and w/ TETA

m/e	Inter	nsity	Scecies	
	w/o TETA	w/ TETA		
838 (836 + 2H*)	8	-		
623 (621 + 2H ⁻)	22	8		
407 (405 + 2H)	63	18	CH CH	
361 (360 + H ⁻)	24	10	CH ²	
216 (215 + H ⁺)	100	100	** -	



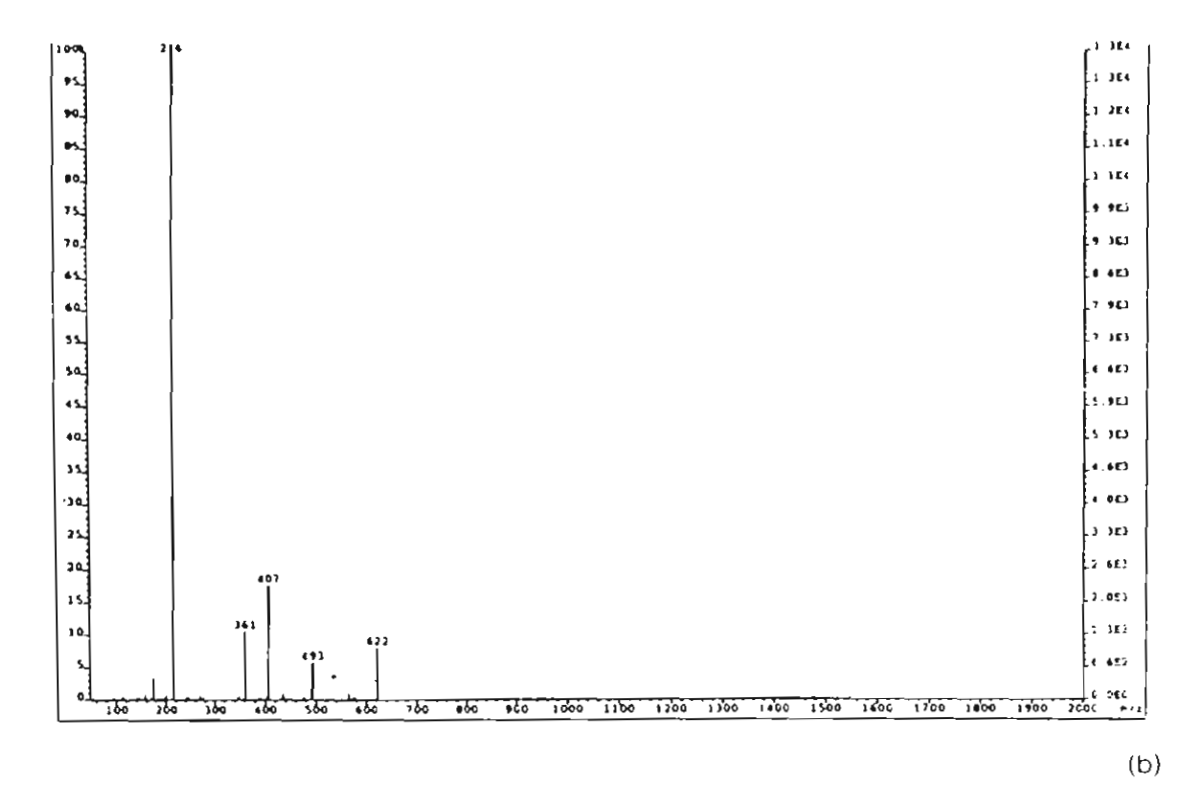


Figure 2.3: FAB*-MS Fragmentation Patterns of Silatrane Complexes, (a) without TETA and (b) with TETA

From the results of FAB*-MS spectroscopy, Figure 2.3 and Table 2.1 indicate that the product without TETA mainly consists of the oligomer that has the molecular ion peak at m/e 838, and the base peak is the monomer silatrane. The second highest intensity is the fragment with m/e 407, which has an intensity of 63%.

The fragmentation pattern of the product with TETA is similar to the pattern of the product from the reaction without TETA, except that the m/e 838 is absent. This is probably because TETA acts like an accelerator in the reaction, which results in the shorter chain of oligomers.

Fourier Transform Infrared Spectroscopy (FTIR)

FTIR spectra show that the precipitated product of the reaction with TETA gives the same peaks found in the reaction without TETA. Both products indicate the presence of strong Si-O-C stretching bands at about 1015-1085 cm⁻¹. The peak at 2800-2976 cm⁻¹ corresponds to the C-H stretching, whereas the peak at 1380-1460 cm⁻¹ is resulted from the C-H bending. The peak at 1270 cm⁻¹ comes from the C-N stretching. The strong peak at 1030-1070 cm⁻¹ corresponds to the C-O stretching and the peak at 560-590 cm⁻¹ refers to the Si—N dative bond.

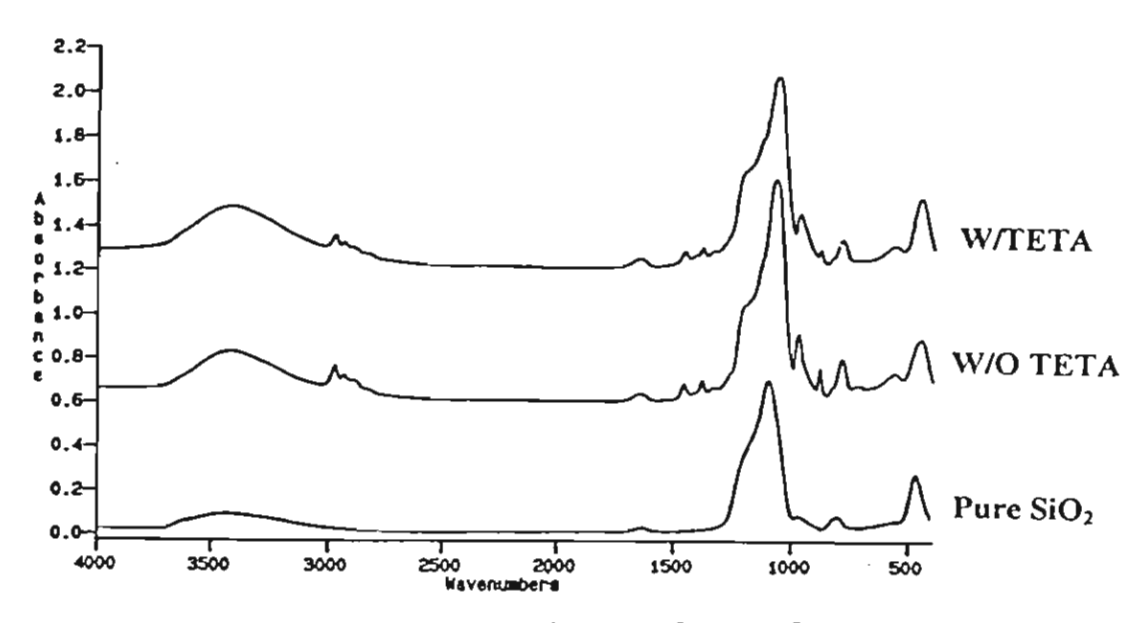


Figure 2.4: FT-IR Spectra of Pure Silica and Silatrane Complexes w/o and w/ TETA

Nuclear Magnetic Resonance Spectroscopy (NMR)

The ¹H-, ¹³C- and ²⁹Si-NMR spectra are used to confirm the structure of silatrane complexes. For the product without TETA ¹H-NMR spectrum in d₆-DMSO shows peaks at 0.96-1.12,

2.86-2.91, 3.3, 3.4-3.5, and 4.0 ppm, which are assigned to CH-C \underline{H}_3 , N-C \underline{H}_2 , C \underline{H}_2 -O, CH₂O \underline{H} of EG, and C \underline{H} -CH₃, respectively. The ¹³C-NMR spectrum shows peaks at 20-21, 23, 57.7, 59.2, and 62.5-65 ppm which can be attributed to H₂C-CH- \underline{C} H₃, H₂C- \underline{C} H-CH₄, N- \underline{C} H₂-O, \underline{C} H₂OH of EG, respectively.

¹H- and ¹³C-NMR spectra of the silatrane complexes with TETA show similar peaks to those obtained from the reaction without TETA, except that ¹H-NMR spectrum shows the peaks at 2.6-2.7, which is the group of NH₂-CH₂ in TETA. ¹³C-NMR spectrum also shows peaks at 39-41 ppm indicating the NH₂-CH₂ group of TETA. All results are summarized in Table 2.2.

Table 2.2: Compared Peak Positions of Products

Position	Groups	¹H-NMR	¹³ C-NMR
		(ppm)	(ppm)
а	N-C <u>H</u> ₂	2.86-2.91	57.7
b	CĤ-CH³	4.0	23
С	СН-С <u>Н</u> ₃	0.96-1.12	20-21
d	C <u>H</u> ₂-O	3.3	59.2
е	CH₂OḤof EG	3.4-3.5	62.5-65
f	NH ₂ -C <u>H</u> 2 of TETA	2.6-2.7	39-41
g	NH-C <u>H</u> ₂ of TETA	2.9-3.1	60.4-60.7

²⁹Si NMR spectra of precipitated products of the reactions without and with TETA show the peaks at 96 and 98 ppm, respectively, identifying a pentacoordinate Si with dative bond ¹⁸, as shown in Figure 2.5. One silica atom is bonded not only with 4 oxygen atoms, but also has a transannular dative bond, which interacts with N atom of TIS. Transannular dative bond is not like a "normal" siliconnitrogen bond because internuclear distance (r_{Si-N}) is considerably shorter than the vander waal but longer than Si-N covalent bond. This is confirmed by the detailed X-ray crystalliographic studies by Boer and Turley in 1968¹⁹.

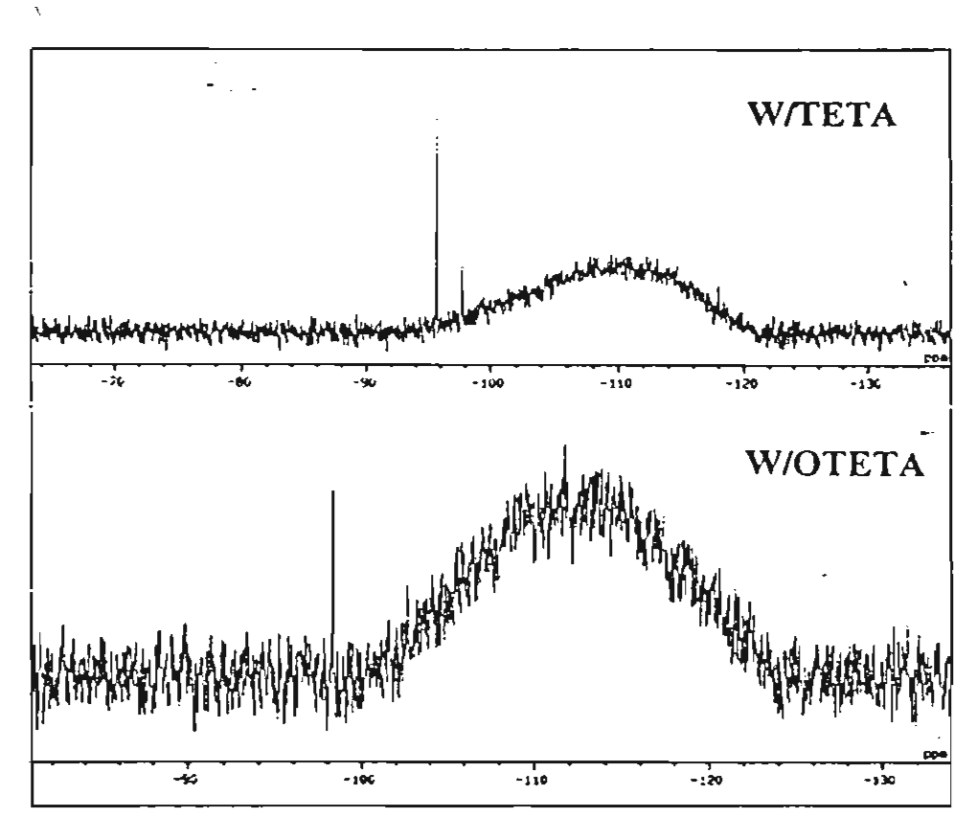


Figure 2.5: 29Si-NMR Spectra of Silatrane Complexes w/ and w/o TETA

CONCLUSIONS

The silatrane complexes can be synthesized directly from widespread available SiO₂ and TIS via the "Oxide One Pot Synthesis" process in the presence and absence of TETA. When TETA is present, the reaction time is twice faster. Thus, TETA could be used as an accelerator for this reaction. The purified products from the reaction with and without TETA are white solid powder which give molecular ion peaks at m/e=623 and 838, respectively. Other characterization studies show that both products display similar properties.

REFERENCES

- 1. Kirk-Othmer Encyclopedia of Chemical Technology (1979), 3rd Ed., "Silica", Vol. 20, p. 750
- R. Tacke and H. Linoh (1989), "Bioorganosilicon Chemistry, in S. Patai and Z. Rappoport", The Chemistry of Organic Silicon Compounds, Wiley-Interscience, New York.
- 3. E. Lukevics and L. Ignatovich (1992), "Comparative Study of the Biological Activity of Organosilicon and Organogermanium Compounds", *Appl. Organomet. Chem.* 6, 113
- M.G. Voronkov, M.S. Sorokin, V.A. Klyuchnikov, G.N. Shvetz and V.J. Pepekin (1989), "Thermochemistry of Organosilicon Compounds", *J.Organomet. Chem.* 359, 301

- G. Cerveau, C. Chuit, E. Colomer, R.J.P. Corriu and C. Reye (1990), "Ferrocenyl Compounds Containing Two Hypervalent Silicon Species", *Organometallics* 9, 2415
- M. Nasim, L.J. Livantsova, P.D. Krutko, G.S. Zaitseva, J. Lorbertth and M. Otto (1991), "Synthesis of 2-Silatranyl-and 2-(3,7,10-trimethylsilatranyl) acetaldehydes", J. Organomet. Chem. 402, 313
- 7. P. Hencsei (1991), "Mass-spectrometric Study of Ring Substituted Silatranes", Struct. Chem. 2, 21
- 8. R.J.P. Corriu and J.C. Young (1989), "Hypervalent Silicon Compounds, in: S. Patai and Z. Rappoport", The Chemistry of Organic Silicon Compounds, Wiley-Interscience, New York
- C. Chuit, R.J.P. Corriu, C. Reye and J.C. Young (1993), "Reactivity of Penta- and Hexacoordinate Silicon Compounds and Their Role as Reaction Intermediates", Chem. Rev. 93, 1371
- 10. V. Gevorgyan, L. Borisova, A. Vjater, J. Popelis, S. Belyakov and E. Lukevics (1994), "Synthesis and Structure of Silylmethylsilatranes RR'R"SICH2SI(OCH2CH2)(3)N", J.Organomet.Chem. 482, 73
- 11. M.G. Voronkov, V.M. Dyakov and S.V. Kirpichenko (1982), "Silatranes", J. Organomet. Chem. 233, 1-147
- M.G. Voronkov (1966), "Silatranes:Intra-Complex Heterocyclic Compounds of Pentacoordinated Silicon", Pure Appl. Chem. 13, 35
- 13. J. Dirk Nies, J.M. Bellama, B-Z. Nava (1985), "Multiphoton Infrared Laser-induced Degradation of Polydimethylsiloxane and Hexamethyldisilane", J. Organomet. Chem. 296, 315
- 14. Rangsitphol, J. (1995), <u>Aryloxysilane Synthesis Directly from silica and Catechol</u>, Master Thesis, The Petroleum and Petrochemical College, Chulalongkorn University.
- 15. R. Laine, K. Blohowiak, T. Robinson, M. Hoppe, P. Nardi, J. Kampf and J. Uhm (1991), "Synthesis of Pentacoordinate Silicon Complexes from SiO₂", *Nature* 353, 642-644
- 16. K. Blohowiak, D. Tradewell, R. Mueller, M. Hoppe, S. Jouppi, P. Kansal, K. Chew, C. Scotto, F. Babonneau, J. Kampf and R. Laine (1994), "SiO₂ as a Starting Material for the Synthesis of Pentacoordinate Silicon Complexes", *Chem.Mater.* 6, 2177-2192
- 17. C. Bickmore and R. Laine (1996), "Synthesis of Oxynitride Powders via Fluidized-Bed Ammonolysis, Part I: Large, Porous, Silica Particles", *J.Am. Ceram.Soc.* 79, 2865-77
- L. Sommer and O. Bennett (1957), "Anomalous Spin-Spin Splitting in NMR Spectra of Cyclobutenes",
 J.Am. Chem. Soc. 79, 1008
- 19. J. Turley and F. Boer (1968), "Structural Studies of Pentacoordinated Silicon. I Phenyl-(2,2',2"-nitrilotriethoxy)silane", *ibid.* 90, 4026

CHAPTER III SYNTHESIS OF ALUMATRANE

ABSTRACT

Preparations of alumatrane complexes generally are high cost because of multistep synthesis and expensive starting materials. Recently, a new one step method was developed for synthesizing alumatrane directly from aluminum hydroxide [Al(OH)₃] and triisopropanolamine (TIS) both of which are inexpensive and readily available. When 45.5 mmol of Al(OH)₃ are reacted with 70 mmol of TIS at 200°C, the reaction is complete in 3 h. The product can be purified by precipitation. Triethylenetetramine (TETA), a stronger base than TIS, was found to accelerate the dissolution rate of Al(OH)₃. The kinetics of TIS-Al formation were studied and TIS-Al was fully characterized using DSC, TGA, FAB*-MS, NMR (¹H-, ¹³C-, ²⁷Al-), and FTIR. The integral method was used to study the dissolution kinetics as a function of different conditions. The activation energy of reaction was 24 ± 2 kJ mol⁻¹.

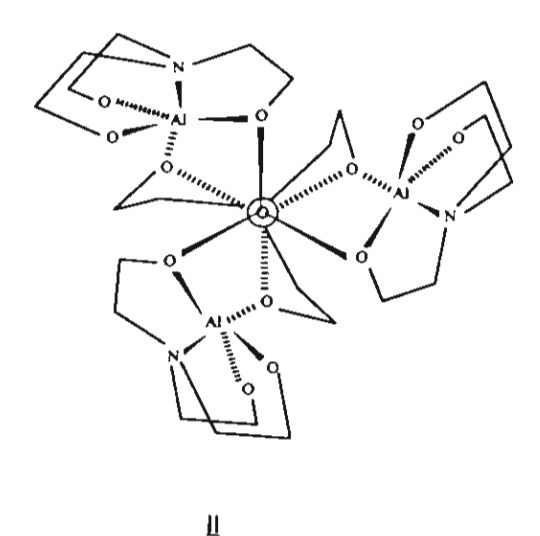
INTRODUCTION

Atranes, I, with M = B, Al, Si, Ge, Sn, Pb, P, Ti, V, Mo, etc. have been synthesized and studied during the last three decades¹⁻⁵. These compounds are of interest because of their cage structure, physical/chemical properties, and especially biological activity. The behavior of alumatrane, where M = Al, 2,8,9-trioxa-1-alumatricyclo [3.3.3.0^{1.5}]undecane, and oligomeric alumatrane has been described previously⁶⁻⁹.)]. In benzene solution, cryoscopy and ebullioscopy indicate tetrahedral and octameric behavior. A mass spectroscopic (El 70 eV) study showed the stability of the dimer I' in the gas phase.

There are several methods of preparing alumatranes. Alumatrane is prepared readily in high yield by reaction of aluminum alkoxides with triethanolamine in an aromatic solvent¹⁰⁻¹¹ or with no solvent¹²⁻¹⁴.

Triethylaluminum also reacts with triethanolamine in toluene or hexane at -78°C to form alumatrane ¹⁵. VERKADE ¹⁶ prepared alumatrane by the alcoholysis of tris-(dimethylamido) aluminum with triethanolamine and also the transligation of monomeric and dimeric alumazatranes with triethanolamine.

According to ²⁷Al-, ¹H-, and ¹³C-NMR data, they found tetramers, [], in solution and dimeric [' by mass spectra in the gas phase. Alumatrane precursors, aluminum alkoxides [Al(OR)₃] or aluminum alkyls [Al(R)₃], are expensive and the syntheses are multistep. LAINE et al. have developed an inexpensive way to convert metal oxides, namely, alumina and silica, into novel materials ranging from ion conducting, liquid crystalline polymers to oligomeric and polymeric precursors¹⁷⁻¹⁸.



LAINE also found that higher boiling point amine bases (b.p.>200°C), such as triethanolamine and triethylenetetramine can be used either in catalytic or stoichiometric quantities to dissolve SiO₂. Moreover, they also found that approximately stoichiometric quantities of TEA will effectively dissolve Al(OH)₃. The "Oxide One Pot Synthesis Process (OOPS)" for alkoxyalanes was developed after it was discovered that stoichiometric amounts of TEA would dissolve aluminum hydroxide, the source material for most pure alumina.

The purpose of this work is to extend previous efforts to reactions of aluminum hydroxide (Al(OH)₃) and triisopropanolamine (TIS) and study the kinetics of the product formation, which includes the reaction order, rate constant and activation energy. Along with this, the effect of triethylenetetramine (TETA) on the reaction was also studied to improve the solubility of this novel aluminum alkoxide in non-polar solvents for use as a catalytic intermediate in the sol-gel processing.

EXPERIMENTAL

Materials

The starting materials and products are moisture and air sensitive. Therefore, all operations were carried out with careful exclusion of air by purging with nitrogen gas.

UHP grade Nitrogen; 99.99% purity was obtained from Thai Industrial Gases Public Company Limited (TIG). Aluminum hydroxide hydrate [Al(OH)₃.xH₂O] containing 57.5% Al₂O₃ content by TGA was purchased from Aldrich Chemical Co. Inc. (USA) and used as received. Ethylene glycol (EG), used as solvent in the reaction, was purchased from Farmitalia Carlo Erba (Barcelona) and purified by fractional distillation at 200°C, under N₂ before use. Triisopropanolamine (TIS) was obtained from Fluka Chemika-BioChemika (Switzerland) and used as received. Triethylene Tetramine (TETA) was obtained from Union Carbide Thailand Limited (Bangkok, Thailand) and distilled under vacuum (10°2 torr) at 120°C. Acetonitrile and methanol were purchased from J.T. Baker Inc. (Phillipburg, USA) and purified by standard techniques. Acetonitrile was distilled from calcium hydride powder. Methanol was distilled from magnesium metal activated with iodine.

Instrumentation

Mass spectra were obtained on a 707E-Fison Instrument (VG-Autospec, Manchester, England) with a VG data system, used in the positive fast atomic bombardment (FAB⁺) mode. Thermal analysis was carried out on a Netzsch DSC 200 (Germany) and a Netzsch Gerätebue BmbH Thermal analysis TG 209 (Germany). ¹H- and ¹³C-NMR spectra were obtained using a 500 MHz JEOL (JNM-A500) spectrometer at the Scientific and Instrumental Research Equipment Center, Chulalongkorn University, using deuterated methanol (CD₃OD) and tetramethylsilane (TMS) as the solvent and internal reference, respectively. ²⁷Al-NMR spectra were recorded on Bruker 360 MHz at the University of Michigan. FTIR spectra were recorded on a Bio-Rad FT-45A Fourier transform infrared spectrometer with a resolution of ±4 cm⁻¹.

Procedure

General procedures to obtain tris(alumatranyloxy-*i*-propyl)amine are as follows; aluminum hydroxide, 50 mL of EG, and TIS were added to a 250 mL two-necked round bottomed flask. The reaction mixture was stirred and heated under N₂ in a thermostatted oil bath. When the oil bath temperature reached 200°C, the reaction was considered to have commenced. Fresh EG in the same amount as the distillate was added to maintain the total reaction volume until the reaction mixture turned clear (about 3 hour), indicating reaction completion. After letting the reaction mixture stand without stirring overnight, white product precipitated out. After filtering, the product was stirred with dried acetonitrile overnight to remove excess TIS. The solid product was then filtered off and dried under high vacuum (10°2 torr) at 120°C for 5 h. Dried products were then characterized using DSC, TGA, FTIR, FAB -MS and NMR.

Kinetic studies

The kinetic studies were primarily conducted on the dissolution of Al(OH) as a function of changes in the reaction conditions, namely, the amount of TIS, the amount of aluminum hydroxide, reaction temperature, and time. Each reaction was repeated three times.

The optimum ratio of TIS was studied by fixing the amount of $AI(OH)_3$ (57.5% AI_2O_3 content by TGA) at 22.7 mmol or 10 mmol equivalent of AI_2O_3 . The amount of TIS was varied from 0-50 mmol. The reaction time and temperature were fixed at 3 h and 200°C, respectively.

Dissolution Rate as a Function of Al(OH), Concentration

The amount of TIS was fixed at 3.83 g (20 mmol) and the amount of Al(OH)₃ was varied from 0.89-8.87 g (5-40 mmol). EG was added to make the total volume of reaction mixture 50 mL. The reaction time and temperature were set at 1 h and 200°C, respectively. Each run was repeated three times. The relationship between mmol of unreacted alumina and mmol of alumina added was plotted.

Dissoluion Rate as a Function of TETA Concentration

To study the effect of [TETA] on the rate of reaction, Al(OH)₃ and TIS quantities were fixed at 1.77 g (22.7 mmol) and 0.96 g (5 mmol), respectively. The concentration of TETA was varied from 0-4.3875 g (0-30 mmol). The reaction time and temperature were fixed at 3 h and 200°C. The relationship between mmol dissolved alumina and mmol TETA added was then plotted.

Determination of the Reaction Rate Constant and Activation Energy

Amounts of Al(OH)₃ and TIS were fixed at 1.77 g (22.7 mmol) and 0.96 g (5 mmol), respectively. The reaction time was varied from 15-120 min with increments of 15 min at 150° , 170° , 190° , and 200° C. The relationship between mmol of unreacted alumina versus reaction time at each reaction temperature was then plotted to obtain the reaction rate constant (*k*). The activation energy was then calculated by plotting ln (*k*) versus 1/T (1 K⁻¹).

Dissolution Rate as a Function of Time in the Presence of TETA as a Catalyst

The effect of time on the reaction of Al(OH)₃ and TIS with TETA as a catalyst was studied by fixing the amounts of Al(OH)₃, TIS, and TETA at 1.77g (22.7 mmol), 0.96 g (5 mmol), and 0.18 g (1.25 mmol), respectively. The reaction temperature was fixed at 200°C and the reaction time was varied from 15-120 min. The mmoles of unreacted alumina for each run were then plotted versus time.

RESULTS AND DISCUSSION

In this study, recovered $Al(OH)_3$ was thermally converted to α -alumina to determine the actual amount dissolved. $Al(OH)_3$ used at the beginning and left after the reaction was measured as Al_2O_3 using TGA ceramic yield.

As seen in Figure 3.1, with a fixed amount of aluminum hydroxide hydrate [1.77 g (22.7 mmol)] at a reaction time and temperature of 3 h. and 200 °C, respectively, the reaction went very slowly for TIS quantities less than 20 mmol. However, it went to completion when 35 mmol of TIS was used. It was found also that when 10 mmol of TETA was used with the 22.7 mmol of Al(OH)₃ and 35 mmol of TIS, the reaction was complete within 2 h.

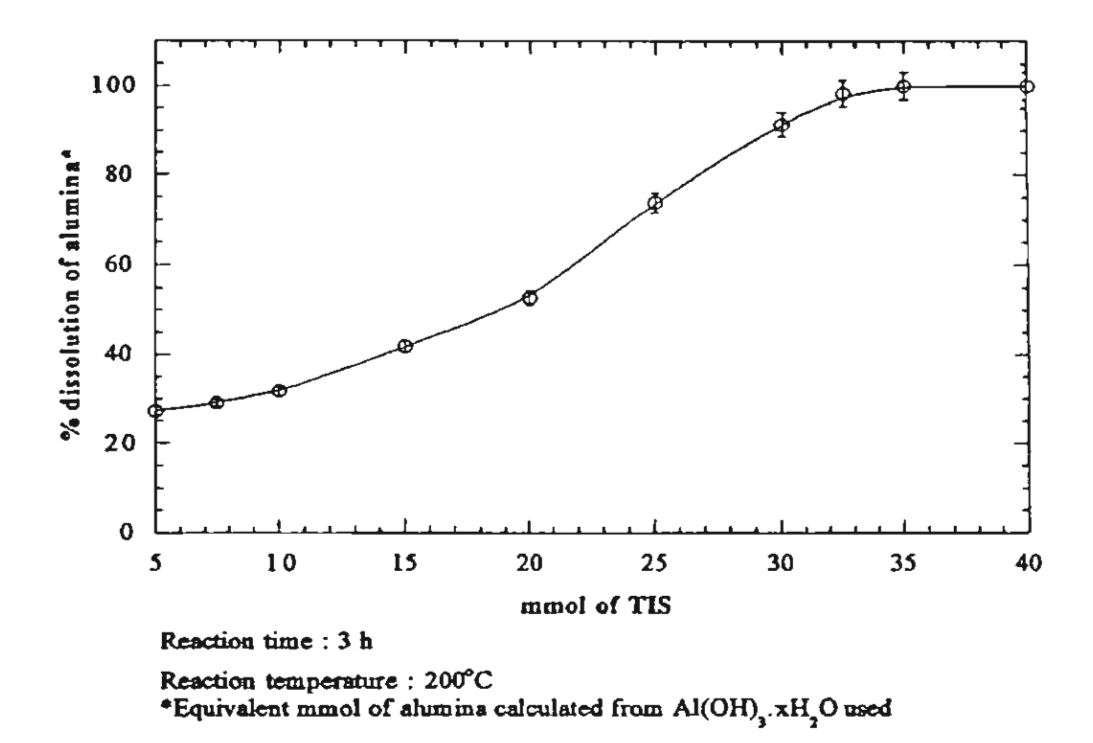


Figure 3.1 Optimization of AI(OH)₃:TIS Ratio for Complete Dissolution of AI(OH)₃.

Dissolution Rate as a Function of Al(OH), Concentration

In this case, determination of a reaction rate, the so-called "method of initial rates", was based upon an accurate analysis of one product at a very early stage of reaction. Therefore, all reactions studied did not proceed to completion. The reaction time and temperature were thus set at 1 h and 200°C. The amount of alumina was varied from 7.5 to 12.5, 15, and 40 mmol while the concentration of TIS was fixed at 20 mmol. The relationship between the dissolved and added alumina is nearly linear, as shown in Figure 3.2. Clearly, the reaction of Al(OH)₃ and TIS also depended on the concentration of Al(OH)₃. The curve was nearly linear, suggesting that the reaction was first order with respect to Al(OH)₃ and first order with respect to TIS. It is worth noticing that the intercept of both curves are not equal to zero. This is because some unreacted Al(OH)₃ was lost during recovery step.

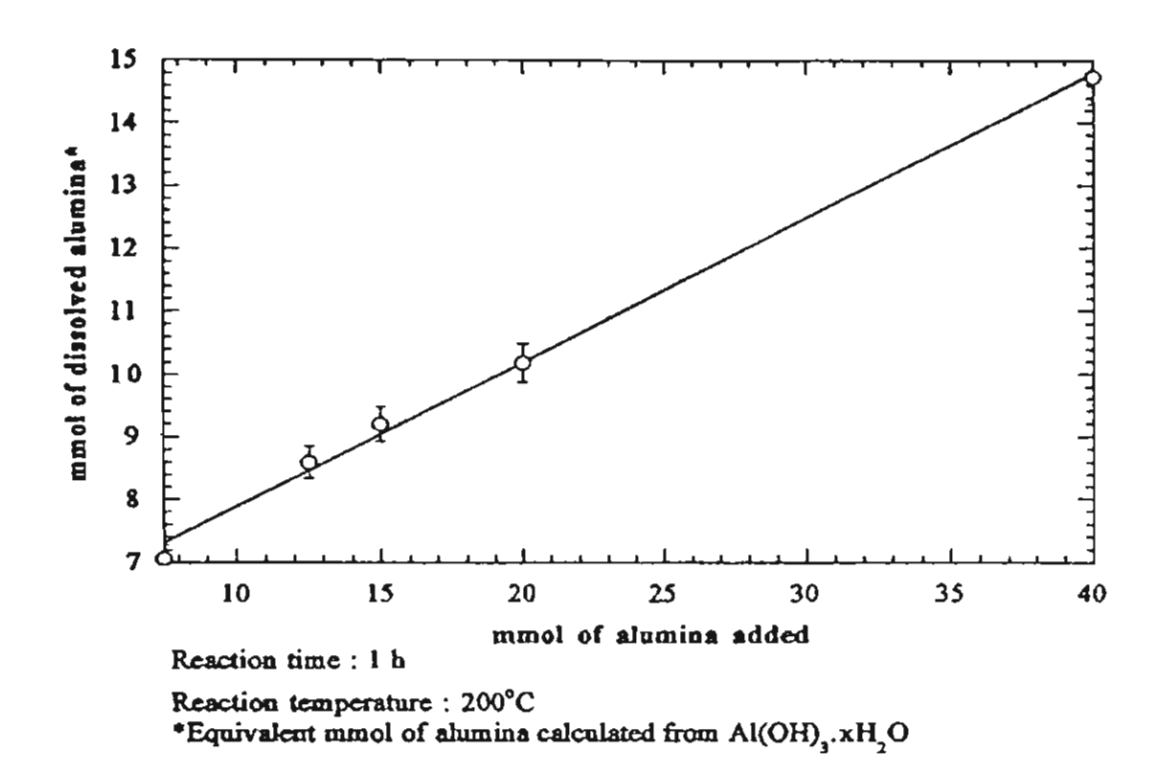


Figure 3.2 Dissolution Rate as a Function of AI(OH)₃ Concentration.

Determination of the Reaction Rate Constant and the activation energy

We used the integral method to determine the reaction order. The reaction order was assumed to be second order overall. Plots of In[(1-rX)/(1-X)] versus reaction time at each temperature are presented in Figure 3.3, (Note:the linearity of the data suggesting that the reaction is most likely to be second order as assumed). The reaction rate constants were obtained from the slope of the plotted data, straight line with different gradients. As expected, the higher temperature showed the higher gradient, meaning that the higher reaction temperature, the higher dissolution rate.

To determine the activation energy, the Arrhenius equation was employed. From section 3.2.3, after obtaining the reaction rate constants (k), In k was plotted versus 1/T(1/Kelvin) as Figure 3.4, which gives a straight line with the slope proportional to the activation energy. The slope obtained is equal to the activation energy devided by the gas constant (8.314 J mol⁻¹ K⁻¹). As a result, the activation energy was 24 ± 2 KJ mol⁻¹.

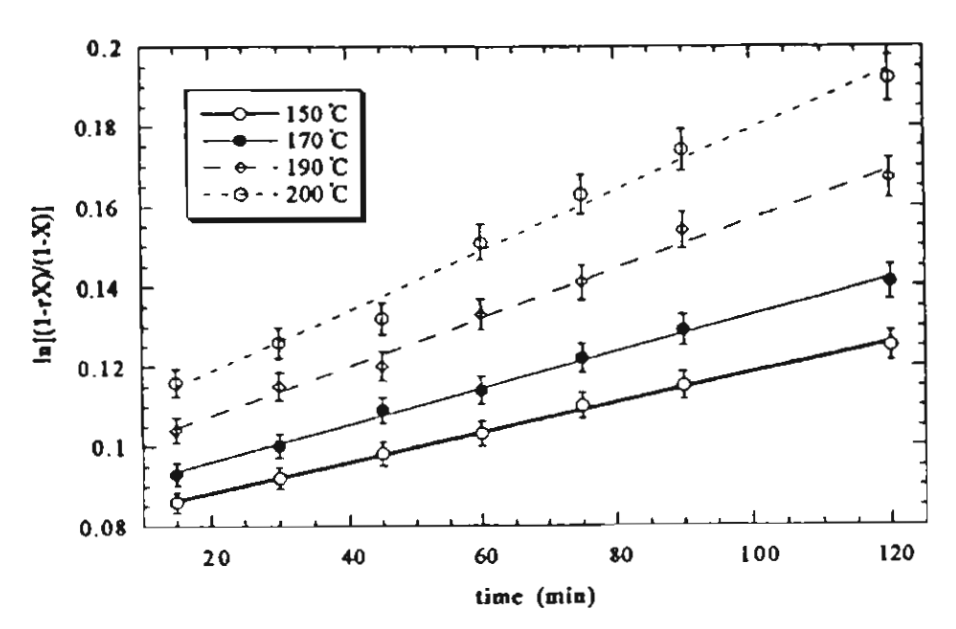


Figure 3.3 The Relationship of Logarithm of Conversion Factor versus Reaction Time for each Variation of Reaction Temperature.

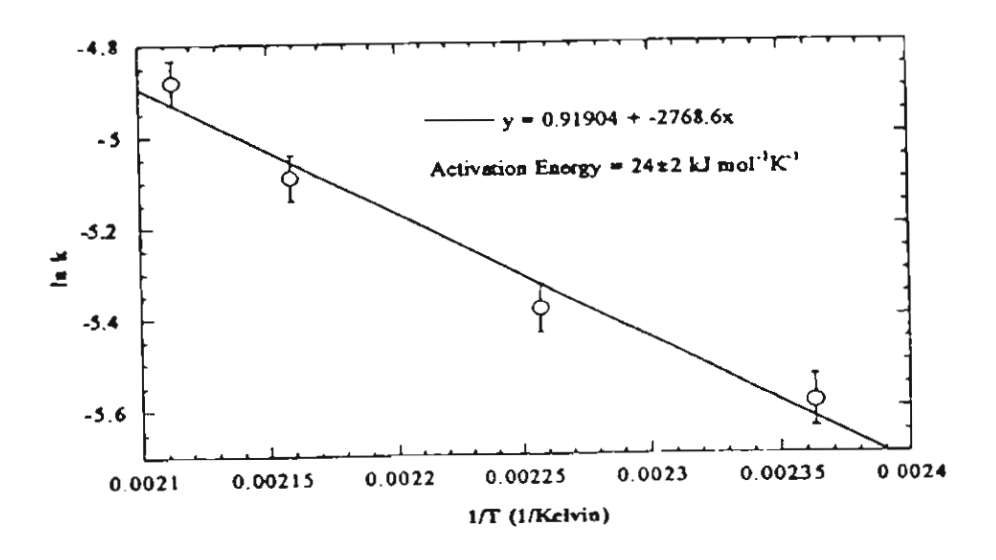
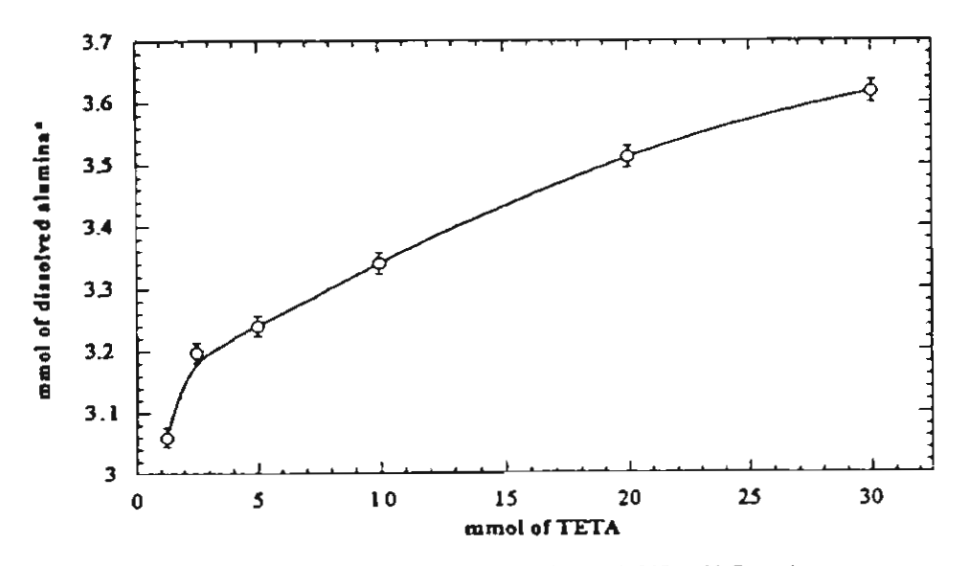


Figure 3.4 The Relationship of Logarithm of Rate Constant and Reaction Temperature.

Dissolution Rate as a Function of TETA Concentration

The plot of the amount of dissoved Al(OH)₃ and amount of TETA is presented in Figure 3.5. The higher the TETA concentration, the greater the amount of dissolved Al(OH)₃. At low TETA concentration (1.25-2.5 mmol), the amount of Al(OH)₃ dissolved increased significantly, as compared to the higher TETA

concentrations. This is due to the role of TETA acting as solubilization catalyst to increase the surface area of Al(OH)₃.

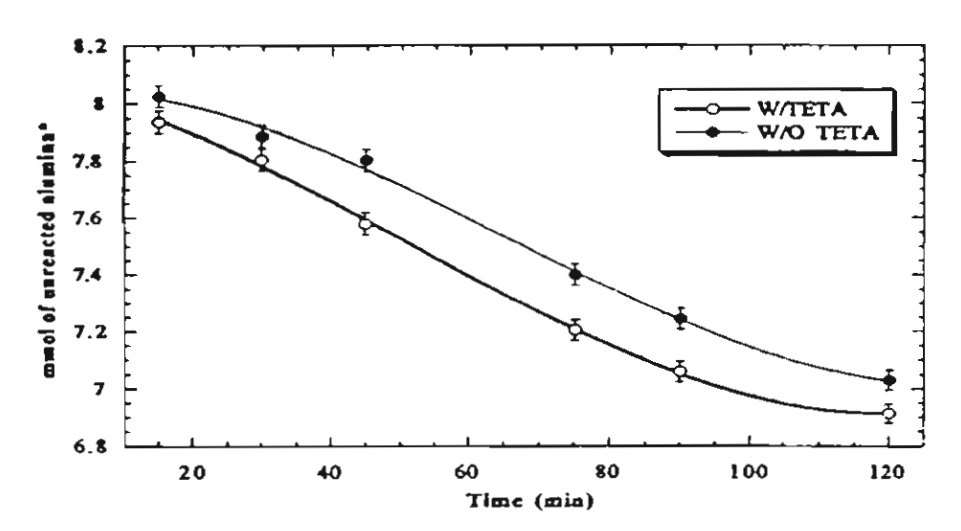


*Equivalent mmol of alumina calculated from Al(OH), xH, O used

Figure 3.5 Effect of the TETA Concentration.

Dissolution Rate as a Function of Time in the Presence of TETA as a Catalyst

Figure 3.6 shows a plot of mmol of unreacted Al(OH)₃ versus reaction time comparing reactions with (1.25 mmol) and without TETA. The dissolution reaction rate with TETA was faster than that without TETA because TETA increased solubility of Al(OH)₃, resulting in increasing its surface area which caused the reaction to go faster, as discussed previously.



*Equivalent mmol of alumina calculated from Al(OH), xH, O used

Figure 3.6 Effect of TETA Concentration with Time.

Characterization

Thermogravimetric Analysis

The TGA data for the product from the reaction without TETA (Figure 3.7 (a)) shows two major regions of mass loss. The first region was between 180°-260°C that indicated the decomposition of TIS which is a component of the product while the second region occurred at about 260°-550°C which corresponded to the oxidative decomposition of the organic ligands and carbon residues. The % ceramic yield of the product was 27.6 %, which was higher than the theoretical ceramic yield (23.7 %) owing to the incomplete combustion of the sample since the final ash was still gray in color.

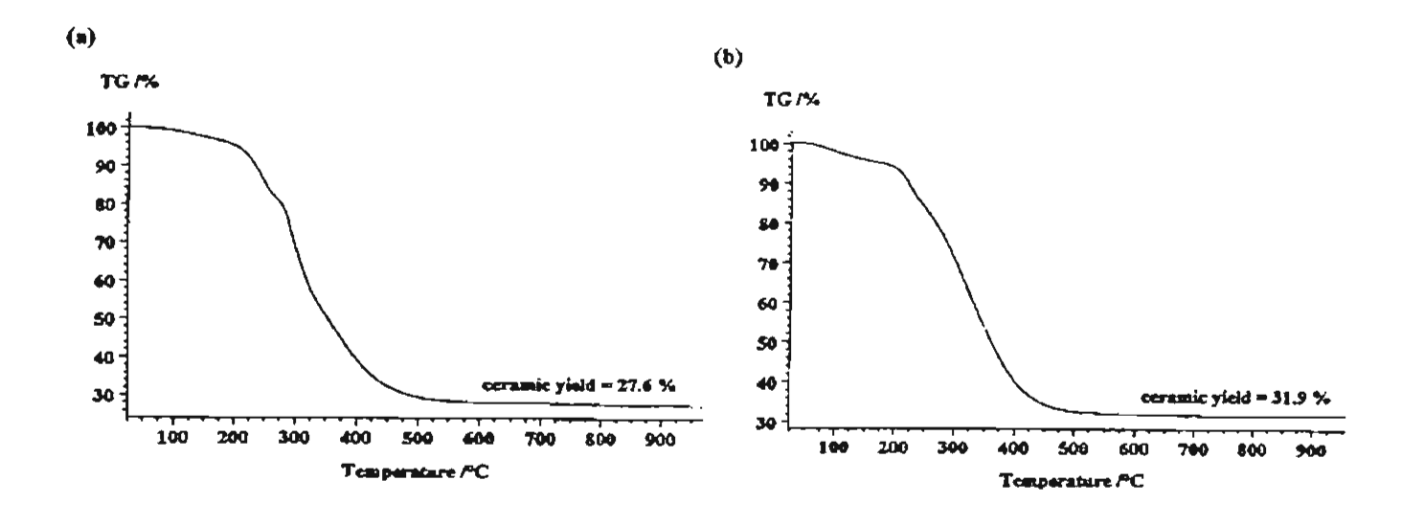


Figure 3.7 TGA Thermogram of the Product from the Reactions: (a) with and (b) without TETA.

Similarly, the TGA of the product synthesized in the presence of TETA (Figure 3.7(b)) also showed two major mass losses at 180°-250°C and 250°-500°C corresponding to the decomposition of TIS ligand and the oxidative decomposition of the organic ligands, and carbon residues, respectively. The % ceramic yield of product was 31.9 %, which was much higher than the theoretical yield. This can be explained along with the mass spectrum which indicated that the product synthesized from the batch with TETA gave more dimer (m/e 431) than the one without TETA because mass spectral data showed that the product consists of monomer, trimer, pentamer, and hexamer. The more smalller unit, the higher ceramic yield. Moreover, the final ash was darker in color.

Differential Scanning Calorimetry

The DSC of the product from the reaction without TETA (Figure 3.8(a)) showed an exotherm at 250°-280°C corresponding to the boiling point of TIS, since when the product was run the second time, there was no exothermic peak in DSC thermogram. An endotherm at 380°-400°C, as

compared to its TGA, correlated to the decomposition temperature of products. The $T_{\rm p}$ was observed at about 167°C.

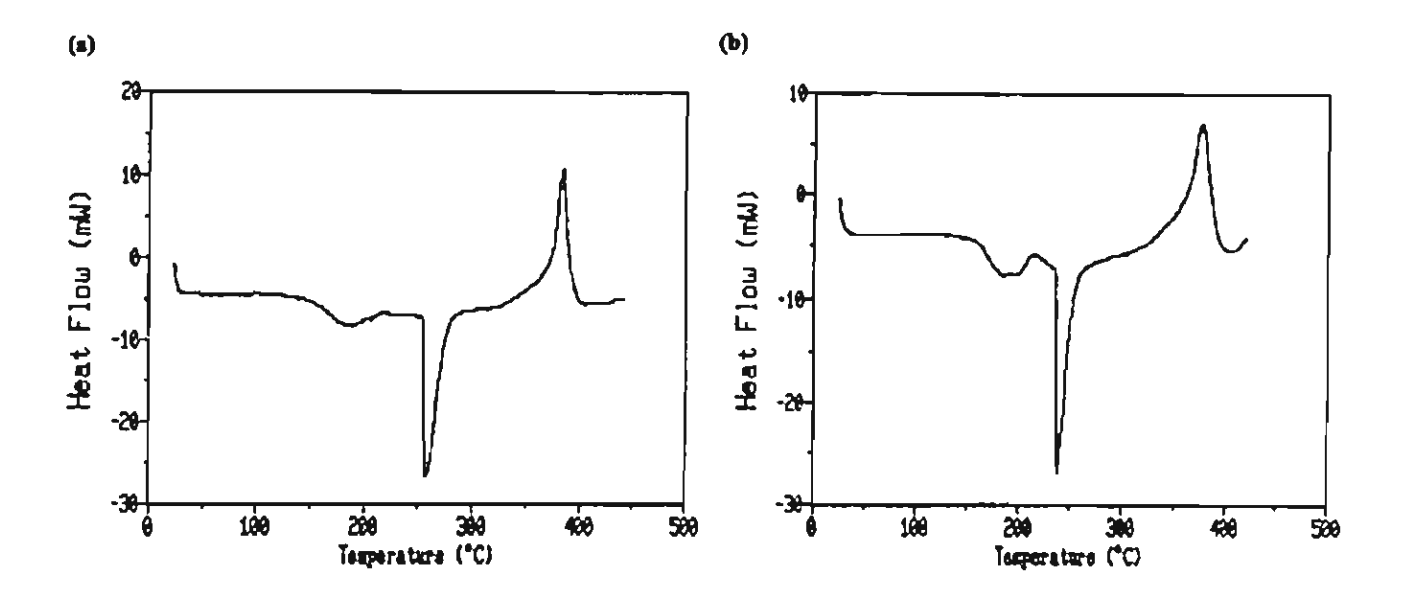


Figure 3.8 DSC Thermograms of the Product from the Reactons (a) with and (b) without TETA.

Similarly, the DSC data of the product from the reaction with TETA (Figure 3.12) showed the exotherm at about 220° - 260° C corresponding to the decomposition of TIS. An endotherm at about 350° - 400° C was again the decomposition temperature of products. The T_g of this product occured at about 166° C

FAB*-Mass Spectroscopy

Mass spectral analysis suggests that there are four different alumatrane complexes; hexamer (m/e 1292), the highest intensity pentamer plus one morpholine (m/e 1250), resulted from losing a molecule of water in TIS, trimer plus one ethylene glycol (m/e 707), and monomer plus one TIS (m/e 409) and the intensities of all proposed structures was shown in table 3.1.

The fragmentation pattern of the product from the reaction with TETA gave higher intensities of the lower unit peaks at m/e 216 and 409, and lower intensity of the peak at m/e 1250. This result can obviously confirm that the reaction carried out without TETA gives the product containing higher molecular weight unit than the one run with TETA owing to the acceleration of TETA resulting in faster completion of the reaction.

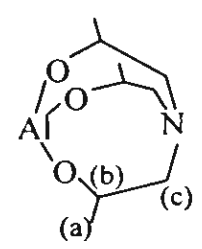
Table 3.1 The Proposed Structures and Fragmentation Pattern of Products

'n

m/e	Intensities	Proposed Structure
216	50	AIN(CH ₂ CH ₃ O) ₃ H ⁺
409	17.5	$\begin{array}{c} O \\ H^{2} \\ O \\ $
492	38.7	Al ₂ [N(CH ₂ CH ₂ CH ₃ O) ₃] ₂ (OCH ₂ CH ₂ O) H ₂ ⁺
707	35.4	AI_O O AI_O O AI O O AI O O O AI O O O O O O O O O
959	7.9	AI ₃ [N(CH ₂ CH ₃ O) ₃] ₂ AI ₂ [N(CH ₂ CH ₃ O) ₂] ₂

1076	15	AI ₅ [N(CH ₂ CH ₂ CH ₃ O) ₃] ₅ H*
1175	46.3	Al-O-Al-O-Al OOH+ OO N N N N N N N N N N N N N N N N N N
1250	100	AI ₂ [N(CH ₂ CH ₂ CH ₃ O) ₃] ₅ N(CH ₂ CH ₂ CH ₃ O) ₂ CH ₂ CH ₂ CH ₃ H
1292	7.8	+HOO AI-O-AI-O-HOO AI-O-O-AI-O-AI +HOO NOOH+ AI ₆ [N(CH ₂ CH ₃ O) ₃] ₆ H'

Nuclear Magnetic Resonance Spectroscopy



The NMR results showed that the products certainly contained several kinds of oligomers, such as monomer, dimer, etc., which are coincided with the mass spectroscopy results. The ¹H-NMR spectrum of the product from the reaction without TETA showed 3 multiple characteristics of quadrapolar coupling peaks indicating the presence of a few species in the product. The peaks at 1.1-1.4 ppm correspond to the -CH₃ group of TIS (position (a)). The peaks at 2.4-3.1 ppm are assigned to the methylene group adjacent to the N-atom of TIS (-N-CH₂) at position (c). The peaks at 3.6-4.2 ppm are assigned to the tertiary carbon adjacent to the O-atom of TIS, position (b). The ¹H-NMR spectrum of the product from the reaction with TETA gave a similar one.

Similarly, the 13 C-NMR spectrum of the product from the reaction without TETA showed a multiple peak at 22.0 ppm corresponding to $^{-}$ CH₃ groups at position (a) coupled to itself and proton of the tertiary carbon. The sharp peak at 64.3 ppm belongs to the carbon adjacent to N-atom of TIS (-N-CH₂) at position (c). The multiple peak at 79.0 ppm is associated with the carbon adjacent to O-atom of TIS (position (b)) due to the coupling with $^{-}$ N-CH₂ and $^{-}$ CH₃. The spectrum of both reactions showed the similar positions.

The ²⁷Al-NMR spectra of the products from the reaction with and without TETA coincidentally showed 3 multiple peaks, as shown in Table 3.2, at around 65, 49 and 7 ppm at the ratio of 1:1:1. Again, these three peaks indicated the presence of both hexa- (at 7 ppm) and tetracoordinated (at 65 and 49 ppm) aluminum compounds.

Fourier Transform Infrared Spectroscopy

The FTIR spectra of the products from the reactions with and without TETA show similar functional groups (Table 3.3). Due to the moisture sensitivity of the products, the \mathbf{V} O-H appears at 3300-3700 cm⁻¹, and the wave number at 2750-3000 cm⁻¹ corresponds to \mathbf{V} C-H. The single peak at about 1650 cm⁻¹ is O-H overtone and C-H bending. The strong peak at 1000-1250 cm⁻¹ results from the \mathbf{V} C-N and/or O-H bending. The broad peak at 500-800 cm⁻¹ represents the \mathbf{V} Al-O of the product.

Table 3.2 Peak Positions of ¹H-, ¹³C-, and ²⁷Al-NMR of Products

Compounds	¹ H-NMR (ppm)	¹³ C-NMR (ppm)	²⁷ Al-NMR (ppm)	
Product w/o TETA	1.07-1.41 (a)	21.59-22.45 (a)	7.5	
	2.36-3.15 (c)	64.30 (c)	49.6	
	3.65-4.23 (b)	78.56-79.21	66.0	
Product w/ TETA	1.07-1.88 (a)	20.79 (a)	7.4	
	2.23-2.85 (c)	64.30-65.63 (c)	48.8	
	3.73-4.11 (b)	78.79-79.48 (b)	64.9	

Table 3.3 Peak Position and Assignments of FTIR Spectra of Products with/without TETA

peak positions	assignments		
AI-TIS	TIS-AI-TETA		
3000-3700	3000-3700	u O-H and u C-H	
2750-3000	2750-3000	u C-H	
1650	1630	O-H overtone;	
		C-H bending	
1450	1450	δ с-н	
1000-1200	1000-1250	u C-N; O-H bending	
500-800	500-800	u Al-O	

CONCLUSIONS

In this work, alumatrane complexes were synthesized directly from inexpensive starting material, aluminum hydroxide, and TIS, via the one step process, called "OOPS" process. Mass spectra revealed that products were oligomers. The main product was pentamer bonded with TIS that lost one H₂O molecule. From TGA data, the % ceramic yields of the product from the reactions without and with TETA were 27.6 and 31.9 %, respectively, which are higher value than the theoretical yield (23.7%). The higher percent ceramic yields were due to the small unit of oligomers in the product and the small amount of unreacted Al(OH)₃ remaining in the product.

The reaction order was second order overall, first order with respect to aluminum hydroxide and first order with respect to TIS. The dissolution rate increased when the reaction temperature increased. The activation energy of this reaction was about 24 ± 2 KJ mol⁻¹.

REFERENCES

- 1. Voronkov, M. G., Seltschan, G. I., Lapsina, A. and Pestunovitsch, V. A., Z. Chem., 1968, 8.
- 2. Voronkov, M. G., Vestnik Akad. Nauk SSSR, 1968, 38, 48
- 3. Voronkov, M. G. and Zelchan, G. I., Khim. geterotsikl. soed., 1965, 51.
- 4. Bradley, D. C., Mehrotra, R. C., Gaur, D. P., Metal Alkoxides; Academic Press: N. Y., 1978, 266.
- 5. Pinkas J., Verkade G., *Inorg. Chem.*, 1993:32:2711.
- 6. Hein, F. and Albert, P. W. Z., Anorg. Allg. Chem., 1952, 269, 67.
- 7. Mehrontra, R. C. and Mehrotra, R. K., J. Indian Chem. Soc., 1962, 39, 677.
- 8. Mehrotra and Rai, A. K., Polyhedron, 1991, 10, 1967.
- Shklover, V. E., Struchkov, Yu. T., Voronkov, M. G., Ovchinnikova, Z. A. and Baryshok, V. P., Dokl. Akas. Nauk (Engl. Transl), 1984, 227, 723.
- 10. Voronkov, M.G., Baryshok, V.P., Organomet. Chem., 1982:239:199.
- Thomas, W. M., Groszos, S. J and Day, N. E., U.S. Patent 2, 1961, 985, 685; Chem. Abstr., 1961, 55, 20966.
- 12. Icken, J. M. and Jahren, E. J., Belg. Patent 619, 1963, 940; Chem. Abstr., 1963, 60, 2768.
- 13. Stanley, R. H., British Patent 1, 1968, 123,559; Chem. Abstr., 1968, 69, 78532.
- Elbing, I. N. and Finestone, A. B., German offen 1., 1964, 1,162,439; Chem. Abstr., 1964, 60, 17/4705.
- 15. Higashi, H. and Namikawa, S., Kogyo Kagaku Zasshi, 1967, 70,97.
- 16. Verkade, J. K., Acc. Chem. Res., 1993, 26, 483.
- 17. Blohowiak, K., Tradewell, D., Mueller, R., Hoppe, M., Jouppi, S., Kansal, P., Chew, K.W., Scotto, C., Babonneau, F., Kampf, J. and Laine, R.M., *Chem. Mater.*, 1994:6:2177-92
- 18. Ray, D. G., Laine, R. M., Robinson, T. R., Viney, C., Mol. Crys. Liq. Crystal, 1992, 225,153.
- 19. Laobuthee, A., Wongkasemjit, S., Traversa, E. and Laine, R., J. Eur. Cer. Soc., 2000, 20,185-191.

CHAPTER IV SOL-GEL PROCESSING OF SILATRANES

ABSTRACT

Silatrane complexes are organositicon compounds synthesized by direct reaction of SiO₂ and trialkanolamines. Here, we explore their potential as ceramic precursors via the hydrolytic sol-gel processing method. Viscoelastic analysis is used to characterize the gelation behavior of silatranes based on triisopropanolamine, under different hydrolysis conditions. Pyrolysed ceramic products are characterized in terms of surface area and morphology and found to have a homogeneous microporous structure with high surface areas (313-417 m²/g). Faster hydrolysis rates lead to shorter gelation times, and smaller pore sizes in the derived ceramic.

INTRODUCTION

Organosilicate polymers are of interest for their potential as precursors in sol-gel processing to form complex preceramic shapes and structures, not readily accessible by melt processing ¹⁻². Due to widespread availability and low cost, silica, (SiO₂) is the ideal starting material to make organosilicon polymers. However, the Si-O bond is very strong and difficult to manipulate chemically³. As a corollary, organosilicate polymers, once formed, are very easy to hydrolyze back to SiO₂. Such high reactivity can create problems in chemical processing, therefore it is advantageous to be able to create precursors with reduced hydrolytic activity.

Silatrane complexes are a family of organosilicate compounds derived from reaction of SiO₂ with trialkanolamines such as triethanolamine or triisopropanolamine⁴⁻⁶. These materials are hydrolytically stable in air for periods up to several weeks. For this reason, they are candidates for use as precursors in ceramic processing via the sol-gel technique. Here, we report some preliminary viscoelastic studies of sol-gel processing of silatranes under different hydrolysis conditions, and investigate the characteristics of glasses formed by pyrolysis of the products.

EXPERIMENTAL

Synthesis of Silatrane Complex

Materials

Fumed silica (surface area 280 m²/g, average particle size of 0.007 μ m) was purchased from Aldrich Chemical Company, and dried in an oven at 90 °C for 10 hr. Ethylene glycol, purchased from Labscan, was used as reaction solvent, and purified by fractional distillation at 200 °C under N₂ atmosphere. Triisopropanolamine [TIS, N(CH₂CHCH₃OH)₃] was obtained from Fluka Chemical Company, and dried in a desiccator. Commercial grade triethylenetetramine [TETA,

H₂NCH₂(CH₂NHCH₂)₂ CH₂NH₂], supplied by Union Carbide Thailand, Limited, was purified by vacuum distillation at 120 °C (1mm Hg).

Anhydrous diethyl ether and dichloromethane, used as precipitants, were purchased from Baker Analytical Co. Dichloromethane was distilled over anhydrous calcium chloride under N₂ atmosphere. Anhydrous diethyl ether was dried by adding anhydrous calcium chloride, let stand for 24 hr with occasional shaking, and then filtered into a clean dry bottle. HPLC grade tetrahydrofuran, used as solvent for molecular weight determination by gel permeation chromatography, was purchased from J. T. Baker Inc., and used as received.

Reaction conditions

As discovered by Piboonchaisit⁶, silatrane complexes were formed by mixing fumed silica with TIS (and TETA as catalyst) in ethylene glycol (EG) as solvent. The reaction temperature was set at the distillation point of EG (200 °C). Water formed during the reaction, and EG were continuously removed and replaced by an equivalent amount of fresh EG distillate. After reaction, the residual EG was removed by vacuum distillation (1 mm Hg). Based on GPC analysis described below, four distinct chemical species may be formed during the reaction, with proposed structures shown in Fig. 4.1, whose relative abundance depends on the molar ratio of TIS:SiO₂, the amount of TETA catalyst present, the temperature at which the vacuum distillation of EG is carried out, and on the duration of this distillation procedure. Of the four structures shown, that with molecular weight 407 is particularly undesirable, because the silicon content is low, and hence the % ceramic yield is poor, which makes the product unsuitable as a ceramic precursor. The optimal reaction condition, at which minimal formation of this species occurs, was found to be at a 1: 1 molar ratio of TIS:SiO₂, (with TETA in the amount of 5 mol% of silica⁶). As the vacuum distillation temperature increases, the amount of high molecular weight species increases up to 180 °C, after which it decreases again, as shown in Fig. 4.2. The optimum temperature for high ceramic yield is therefore 180 °C.

(a)
$$O = Si = OH$$

(b) $O = Si = OH$

(a) $O = Si = OH$

(b) $O = Si = OH$

(c) $O = Si = OH$

(d) $O = Si = OH$

(e) $O = Si = OH$

(in) $O = Si$

Figure 4.1 The proposed structures of silatrane complexes using 1:1 ratio of [TIS]: [SiO₂].

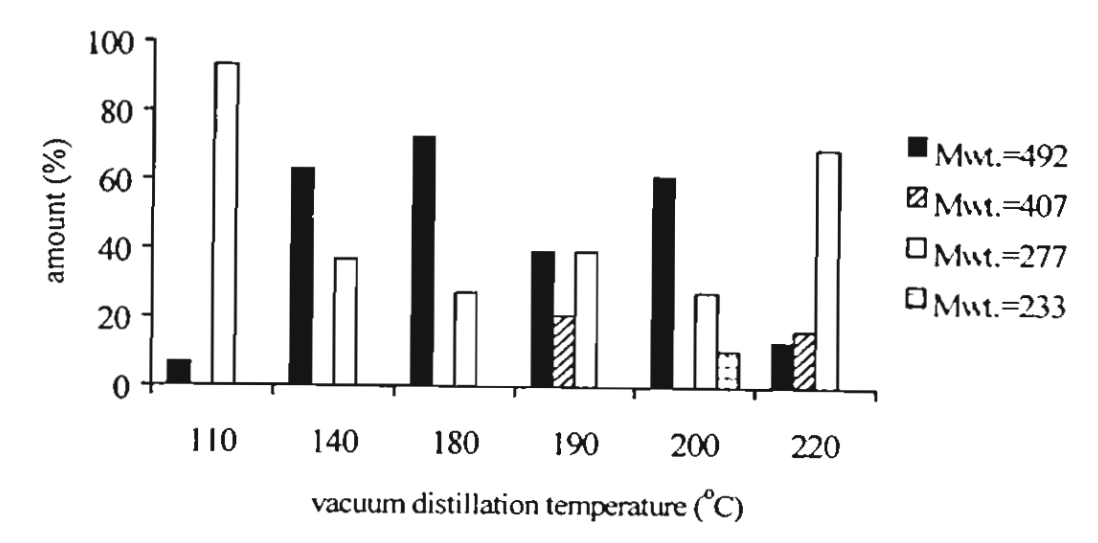


Figure 4.2 Silatrane complexes obtained at 1:1 [TIS]:[SiO₂] and various vacuum distillation temperature.

Characterisation of Silatrane Complexes

FTIR Spectroscopy

FTIR spectroscopic analysis was performed using a Bruker instrument with a resolution of 4 cm⁻¹. Powdered specimens containing 1.0% sample mixed with 99% crystalline KBr were compressed into pellets. The pellets were placed in the sample chamber purged with N₂ for 20 minutes to remove CO₂.

NMR Spectroscopy

¹³C and ¹H NMR spectra of silatrane complexes were obtained using a 500MHz JEOL spectrometer. Samples were dissolved in deuterated DMSO. Tetramethylsilane was used as the internal reference for both proton and carbon NMR.

Gel Permeation Chromatography

GPC chromatograms were performed using a Waters 600E Instrument equipped with UV and RI detectors (Waters 486 and 410, respectively). The column used was Styragel of pore size suitable to separate molecular weights in the range 0 to 1,000. Calibration was performed using polystyrene standards of narrow molecular weight distribution. THF was the solvent at ambient temperature. The silatrane samples were dissolved in THF at concentration below 0.3% weight, and filtered through 0.45 μ m membrane filters prior to GPC analysis.

Rheological determination of the sol-gel transition

The transformation from a sol to a gel can be monitored rheologically by following the change in viscoelastic properties. The silatrane reaction product, after removal of residual ethylene glycol, has the appearance of a hard plastic, and was used without further punfication. The material was dissolved in the hydrolysis solvent at a concentration of 150% w/v. The hydrolysis temperature was selected to be 40 °C, 50 °C, or 60 °C. The solution was stirred until homogeneous and preheated in a water bath at

the hydrolysis temperature, until the solution was viscous enough to be transferred to the meometer. The cone and plate attachment of the meometer was pre-heated to the hydrolysis temperature. The gelation time was determined from the point during pre-heating at which the solution reached the hydrolysis temperature in the water bath. Measurements of storage $(G'(\omega))$ and loss $(G''(\omega))$ moduli were made in a Rheometrics ARES rheometer with a 10g-cm transducer, in cone and plate geometry (cone radius 50 mm, cone angle 0.04 radians). Measurement of $G'(\omega)$ and $G''(\omega)$ was performed at 10 frequencies ω ranging from 0.1 to 1.6 rad/sec. Each frequency scan required 10 sec.

The precise location of the gel point as determined from viscoelastic measurements has been discussed in the previous literature⁷. Initially, the material in the sol state is a viscous fluid such that $\tan\delta=G''(\omega)/G'(\omega)>>1$. As gelation proceeds, G' and G'' increase and, ultimately, the material becomes an elastic gel, $\tan\delta<<1$. Frequently, it is assumed that the gel point occurs at the location of the crossover of the loss (G'') and storage (G') moduli (i.e. where $\tan\delta=1$). However, experimentally, this crossover point is often found to depend on the deformation frequency, ω . A more definitive analysis is now possible following more recent experimental and theoretical work⁷⁻⁸. At the gel point, power-law behavior is observed in the frequency dependence of dynamic mechanical experiments. Specifically, the storage and loss moduli follow the relationships⁷⁻⁸:

$$G'(\omega) = G''(\omega)/\tan(n\pi/2) = \Gamma(1-n)\cos(n\pi/2)S\omega^{n}$$
 (4.1)

where Γ (1-n) refers to the gamma function of argument (1-n). The phase angle δ between stress and strain is independent of frequency and proportional to the relaxation exponent, n:

$$\delta = n\pi/2 \tag{4.2}$$

A variety of experimental studies have been reported $^{7, 9-12}$, which support the validity of this viscoelastic definition of the gel point, including both chemically and physically cross-linked systems. Experimental values of the relaxation exponent n vary from $n \cong 0.2$ to $n \cong 0.8$. For certain chemically cross-linked systems, n depends on stoichiometry. Theoretical predictions, which support various values of the dynamical exponent, n, have been reported $^{7, 13-14}$. Physically, the power law dependence of the moduli originates in the fact that the gel point occurs when the first sample-spanning gel cluster forms. Hence, the magnitude of the dynamical exponent is determined by the structure and hydrodynamic properties of the critical cluster. The power-law behavior originates in the fact that the structure of the critical gel has a fractal character 14 .

Characterisation of Pyrolysis Products

1

BET Surface Area Measurement

The surface area of pyrolysed polysilatrane gels was determined using an Autosorb-1 Gas Sorption System (Quantachrome Corporation) via the Brunauer-Emmett-Teller (BET) method. A

gaseous mixture of nitrogen and helium was allowed to flow through the analyser at a constant rate of 30 cc/min. Nitrogen was used to calibrate the analyser, and was also used as the adsorbate at liquid nitrogen temperature. Each sample was degassed at 300 °C for 2 hr before analysis. The surface area was obtained from a five-point isotherm at P/P_o ratio less than 0.3. The results were computed based on the desorption surface area and the dried weight of the sample after analysis.

Scanning Electron Microscopy

SEM micrographs were obtained using a JEOL 5200-2AE(MP 15152001) scanning electron microscope. Samples were prepared for SEM analysis by attachment to Aluminum stubs, after pyrolysis at 800 °C. Prior to analysis, the specimens were dried in a vacuum oven at 70 °C for 5 hr, and then coated with gold by vapor deposition. Micrographs of the pyrolysed sample surfaces were obtained at 2,000 and 7,500 magnification.

RESULTS AND DISCUSSION

Structural Characterisation of Silatrane Complex

Silatrane complexes produced by the synthetic method described above are a mixture of four molecular species, based on GPC analysis. Proposed structures of each species are shown in Fig. 4.1. Evidence for the formation of silatrane complexes includes observation of characteristic absorption bands in FTIR analysis (Table 4.1) and resonance frequencies in ¹³C and ¹H NMR spectroscopy (Table 4.2).

Table 4.1 Assignments of infrared spectra of the products.

Characterization	Silatrane Complexes
Si-N stretching ^a	560-590 cm ⁻¹
Si-O-CH ^b	970,883 cm ⁻¹
C-Oª	1013-1070 cm ⁻¹
Si-O-CH ₂ ^b	1015-1085 cm ⁻¹
C-N ^a	1270 cm ⁻¹
C-H bending ^a	1380-1460 cm ⁻¹
C-H stretching ^a	2800-29760 cm ⁻¹

a: Silverstein et al. 1991.

b: Anderson D.R., 1974.

Table 4.2 H-and ¹³C-NMR chemical shifts of silatrane complexes

Position	Groups	¹ H-NMR (ppm)	¹³ C-NMR (ppm)	
(a)	N-CH ₂	2.86-2.91	57.7	
(p)	CH-C <u>H</u> ₃	4.0	23	
(c)	CH-CH ₃	0.96-1.12	20-21	
(d)	CH₂-O	3.3	59.2	
(e)	C <u>H</u> ₂-OH	3.4-3.5	62.5-65	

Rheological analysis of Sol-Gel transition of Silatranes

Silatrane complex formed after vacuum distillation of ethylene glycol was dissolved in one of three hydrolysis solvents at a concentration of 150 % w/v. The hydrolysis solvents were: distilled deionized water with measured pH = 6.7; MgO solution prepared by dissolving 0.5 g MgO in 1 liter distilled de-ionized water with measured pH = 11.3; and a solution of methanol in distilled de-ionized water at a ratio 1:1 (pH = 8.1). The change in G' and G" was observed following procedures described above. In Fig. 4.3, we show frequency scans of G' and G" during hydrolysis in water at 40 °C at three times, viz. before the gel point, at the gel point, and after the gel point. The location of the gel point was identified following the discussion of Chambon and Winter⁷, summarized above in equations (4.1) and (4.2), as the point where G' and G" follow the same power law with exponent n, i.e. a frequencyindependent $\tan \delta$. As evident in Fig. 4, this occurs at gel time t = 15600 s \pm 1100 s, when n ~ 1.0 and $\tan \delta \sim 1.0$. The corresponding variation of $\tan \delta$, the apparent frequency exponents of G' and G'', and the change in magnitude of the dynamic viscosity, $\eta^*(\omega)$, during hydrolysis are shown in Figs. 4.4, 4.5. and 4.6, respectively. As evident in Figs. 4.4 and 4.5, there is considerable uncertainty (~± 7%) in deciding the location of the gel point based on the frequency-independence of $tan\delta$, and, therefore, a corresponding uncertainty in the precise values of the dynamic exponent $n = 0.55 \pm 0.15$. Fig. 4.6 confirms that, as expected, the dynamic viscosity increases dramatically at the gel point and, after gelation, exhibits a strong dependence on deformation frequency.

Hydrolysis experiments were carried out at three temperatures, and the gel times determined are tabulated in Table 4.3. At each temperature, as illustrated by Roy and McCarthy¹⁵⁻¹⁶, the shortest gel times are observed in the most ionic MgO solvent, where the hydrolysis rate is fastest, and the longest gel times are in the least ionic MeOH solvent, which has the slowest hydrolysis rate. Also increase of temperature increases the rate of hydrolysis and thus decreases the gel times.

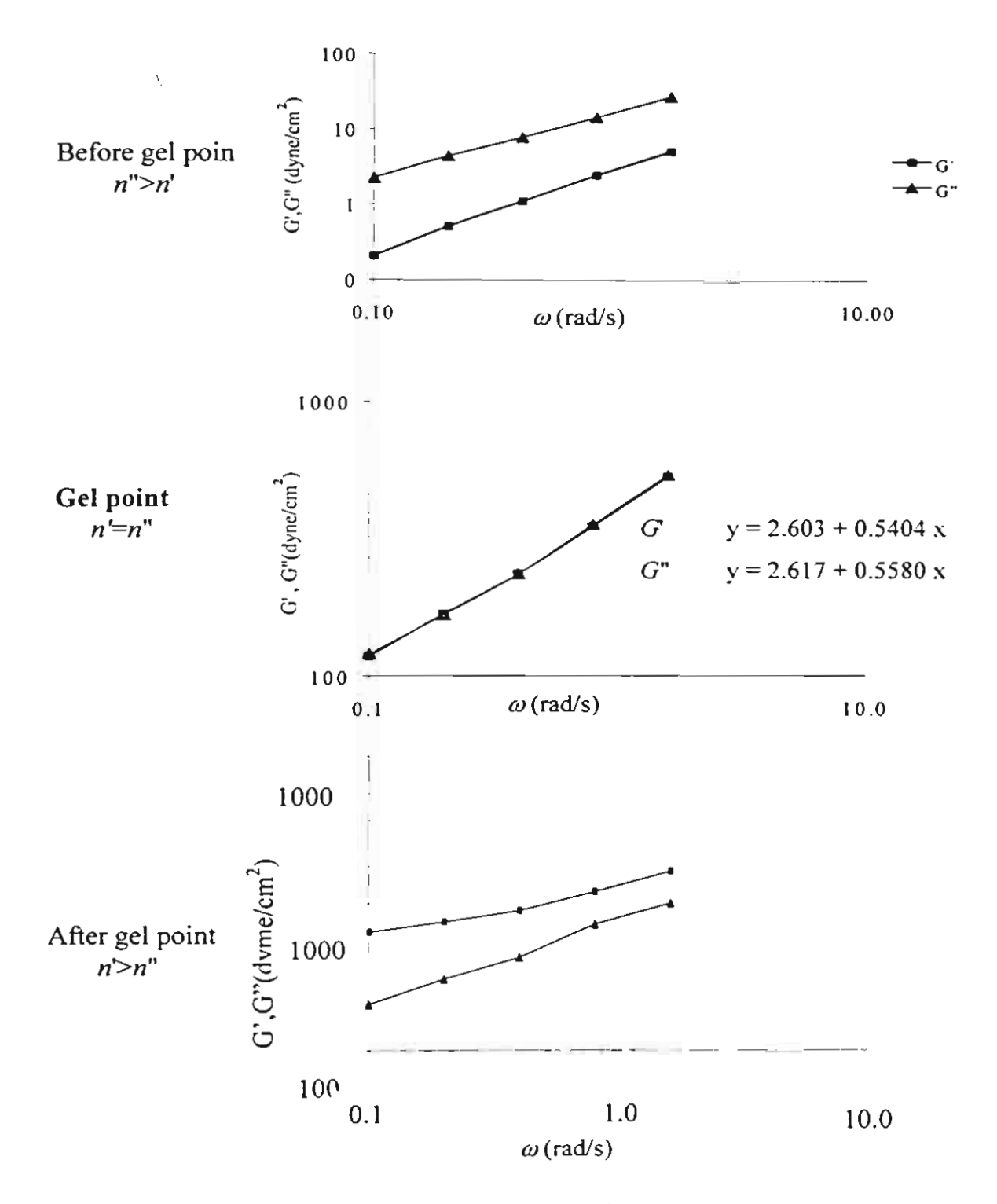


Figure 4.3 The relationship of log G' and log G'' vs. log frequency of 150% w/v silatrane complex hydrolyzed in water at T = 40°C.

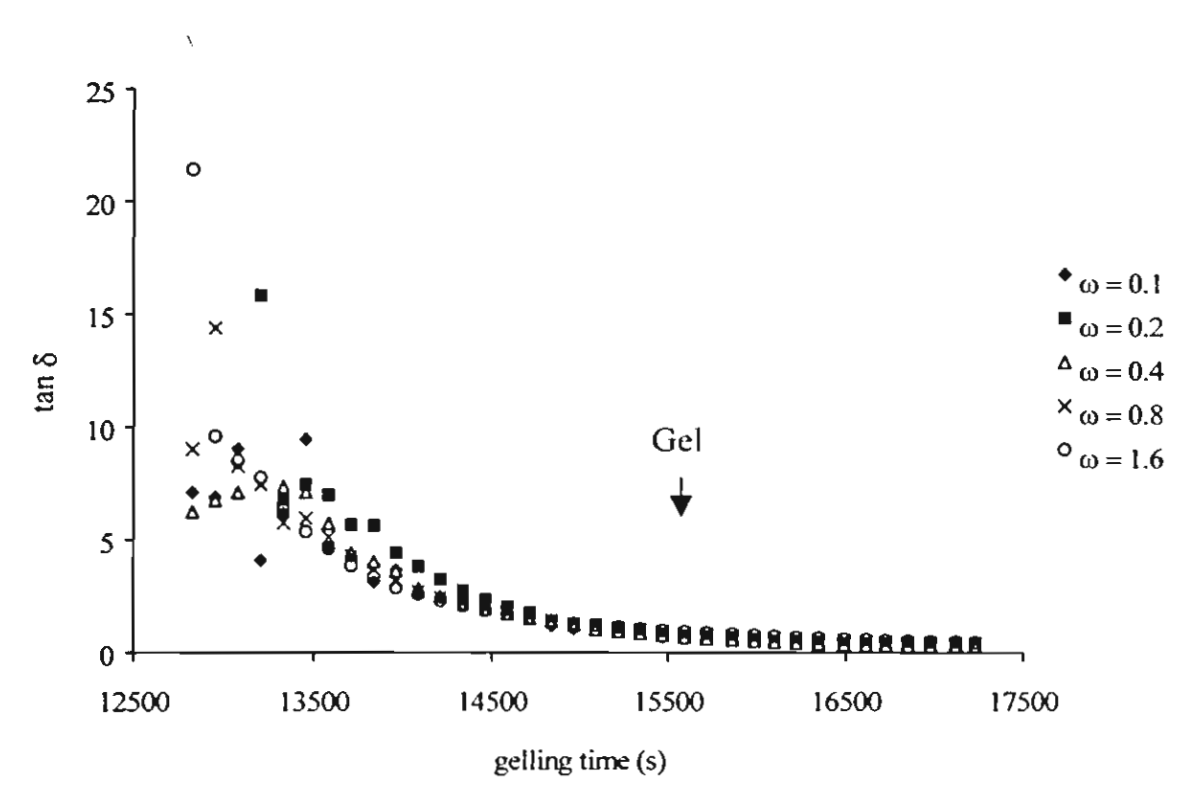


Figure 4.4 Multi-frequency plot of $\tan\delta$ vs. gelling time of 150% w/v silatrane complex hydrolyzed in water at T = 40°C.

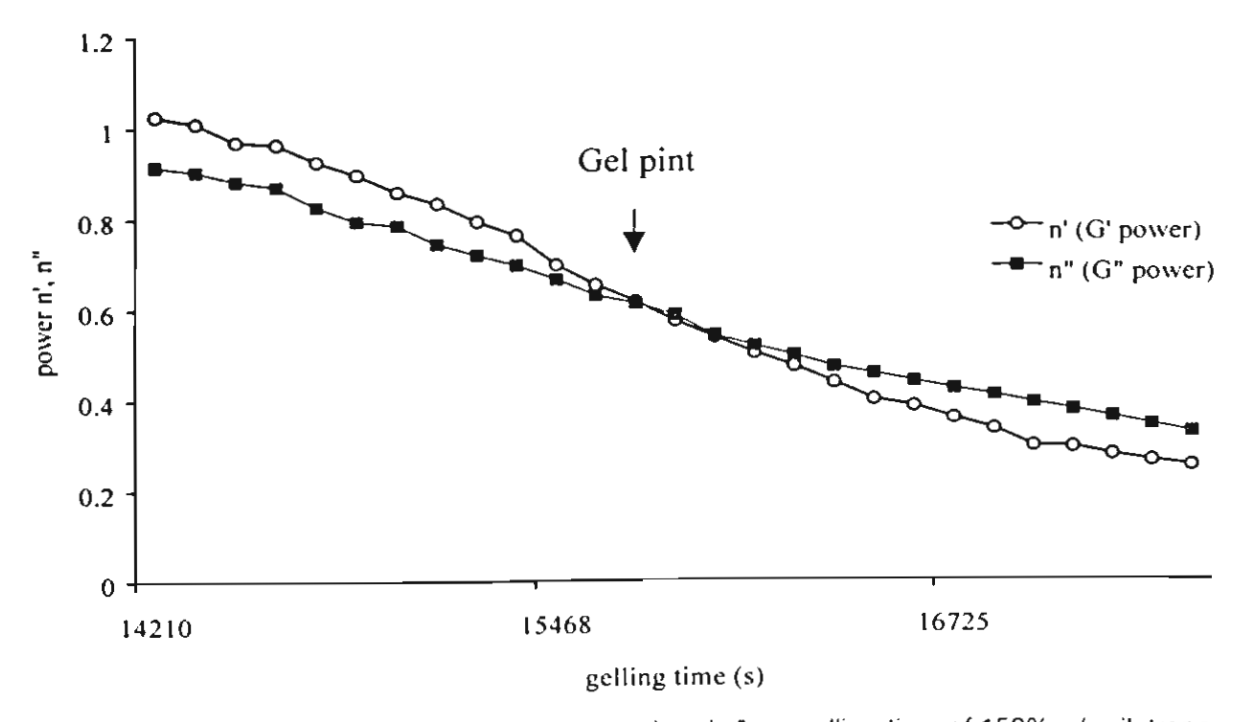


Figure 4.5 The plot of power-law exponent n' and n' vs. gelling time of 150% w/v silatrane complex hydrolyzed in water at $T = 40^{\circ}C$.

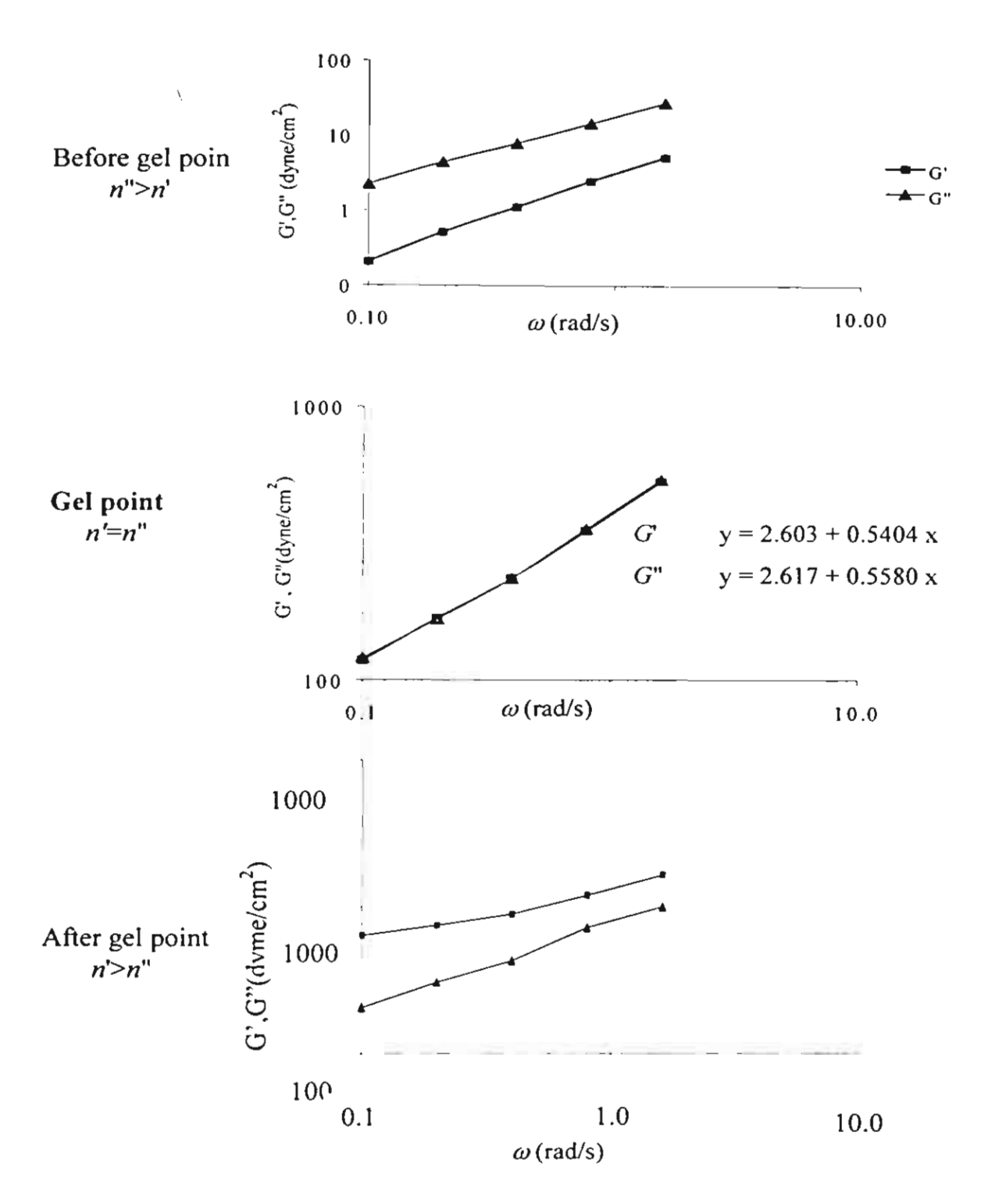


Figure 4.3 The relationship of log G' and log G'' vs. log frequency of 150% w/v silatrane complex hydrolyzed in water at $T = 40^{\circ}C$.

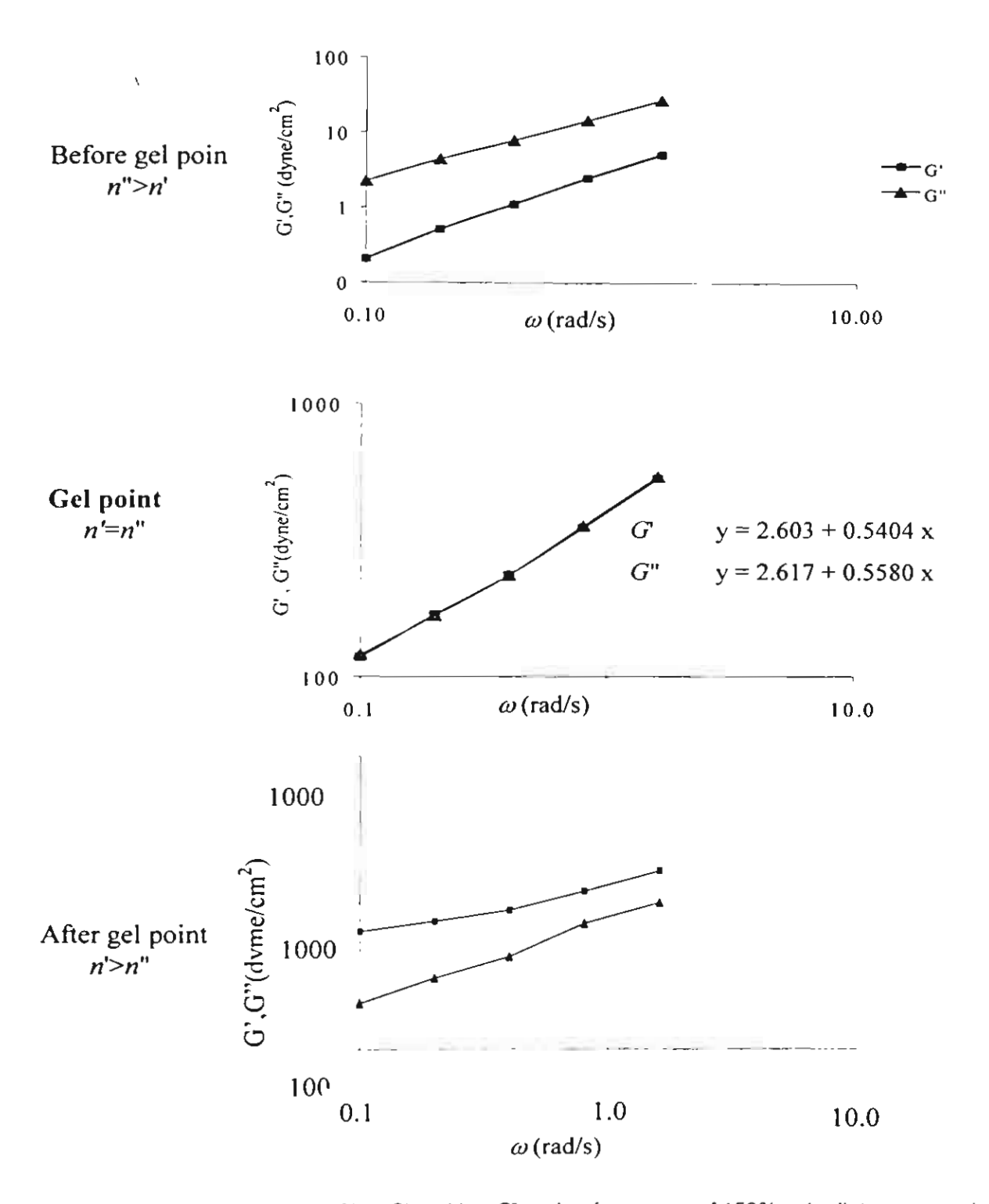


Figure 4.3 The relationship of log G' and log G'' vs. log frequency of 150% w/v silatrane complex hydrolyzed in water at T = 40°C.

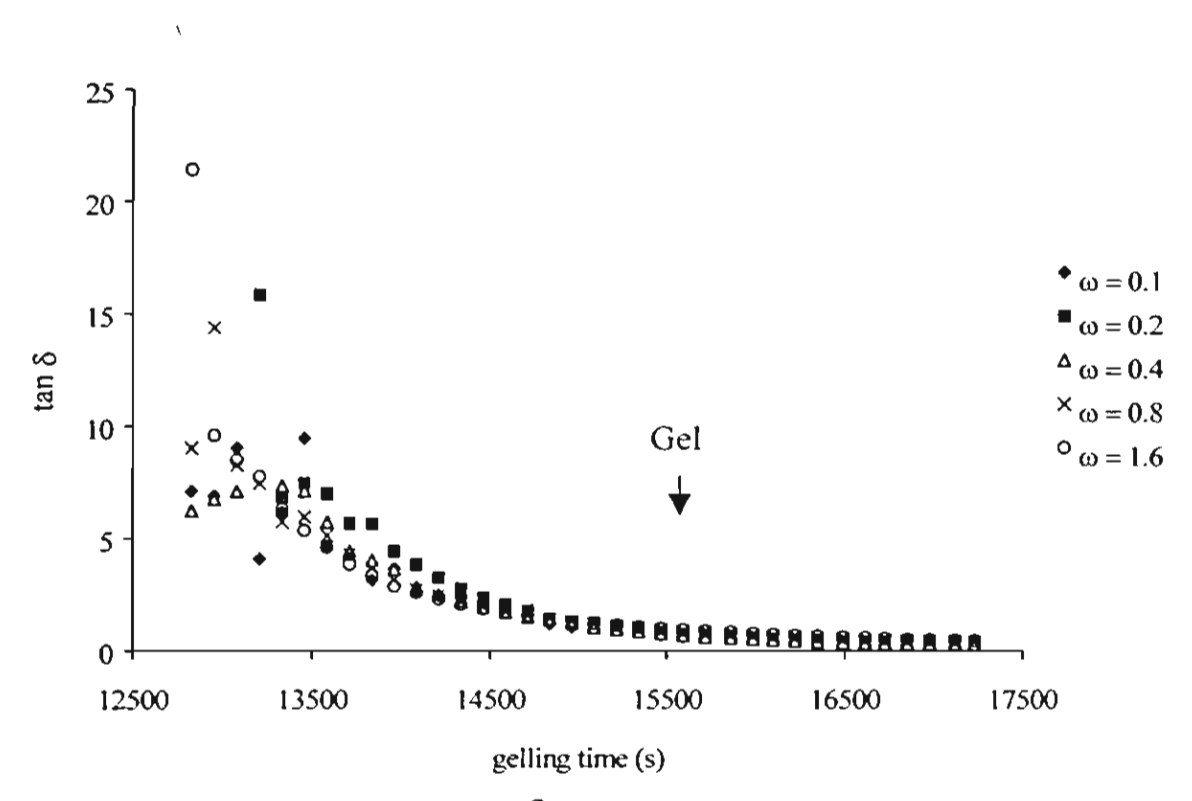


Figure 4.4 Multi-frequency plot of $\tan\delta$ vs. gelling time of 150% w/v silatrane complex hydrolyzed in water at T = 40° C.

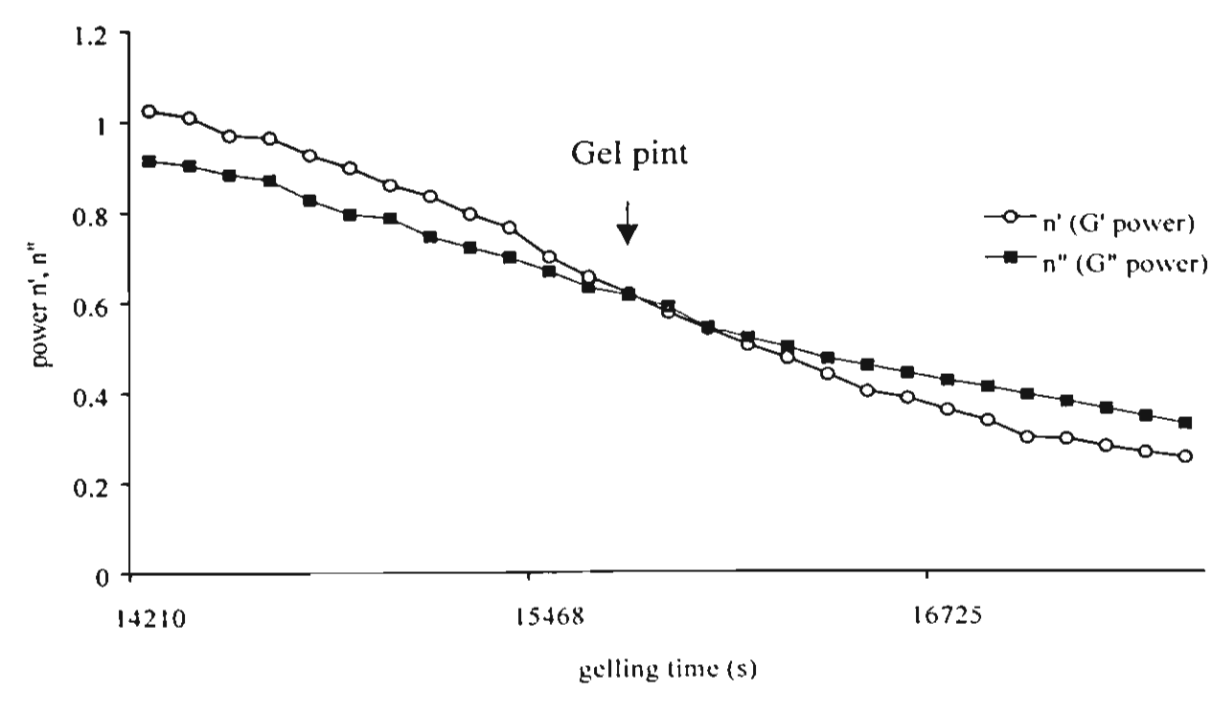


Figure 4.5 The plot of power-law exponent n' and n' vs. gelling time of 150% w/v silatrane complex hydrolyzed in water at $T = 40^{\circ}C$.

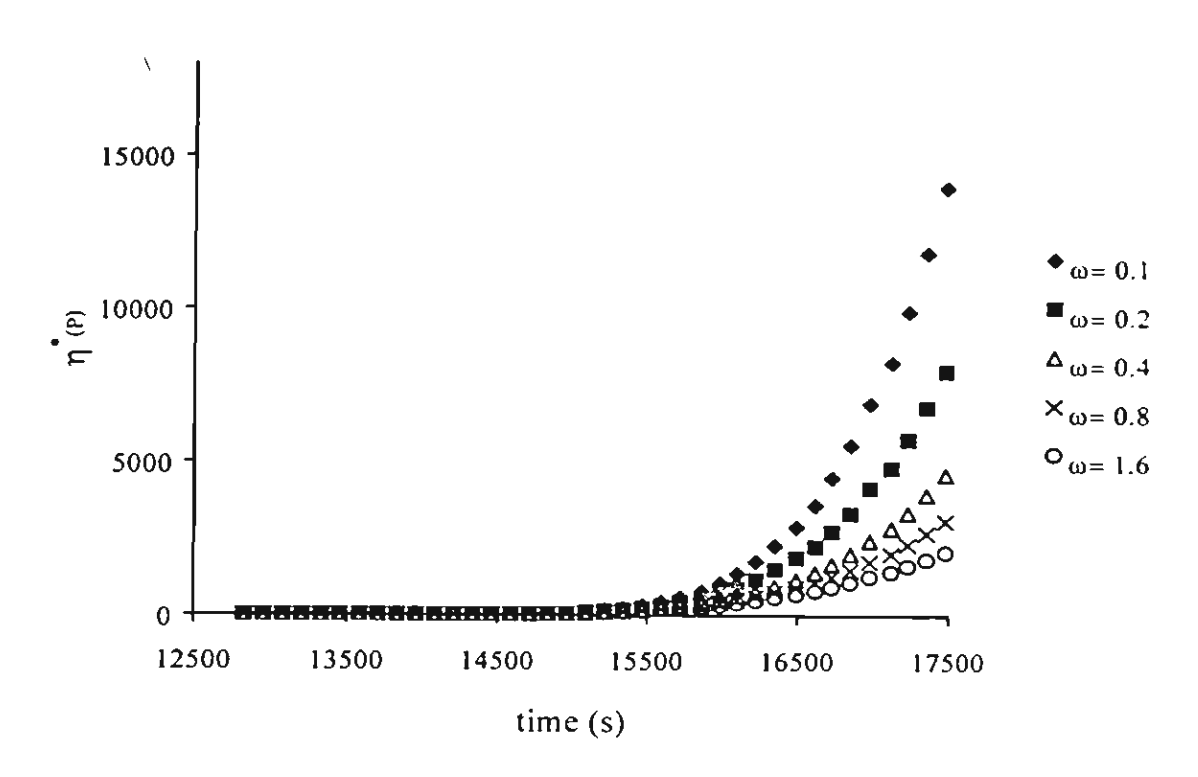


Figure 4.6 Complex viscosity (η^*) at different frequency plotted vs. gelling time of 150% w/v silatrane complex hydrolyzed in water at T = 40°C.

 Table 4.3
 Viscoelastic properties at the sol-gel transition of polysilatrane.

Solvent	Temperature(°C)	Gelling time(s)	$ an \delta$	п
MgO + H ₂ O	60	4500	1.31	0.55
H ₂ O	60	6620	1.62	0.75
MeOH + H ₂ O	60	8260	1.20	0.61
MgO + H ₂ O	50	8950	3.02	0.85
H ₂ O	50	9350	2.24	0.79
MeOH + H ₂ O	50	9560	0.98	0.49
MgO + H₂O	40	14567	1.20	0.62
H ₂ O	40	16200	1.06	0.53
MeOH + H₂O	40	18892	1.42	0.67

Characterization of pyrolyzed ceramics

Polysilatrane gels produced via hydrolysis in the three solvents at 40 °C were pyrolyzed at various temperatures in the range 200 °C to 800 °C. FTIR spectra are shown in Fig. 4.7 and indicate increasing conversion to silica, with increasing temperature such that at 800 °C, essentially pure SiO₂ is

obtained. Thus pure ceramic product can be generated in high yield, using processing temperatures as low as 800 °C. The surface areas of ceramics produced by pyrolysis at 800 °C of gels formed in each of the hydrolysis solvents at 40 °C were determined by the BET method. The results are listed in Table 4.4, and indicate a trend of decreasing surface area with decreasing gel times. At high rates of gelation, it is likely that smaller gel particles are formed, which might lead to smaller pore sizes, and hence higher surface areas in the pyrolysed products. In Fig. 4.8, we show SEM micrographs, taken at a magnification of x7500, of the surfaces of the three pyrolyzed ceramics together with that of the furned silica starting material. Clearly, sol-gel processing via formation of silatrane complexes has converted the silica from a granular porous solid into a homogeneous microporous glass, with a corresponding increase in surface area from 280 m²/g to ~ 410 m²/g. From the micrographs, there appears to be a tendency towards smaller pore sizes with shorter gel times. In particular the ceramic from the MgO hydrolysis solvent has the most finely divided morphology, but shows evidence of contamination by small amounts of precipitated MgO on the surface.

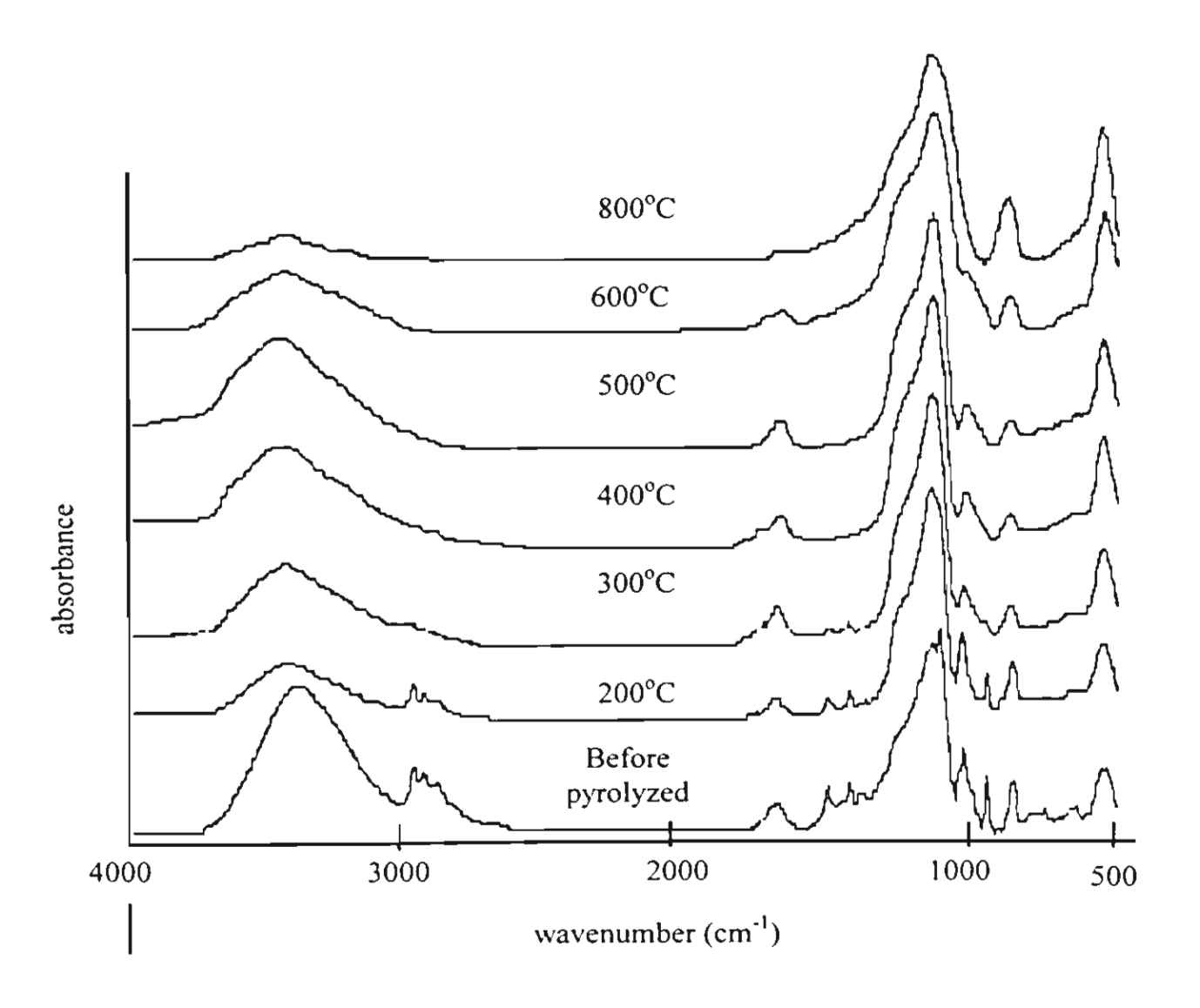


Figure 4.7 FTIR spectra of the pyrolyzed polysilatrane gel at different temperatures.

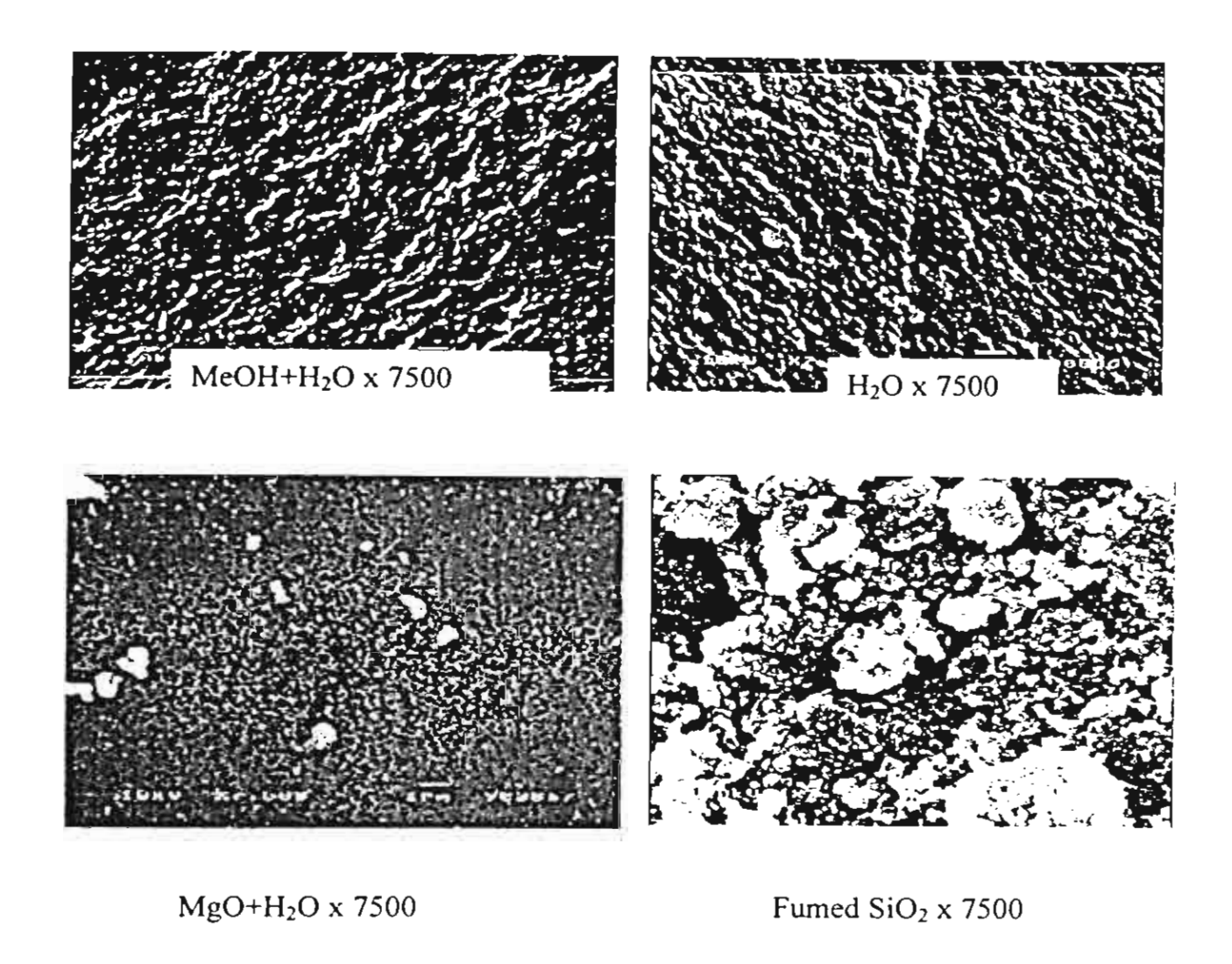


Figure 4.8 SEM micrographs of pyrolyzed polysilatrane hydrolyzed with various solvents, at 800°C, and heating rate of 10°C/min as compared with fumed SiO₂ with magnification of 7500.

Table 4.4 Surface area of polysilatrane gel pyrolyzed at 800°C

Gel	Surface area (m²/g)		
Hydrolyzed MgO+ H ₂ O	417		
Hydrolyzed H₂O	401		
Hydrolyzed MeOH+H ₂ O	313		
Pyrolyzed start from 500°C	414		
Pyrolyzed start from room temp.	388		

CONCLUSIONS

1

The optimal reaction mixture for silatrane synthesis is one with equimilar amounts of TIS and SiO_2 in the presence of 5 mol% of silica. The optimum vacuum distillation temperature is 180 °C. After 12 hours under these conditions, most of the solvent is removed, and the monomer (M = 277) is largely converted to the dimer with M = 492. Gelation of the silatrane complex formed under these conditions is achieved by hydrolysis under ionic conditions. Pyrolysis of the gels at 800 °C produces a homogeneous microporous glass. Glass formed under more ionic conditions (MgO/H₂O) has the smallest pores and largest surface area, but suffers from contamination by precipitated MgO.

RRFERENCES

- Saegusa, T. and Chujo, Y., "Organic Polymer Hybridgs with Silica Gel Formed by Means of the Sol-Gel Method", Advance Polymer Science 1992, 100, 11.
- 2. Varshneya, A., Fundamentals of Inorganic Glassmaking 1994, Boston: Academic Press.
- 3. Iler, R., The Chemistry of Silica 1979, NewYork: John Wiley & Sons.
- 4. Hencsei, P. and Parkanyi, L., "The Molecular Structure of Silatranes", *Review Silicon, Germenium, Tin Lead Compound* 1985, 8(2), 191.
- Bickmore, C., Hoppe, M. and Laine, R., "Processable Oligomeric and Polymeric Precursors to Silicate Prepared Directly from SiO₂, Ethylene Glycol and Base", *Material Research Society* Symposia Processing 1992, 249, 81.
- Piboonchaisit, P., Wongkasemjit, S. and Laine, R., "A Novel Route to Tris(silatranyloxy-i-propyl)amine Directly from Silica and Triisopropanolamine". ScienceAsia, J.Sci.Soc. Thailand 1999, 25, 113.
- 7. Winter, H. and Chambon, F., "Analysis of linear viscoelasticity of a crosslinking polymer at the gel point", *J. Rheol.* 1986, *30*, 367.
- 8. Muthukumar, M. and Winter, H., "Fractal dimension of a crosslinking polymer at the gel point", *Macromolecules* 1986, *19*, 1284.
- Hodgson, D., Qun, Y. and Amis, E., "Dynamic viscoelasticity during thermoreversible gelatin gelation", J. Non-Crst. Solids 1991, 131-133, 913.
- 10. Muller, R., Gerard, E., Dugand, P., Rempp, P. and Gnanou, Y., "Rheological characterization of the gel point: A new interpretation", *Macromolecules* 1991, *21*, 532.
- Izuka, A., Winter, H. and Hashimoto, T., "Molecular weight dependence of viscoelasticity of polycaprolactone critical gels", *Macromolecules* 1992, 25, 2422.
- Hsu, S. and Jamieson, A., "Viscoelastic Behavior at the Thermal Sol-Gel Transition of Gelatin", *Polymer* 1993, 34, 2601.
- 13. Lin, Y., Mallin, D., Chien, J. and Winter, H., "Dynamic mechanical measurement of crystallization-induced gelation in thermoplastic elastomeric poly(propylene)", *Macromolecules* 1991, 24, 850.

- 14. Muthukuma, M., "Screening effect on viscoelasticity near the gel point", *Macromolecules* 1989, 22, 4656.
- 15. Roy, R., "Gel route to homogeneous glass preparation", J. Amer. Cer. Soc. 1969, 344.
- 16. McCarthy, G. and Roy, R., "Gel route to homogeneous glass preparation II, Gelling and desiccation", J. Amer. Cer. Soc. 1971, 639.

CHAPTER V SOL_GEL PROCESSING OF ALUMATRANE

ABSTRACT

Alumina gels were prepared by the sol-gel method using alumatrane or tris (alumatranyloxy-i-propyl)amine as precursor. Alumatrane are aminoalkoxide derivatives of aluminium synthesized directly from the reaction of inexpensive and readily available compounds, aluminium hydroxide and triisopropanolamine, via the one step process. Sol-gel process parameters, such as gelation time, were correlated to variables of the initial stage of the process, such as pH, temperature of hydrolysis and water/alkoxide ratio. The sol-gel transition of alcoholic alumatrane solutions was monitored by multiple waveform rheological measurements. The gelation time could be determined from the evolution of the storage (G') and loss (G'') moduli versus time at different frequencies using the Winter Chambon criterion (convergence of the loss tangents at the gel point). Increasing pH values, hydrolysis ratio and/or temperature accelerates the kinetics of hydrolysis-condensation reactions and thus reduced the gelation time. The gelation times at various temperatures were used to calculate apparent activation energy of the cross-linking leading to the gelation, which was found to be approximately 139 kJ mol¹¹ and independent of hydrolysis ratio. Alumina materials prepared from the heat treatment of obtained gel at 500°C were analyzed using X-ray diffraction and the BET method.

INTRODUCTION

Alumina materials have a wide range of applications in a great number of industrial areas, particularly in catalysis, membrane separation processes, catalytic membrane reactors, adsorbent, composite, coating, fiber, electronic and optic fields. Alumina prepared by sol-gel process is frequently used in such areas. In the development of soft chemistry, the sol-gel process is considered to be the most practical method for the synthesis of inorganic oxides. This process usually involves the hydrolysis and condensation of various metal alkoxide molecules under controlled conditions to form metal-oxygen-metal bridging units. In many cases the metal alkoxide precursors are very sensitive to water and therefore cannot be controlled the hydrolysis reaction. Generally, the aluminium alkoxides, such as aluminium secbutoxide and aluminium isopropoxide, are used to prepare alumina by sol-gel method. However, these commercial precursors are expensive and aluminium secbutoxide can be rapidly hydrolyzed to give the hydrolyzed products dispersed in 2-butanot. Development of applications in a great number of industrial areas.

Alumatrane is aminoalkoxide derivatives of aluminium synthesized directly from the reaction of inexpensive and readily available compounds, aluminium hydroxide and triisopropanolamine, via the one step process. It containing trialkanoamine ligands is hydrolytically stable, thus yielding more controllably chemistry and minimizing special handling requirement. Therefore it should be used as precursors in ceramics processing by sol-gel route. In this work, we investigate the dynamic viscoelastic properties and FTIR studies on sol-gel process of alumatrane under different conditions. This observation is mainly focused on the influence of pH, hydrolysis ratio and temperature on the crosslinking process. In addition, some preliminary thermal studies of an alumina obtained by the sol-gel technique were also observed.

EXPERIMENTAL

Preparation and Heat Treatment of Alumina Gels

Alumatrane or tris(alumatranyloxy-i-propyl)amine was used as an alumina source or the precursor of the sol-gel derived system under investigation with various pH values, temperature and hydrolysis ratio. The preparation of alumatrane has already been reported in a previous paper. To begin with it was dissolved in dried methanol for a period of time. The mixture was checked using FT-IR spectroscopy and TGA in order to confirm the absence of alcohol interchange reactions. Then water was added together with catalyst, except in case of pH = 9 where no catalyst was added. For acid conditions, pH = 3 and pH = 5, HNO₃ was used and for neutral condition, pH = 7, HNO₃ was also used to adjust pH value of alcoholic alumatrane solution (pH = 9). To attain basic conditions, pH = 10 and 11, NH₄OH was added. Two hydrolysis ratios of 9 and 27 and six pH values ranging from 3 to 11 were investigated while the mole ratio of methanol to [AI] was kept equal to 60. The solution was mixed with a vigorous stirring at the range of temperature varied from 20°C to 36°C.

Alumina powders were produced by heat treatment the resulting gels at various pH values in a furnace at 500°C and held at the final temperature for 7 hours.

Measurements

Sol-gel process

Rheological characterizations

The rheological measurements, which were performed to determine sol-gel transition and dynamic viscoelastic properties, were carried out using a Rheometric Scientific Inc. (Model ARES) with a cone-plate configuration covered with the humidity chamber. The humidity chamber filled with methanol to obtain a saturated atmosphere was used to prevent evaporation of solvent during measurement. The dimensions corresponding to the geometry were 25 mm for the diameter and 0.04° for the angle. The

minimum distance between plate and truncated cone was 0.051 mm. The temperature control was achieved with a thermostated-circulating bath. The sample was stirred until homogeneous and loaded in the rheometer. The time for loading the sample was kept to a minimum so as to reduce the solvent evaporation. The experimental conditions (applied strain amplitude and frequency sweep range) were fixed after preliminary experiments. The amplitude was fixed within the linear viscoelastic range. The multiwave experiments were run with eight frequencies ranging from 0.2 to 1.6 rad s⁻¹ and the strains (γ) were kept at 3% at each harmonic. A narrow frequency range was employed because their properties change markedly with time. In addition, no intersection of the tan δ curves at a certain point identified as gel point was observed at higher frequencies.

Although the time requested for G' and G" to be equal is designated as the gel point by some authors $^{19-20}$, a more accurate investigation of the gel point has been given by Winter and co-workers as the point where $\tan \delta$ (=G"/G') is independent of frequency. The gel point can be precisely identified and located by the study of the evolution of G' and G" as a function of the frequency at various reaction times near the gel point. This criterion was firstly proposed for chemical gels but has also been applied to physical gels. For such systems the linear viscoelastic behavior at gel point is described by the *gel* equation.

$$\tau(t) = S \int_{-\infty}^{\infty} (t - t')^{-n} \dot{\gamma}(t') dt'; \ 0 < n < 1$$
 (5.1)

where τ is the stress tensor, $\dot{\gamma}$ is the rate of deformation tensor, S is the strength of the network at the gel point depending on the flexibility of molecular chains and crosslinks, and on the crosslink density. The value of relaxation exponent, n, varies over about the entire possible range between 0 and 1 indicating a strongly elastic gel (n=0) or a more viscous gel (n=1). The dynamic mechanical behavior at the gel point is given by a power law relation between moduli (G' and G'') and the angular frequency (ω)

$$G'(\omega) \sim G''(\omega) \sim \omega^{n}$$
 (5.2)

i.e., storage (G') and loss moduli (G") are parallel in a log-log plot. Consequently the loss angle (δ) is independent of frequency at the gel point but proportional to the relaxation exponent:

$$\delta_c = n\pi/2$$
 or $\tan \delta_c = G^*/G' = \tan(n\delta/2)$ (5.3)

Therefore the gel point can be conveniently determined by the evolution of $\tan\delta$ at different frequencies as a function of reaction time. The various curves intersect at one critical point, at which $\tan\delta$ becomes independent of frequency. The time at which this occurs is the gel time. ²⁵

In very recent years, some studies have also been used to determine the gel time based on a modification of self-similarity method. It is useful for systems exhibiting no intersection of the curves, but is also applicable to systems whose curves coincide at a specific point. The gel point is associated with the

occurrence of statistical loss factor self-similarity. In this way, the gel time is obtained by the minimum of the curve log (s/(tan δ)) as a function of reaction time where s is the standard deviation of tan δ in a frequency sweep. ²⁶

FT-IR spectroscopic characterizations

The hydrolysis and condensation of alumatrane as a function of the reaction time were followed using Fourier-transform IR spectroscopy. An FT-IR spectrophotometer (Nicolet, NEXUS 670) with 16 scans at a resolution of 4 cm⁻¹ was used in this study.

Characterization of pyrolyzed gels

Alumina supports obtained from annealing the gel at 500°C were characterized using BET method and X-ray diffraction techniques. BET surface area and pore size distribution were measured using nitrogen at 77 K in Autosorb-1 gas sorption system (Quantasorb JR.). Samples were degassed at 200°C under a reduced pressure prior to each measurement. The structure of the phases in the samples, annealed at various temperatures, was obtained at room temperature by using X-ray powder diffraction. XRD spectra were recorded on D/MAX 2000 series (Rigaku Co.) using Cu K α radiation (λ =0.154 nm).

RESULTS AND DISCUSSION

Sol-gel process

Gelation times and dynamic viscoelastic properties by rheological measurements

The evolution of gelation process with time was investigated in eight different frequencies ranging from 0.2 to 1.6 rad s⁻¹. Figures 5.1a and 5.1b show measured values of loss G" and storage G' moduli, respectively, as a function of reaction time for the system with pH = 7 and h = 9 at 25°C. In the initial part of the reaction, G" is greater than G', which is a characteristic feature of liquids. With continuing gelation reaction, both the moduli increased with time. However, G' rises more sharply than G" indicating a gradual formation of gel network with a predominantly elastic character. In Figure 5.1c the complex dynamic viscosity (η *) was plotted as a function of time at different frequencies. The viscosity increases as the gelation grows, because more work must be done to produce flow of the sol. In addition, the complex dynamic viscosity η increased as frequency decreased. These observations are more significant when reaction time increased indicating an evolution from liquid-like to solid-like state.

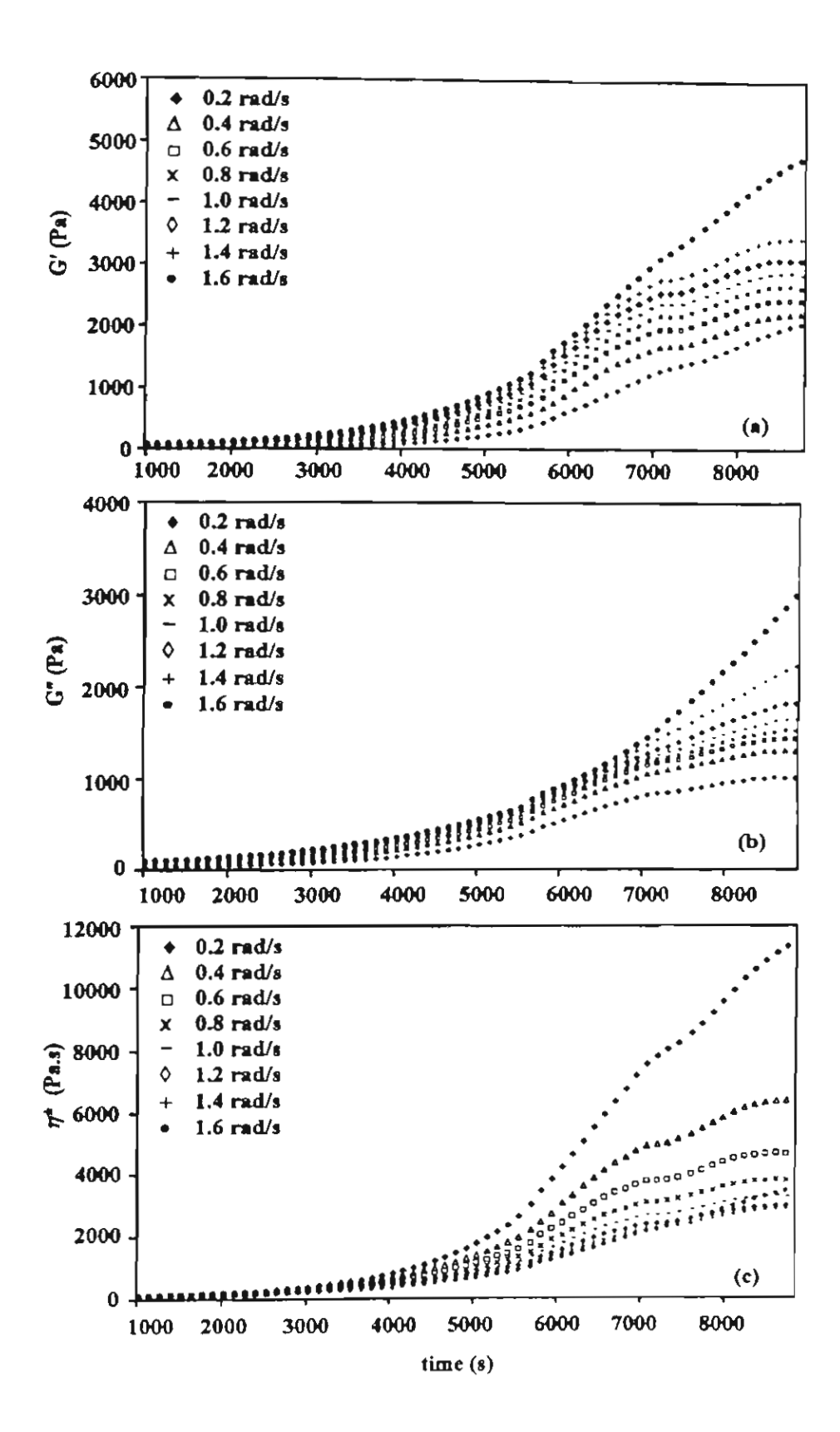


Figure 5.1. Plots showing (a) storage modulus (G'): (b) loss modulus (G"), and (c) complex viscosity (η^*) as a function of the reaction time for the system pH 7 and h = 9 at 25 C

According to eq 5.3 the critical gel is identified by a loss tangent, $\tan \delta = G''/G'$, which is independent of frequency. Therefore, $\tan \delta$ was investigated as a function of time at different frequencies. For the system with pH = 7 and h = 9 at 25°C, the various curves intersect at one point, at which tan becomes independent of frequency (Figure 5.2). The time at which this occurs is the gel time (8114 s) as depicted previously. Before the gel point, $\tan \delta$ decreased with increasing frequency, which is typical for a viscoelastic liquid. After the gel point, $\tan \delta$ increased with frequency, as is characteristic of a viscoelastic solid. Apparently, the sample had changed from a viscoelastic liquid to a viscoelastic solid. Equivalently, the gel time can be calculated by the method of statistical loss factor self similarity as noted above by observation of the minimum of the curve log (s/($\tan \delta$)) against reaction time. Figure 5.3 illustrates that the time at the minimum point compared very well with the experimental value observed for the frequency independence of loss tangent.

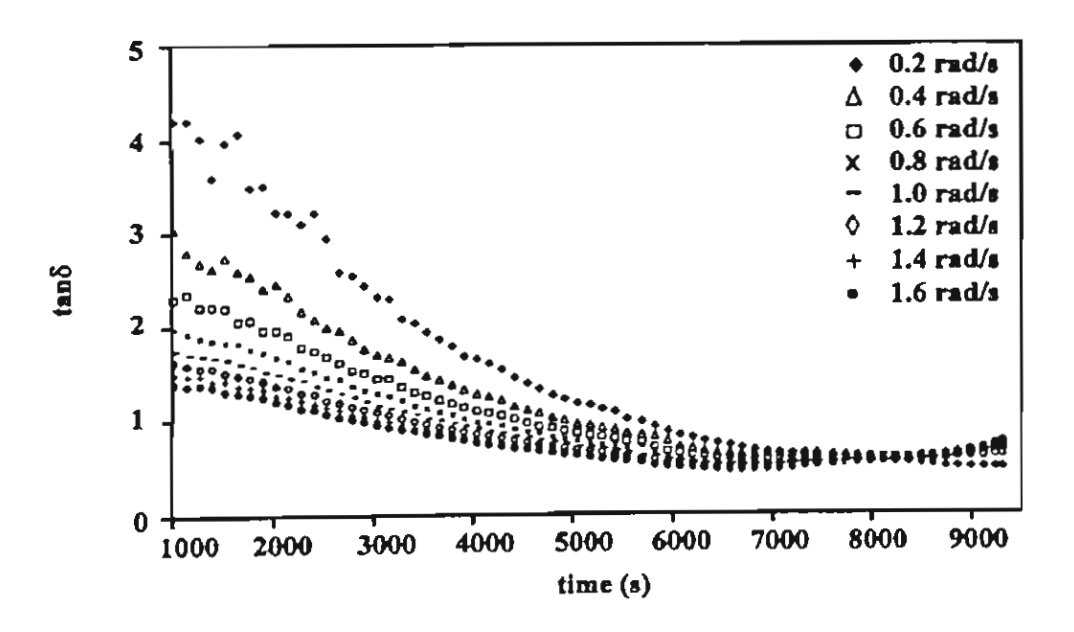


Figure 5.2. Variation of $\tan\delta$ during sol-gel process as a function of the time for pH 7 at h = 9 and temperature of 25°C.

The frequency dependence of G' and G" for several measurement times with pH = 7 and h = 9 at 25°C was exhibited in Figure 5.4. Early in the reaction G' is smaller than G". As gelation proceeds at the instant, the traces of G' and G" became parallel to each other showing power law behavior. Such a condition corresponds to a sol-gel transition according to the criterion suggested by Winter and Chambon. As noted above, values of n near the gelation critical point can be identified from power law character. The slopes of these lines gave n, the viscoelastic exponent in eq.5.2, for the frequency dependence of the

moduli. The changes of n with extent of reaction were shown in Figure 5 where n' and n'' for storage and loss moduli, respectively, were plotted against time. Both decreased and then merged to 0.36 at 8114 s. These values of n component were in good agreement with the values obtained from Figure 5.2 and eq.3 At the gel point, $\tan \delta$ equals 0.56, which corresponds to a relaxation exponent of n = 0.33.

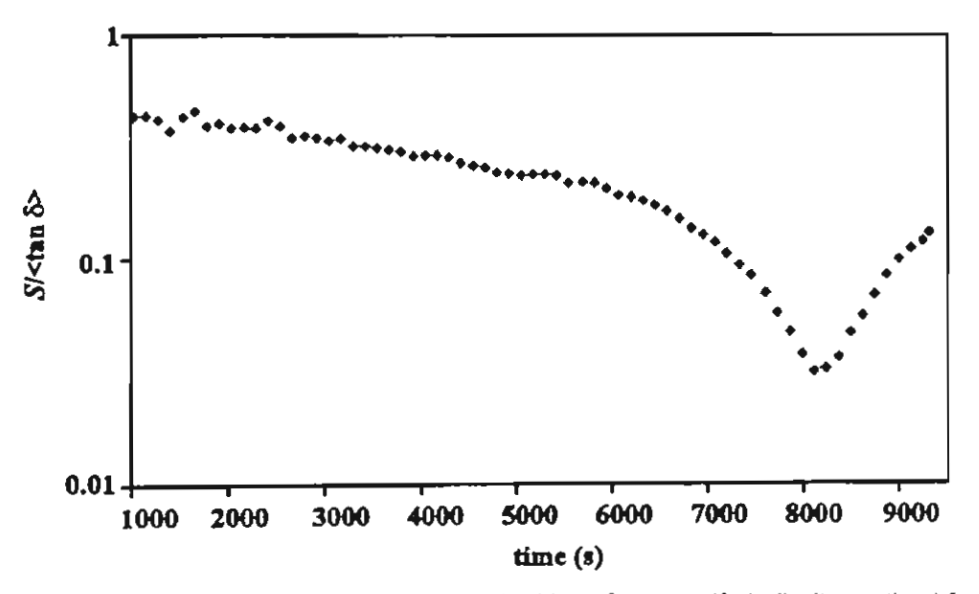


Figure 5.3. Determination of the gel time by the statistical loss factor self-similarity method for pH 7 at h = 9 and temperature of 25°C.

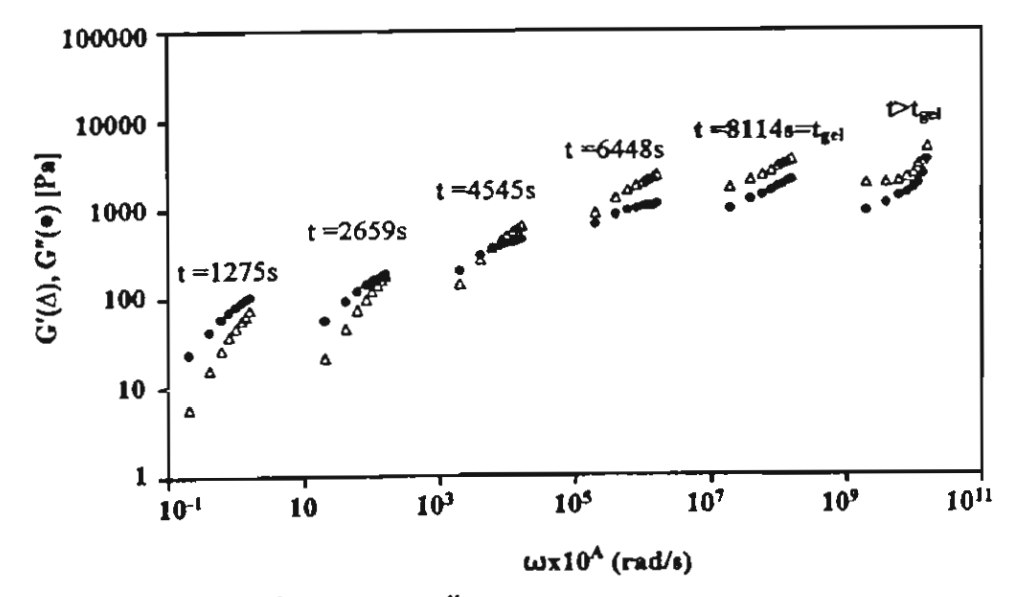


Figure 5.4. Dynamic storage (G') and loss (G") moduli for as a function of the frequency (ω) for the system pH 7 and h = 9 at 25°C. The curves were horizontally shifted by the factor, A = 10^2 for t = 2659 s, A = 10^4 for t = 4545 s, A = 10^6 for t = 6448 s, A = 10^8 for t = 8114 s, and A = 10^{10} for t > t_{oel} .

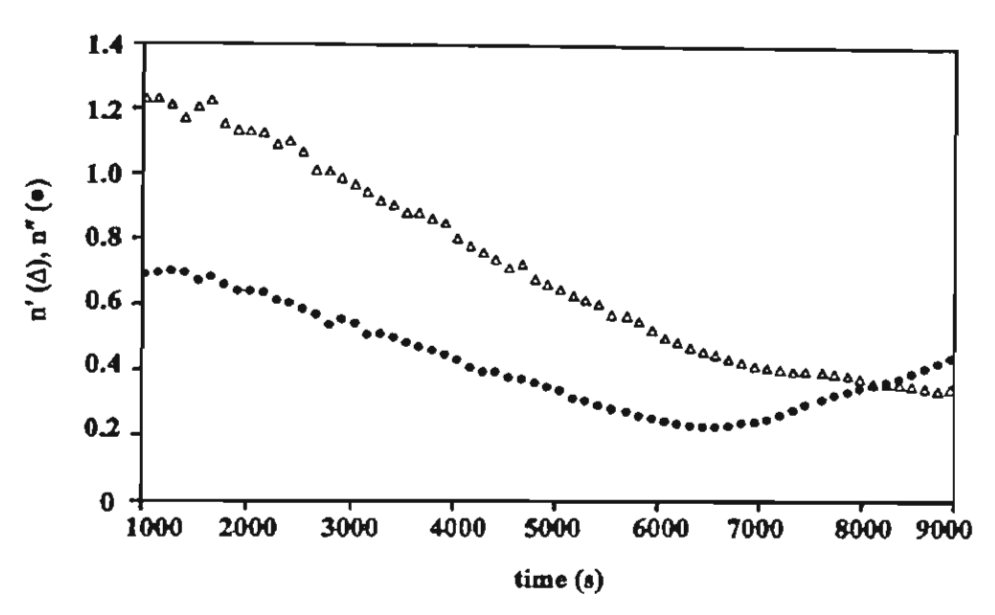


Figure 5.5. Changes of viscoelastic exponent for n' the storage and n'' the loss shear moduli during the gelation reaction as obtained from fits, such as those shown in Figure 5.4.

Many studies of critical gel rheological properties were found that most results show $n \ge 0.5$. Values of n below 0.5 have also been found.^{23, 27-30} Winter reported that if n > 0.5, the gel point preceded the intersection of G' and G". In contrast, if n < 0.5, the intersection occurs before the gelation. This is coincident with the results from our system.

The value obtained in our system was very close to the one found for polycaprolactone. Izuka et al. suggested that a low n value implies that the material at the gel point is a mostly elastic body with the limit of G'' = 0 at n = 0 and vice versa. The low value of n found for our case is probably due to the presence of physical crosslinks with a finite lifetime, in addition to the permanent chemical crosslinks leading to a denser network with elastic behavior.

Effect of pH

The systems with the pH ranging from 3 to 11 at h = 9 and temperature of 25°C were also studied. The values of rheological properties at the gel point were provided in Table 5.1. The gel time at each pH was obtained from plots of tan δ against time in the same manner as Figure 5.2. The relaxation exponent n was calculated from eq.5.3 at 0.8 rad s⁻¹. The maximum gelation rate was observed near pH 11, with the rate decreasing significantly at lower pH. As is investigated, the value of t_{gel} at higher pH is less than at lower pH. The maximum at around pH 9 corresponds to the isoelectric point of alumina. However, it is also evident, Table 5.1, that the strength of the gel network formed at lower pH (determined from the value of G'/G" at t_{gel}) is substantially higher than that obtained at higher pH. This is consistent with a

decrease of n values with decreasing pH. As pointed out above, a lower value of n is related to higher elastic body implying that intermolecular crosslinks were stronger.

Table 5.1. pH effect on the gel time, and dynamic properties for h = 9 at 25°C

На	t _{gel} (s)	G' (Pa)	G" (Pa)	η* (Pa.s)	G'/G"	n
3	16891	4800.45	1105.54	6157.63	4.34	0.14
5	13109	2875.11	1293.79	3941.00	2.22	0.27
7	8114	2556.35	1424.30	3657.94	1.79	0.33
9	17798	5802.23	1200.03	7406.28	4.83	0.13
10	5548	1500.92	989.11	2246.91	1.52	0.37
11	3076	1003.24	750.18	1565.88	1.34	0.41

Effect of hydrolysis ratio

The dynamic viscoelastic properties at the gel point were demonstrated in Table 5.2 for each set of reaction conditions at 25° C. The increase of hydrolysis ratio reduces the times required for gelation. Also, G' outweighs G" for all systems showing that the elastic component appreciably predominates over the viscous one at the gel point. Furthermore, G' and η^* decrease with increase of hydrolysis ratio while the relaxation exponent increases with increase of hydrolysis ratio. It could be justified that when the hydrolysis ratio is greater, gel formation evolving quickly through the reaction of hydrolysis and condensation contain low interconnected networks. Consequently, the network is looser with lower value of G'. On the other hand, a system with a lower hydrolysis ratio grows slowly resulting in a denser network with higher G'. Correspondingly, a higher value of n is related to a lower elastic system indicating that intermolecular crosslinks are weaker.

Table 5.2. Hydrolysis ratio effect on the gel time, and dynamic properties for pH = 9 at 25°C.

h	t _{gel} (s)	G' (Pa)	G " (Pa)	η^* (Pa.s)	G'/G"	n
9	17798	5802.23	1200.03	7406.28	4.83	0.13
18	9575	3003.25	1351.46	4116.65	2.22	0.27
27	3642	2116.89	1206.62	3045.79	1.75	0.33

Effect of temperature

The temperature at which the measurement is performed is one of the most important factors influencing the gel time. The results for the systems varying between 20°C and 36°C were reported in Table 5.3. At higher temperatures gelation occurs faster, resulting in a shorter time to gel. The values of the dynamic moduli at the gel point decreased with increasing temperature. The trend of these results is analogous to that of other studies. In addition, the temperature dependence of the complex dynamic viscosity η^* was also similar to that of the dynamic moduli. In contrast, the n-values obtained for all systems increase with temperature. These observations indicate that the network formation proceeded faster with increasing temperature, whereas the gel texture is rather loose. There exhibits some discussion in the literature regarding an apparent activation energy for the gelation reaction calculated from the gel time at different temperatures. Because gelation represents a specific extent of reaction, the temperature dependence of the time to gel should be described by the Arrhenius equation

$$ln(tgel) = A + E_a/RT$$
 (5.4)

where A is a constant, R is the ideal gas constant, and T is temperature. The activation energy Ea of the gelation can be calculated from the slope of a plot of $\log t_{gel}$ against 1/T. The Arrgenius plots for our system are shown in Figure 5.6. The values of Ea were estimated to be approximately the same in each case, varying slightly around 139 kJ mol⁻¹. This implies that E_a of the gelation does not depend on hydrolysis ratio.

Table 5.3. Temperature effect on the gel time, and dynamic properties for pH = 9 and h = 9, 18 and 27.

	t _{gel} (s)	G' (Pa)	G" (Pa)	η* (Pa.s)	G'/G"	n
20°C						
h = 9	34987	7645.23	1287.78	9691.16	5.94	0.11
h = 18	21875	5134.42	2053.77	6912.43	2.50	0.24
h = 27	11265	4211.56	2190.56	5933.99	1.92	0.31
23°C						
h = 9	23142	6178.21	1173.85	7860.92	5.26	0.12
h = 18	12017	4214.25	1727.84	5693.38	2.44	0.25
h = 27	5987	3165.51	1709.37	4496.94	1.85	0.32
25°C						
h = 9	17798	5802.23	1200.03	7406.28	4.83	0.13
h = 18	9575	3003.25	1351.46	4116.65	2.22	0.27
h = 27	3642	2116.89	1206.62	3045.79	1.75	0.33
28°C						
h = 9	9878	5620.17	1348.8	7224.69	4.17	0.15
h = 18	5164	2534.43	1241.87	3527.92	2.04	0.29
h = 27	2132	1676.51	1022.67	2454.76	1.64	0.35
32°C						
h = 9	3985	4802.47	1392.72	6250.42	3.45	0.18
h = 18	2227	2138.73	1176.3	3051.09	1.82	0.32
h = 27	1135	1032.23	650.31	1525.00	1.59	0.36
36°C						
h = 9	2013	4059.12	1380.11	5359.16	2.94	0.21
h = 18	1198	1851.21	1166.26	2734.94	1.59	0.36
h = 27	582	823.17	617.38	1286.21	1.33	0.41

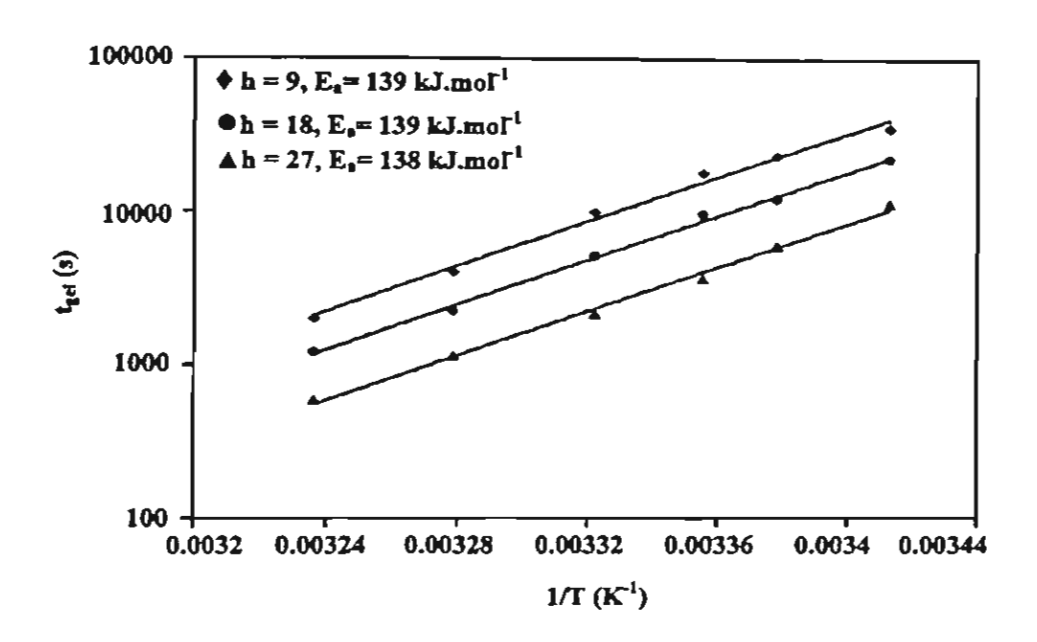


Figure 5.6. Semi-logarithmic plot of gel time versus 1/T where the temperature T is expressed in Kelvin.

FT-IR analysis

The FTIR spectra of the gel as a function of time were compared to elucidate the study of the hydrolyzed alumatrane in sol-gel process. As the reaction proceeds, a decrease in the intensity of the Al-O-C vibration of alumatrane at 1087 cm⁻¹ was observed. Some peaks present in the 900 – 500 cm⁻¹ region disappear, while the width and intensity of this spectral range increase. This result corresponds to the formation of Al-O-Al bonds according to the condensation reaction. Figure 5.7 depicts the FTIR spectra of hydrolyzed systems at different hydrolysis ratio. The intensity of Al-O-Al is maximized at h = 27 with the intensity decreasing at lower hydrolysis ratio. The decrease in intensity of Al-O-C band is accompanied with the increase of Al-O-Al band as hydrolysis ratio increases. This implies that the gelation can be accelerated with increasing hydrolysis ratio leading to the reduction of the gel time.

In order to confirm the above conclusion, a careful deconvolution of the IR profiles using a computer program was also investigated. The results of the analysis are shown in the relationship between the peak ratio of Al-O-C band (1087 cm⁻¹) and Al-O-Al band (683 cm⁻¹) and time (Figure 5.8). This is only a semi-quantitative picture of the gelation of alumatrane molecule. Generally, the gel time is decreased by factors that increase the condensation rate. It is obvious that values of pH, hydrolysis ratio and temperature are the important factors affecting the gel time. The results obtained here compared favorably with earlier study by qualitative FTIR. Furthermore, it was found that these FTIR observations are consistent with the rheological results.

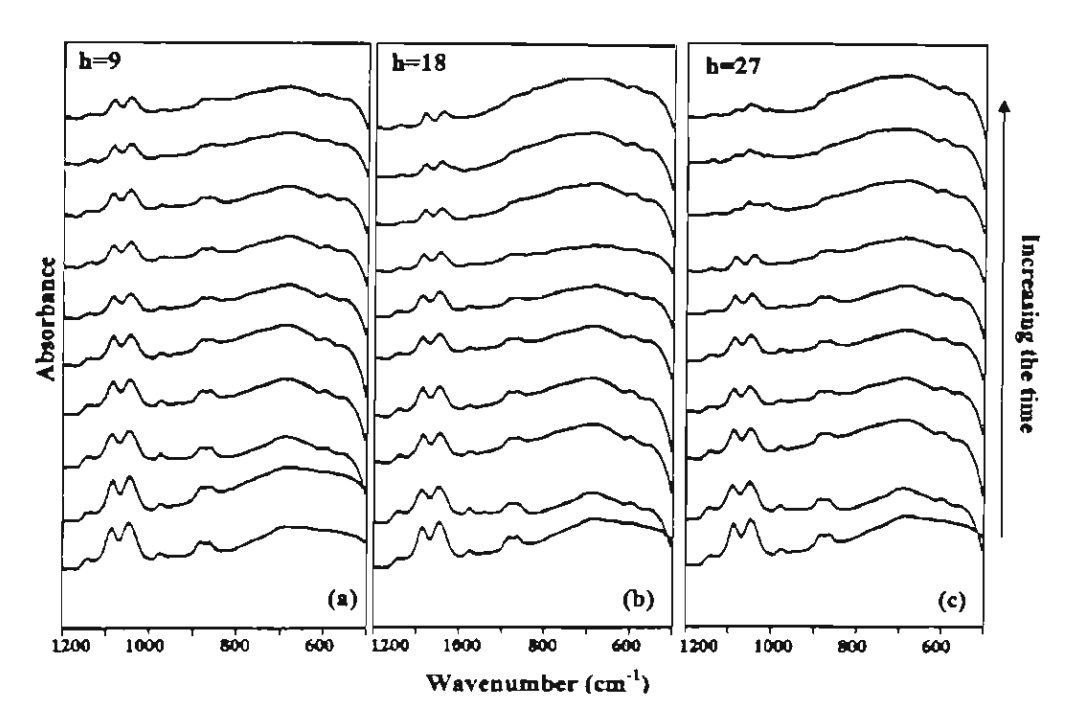


Figure 5.7. FTIR spectra of alumina gel during sol-gel process for pH 9 at 25° C at various hydrolysis ratio (h) (a) h = 9; (b) h = 18; (c) h = 27.

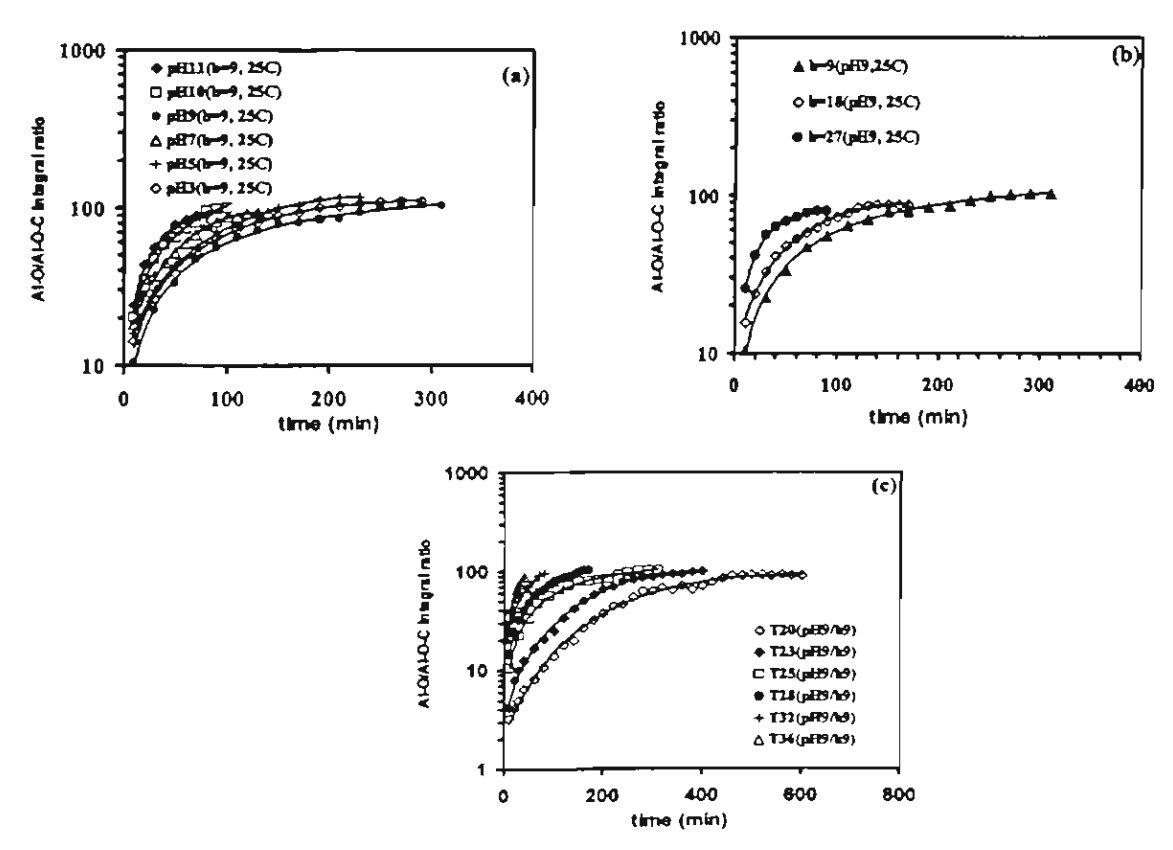


Figure 5.8. Variation of hydrolyzed alumatrane as a function of the reaction time at various conditions

(a) pH dependence; (b) hydrolysis ratio dependence; (c) temperature dependence.

Characterization of pyrolyzed gel

Some preliminary studies of pyrolyzed gel were performed to examine the influence of pyrolysis temperature on the properties of alumina obtained from the heat treatment of alumatrane gels. XRD patterns of pyrolyzed gel at different temperatures ranging between 400 and 1100°C showed amorphous nature at 300°C in Figures 5.9. The sample treated at 500°C presents three γ -alumina peaks (ICDD, File 29-63). At 900°C, the XRD pattern of γ -alumina is better defined, however, characteristic peaks of δ -alumina are not well resolved (ICDD, File 16-394). After heating at 1000°C, two phases of δ -alumina and α -alumina were detected. When the sample was heated from 1000 to 1100°C, the δ -alumina was totally transformed into α -alumina.

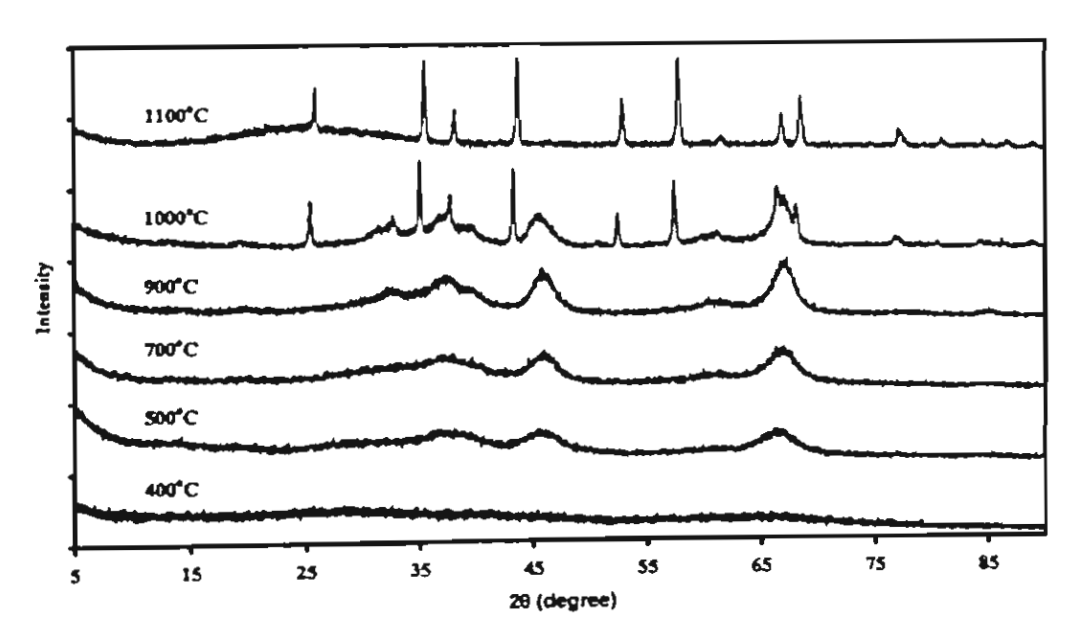


Figure 5.9. XRD patterns of hydrolyzed alumatrane at various pyrolysis temperatures. (a) 400°C; (b) 500°C; (c) 700°C; (d) 900°C; (e) 1000°C; (f) 1100°C.

The sample treated at 500°C shows the monomodal pore size distribution in the mesopore range having a maximum center around a pore diameter of 70 Å (Figure 5.10a). Also, the resulting powder shows the nitrogen adsorption/desorption isotherms of type IV (IUPAC classification) which exhibit hysteresis loops mostly of type H2 (Figure 5.10b).³³ Further investigations on the pyrolysis of alumina gel obtained various reaction conditions are in progress and will be reported later.

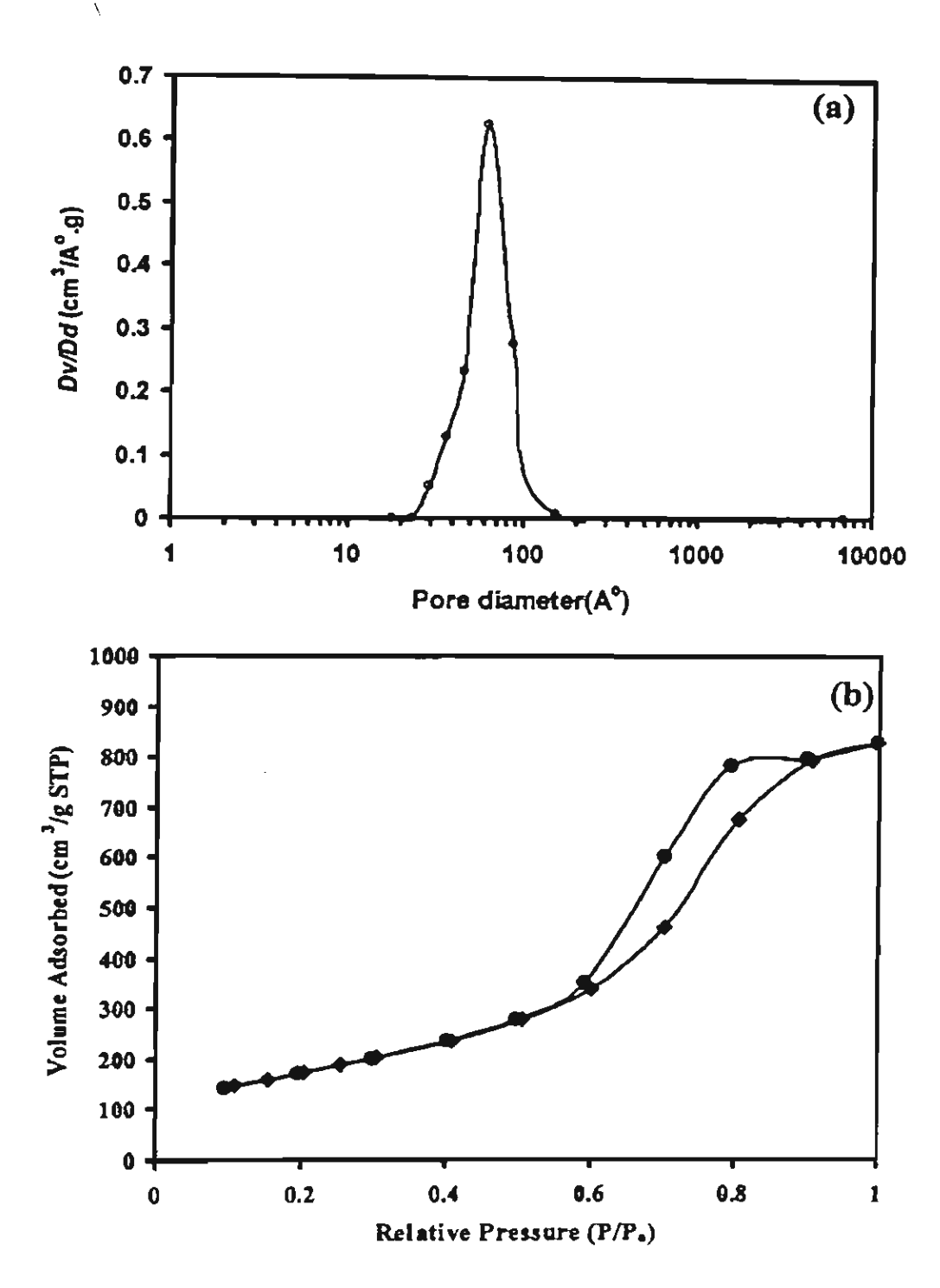


Figure 5.10. Plots showing (a) Pore size distribution; (b) Nitrogen adsorption/desorption isotherms of the alumatrane gel pyrolyzed at 500°C for 7 h.

CONCLUSIONS

Alumatrane can be used as metal alkoxide precursor for preparing high surface alumina powders via sol-get route. The multiple-waveform rheological technique and FTIR were found to be effective for

studying the gelation of alumatrane. The operation variables, viz. pH, hydrolysis ratio and temperature, affect dramatically the gel time. An increase of these parameters leads to the reduction of gel time. However, the strength of the gel network formed more quickly is lower than that obtained gradually. The value of n for our systems was found to be fairly low indicating high elastic gel. The apparent activation energy of the gelation reaction determined directly from the gel time measurement at different temperatures was around 139 kJ mol⁻¹. Heat treatment of the resulting alumatrane gels at 500°C produces a homogeneous mesopore alumina having high surface area.

REFERENCES

- 1. Guizard, C.G.; Julbe, A. C.; Ayral, A. J. Mat. Chem. 1999, 9, 55
- Quanttrini, D.; Serrano, D.; Perez Catán, S. Granular Matter 2001, 3, 125.
- Livage, J. Solid State Ionics 1996, 86-88, 935.
- 4. Suda, S.; Yamashita, K.; Umegaki, T. Solid State Ionics 1996, 89, 75.
- Browne, C. A.; Tarrant, D. H.; Olteanu, M. S.; Mullens, J. W.; Chronister, E. L. Anal. Chem. 1996, 68, 2289.
- Kuraoka, K.; Tanaka, H.; Yazawa, T. J. Mater. Sci. Lett. 1996, 15, 1.
- 7. Skapin, T.; Kemnitz, E. Catal. Lett. 1996, 40, 241.
- 8. Roger, A.A.; Bruce, D. K. J. Non-Cryst. Solids 1988, 99, 359
- 9. Blanchard, J.; Barboux-Doeuff, S.; Maquet, J.; Sanchez, C. New J. Chem. 1995, 19, 929.
- 10. Jarayaman, V.; Guanasekaran, T.; Periaswami, G. Mater. Lett. 1997, 30, 157.
- 11. Yoldas, B. E. J. Non-Cryst. Solids 1992, 147/148. 614.
- 12. Uchilhashi, H.; Tohqe, N.; Minami, T.; J. Ceram. Soc. Jpn. Int. 1989, 97, 389.
- 13. Yoldas, B. E. J. Appl. Chem. Biotechnol. 1973, 23, 803
- 14. Yoldas, B. E. Ceram. Bull. 1975, 54, 286.
- 15. Yoldas, B. E. Ceram. Bull. 1975, 54, 289.
- 16. Pierre, A. C.; Uhlmann, D. R. J. Am. Ceram. Soc. 1987, 70, 28
- 17. Ogihara, T.; Nakajima, H.; Yanagawa, T.; Ogata, N.; Yoshida, K. J. Am. Ceram. Soc. 1991, 74, 2263.
- 18 Opornsawad, Y.; Ksapabutr, B.; Wongkasemjit, S.; Laine, R. M. European Polymer Journal. 2001, 37, 1877.
- 19 Djabourov, M., Leblond, J. and Papon, P. J. Phys. France 1988, 49, 333
- 20 Tung, C. M. and Dynes, J. J. Appl. Polym. Sci. 1982, 27, 569
- 21 Winter, H. H., Chambon, F. J. Rheol. 1987, 31, 683
- 22 Winter, H. H., Chambon, F. J. Rheol. 1986, 30, 367

- 23. Lin, Y. G.; Mallin, D. T.; Chien, J. C. W.; Winter, H. H. Macromolecules, 1991, 24, 850.
- 24. Yu, J. M.; Jerome, R.; Teyssie, P. Polymer, 1997, 38, 347.
- 25. Izuka, A.; Winter, H. H.; Hashimoto, T. Macromolecules 1992, 25, 2422.
- 26. Rude, E.; Llorens, J.; Mans, C. Progress and Trends in Rheology, 1998, 613.
- 27. Scanlan, J.; Winter, H. H. Macromolecules, 1991, 24, 47.
- 28. Hodgson, D. F.; Amis, E. J. Macromolecules, 1990, 23, 2512.
- 29. Raghavan, S. R.; Chen, L. A.; Mc Dowell, C.; Khan, S. A. Polymer, 1996, 37, 5869.
- 30. Ponton, A.; Barboux-Doeuff, S.; Sanchez, C. Colloids and Surface A: 1999, 162, 177.
- 31. Srinivasa, R.R.; Li Ang Chen.; Christopher, M.; Saad, A. K. Polymer, 1996, 37, 5869.
- 32. Gough, L. J.; Smith, I. T. J. Appl. Polym. Sci., 1960, 3, 362.
- 33. Leofanti, G.; Padovan, M.; Tozzola, G.; Venturelli, B. Catal. Today 1998, 41, 207.

CHAPTER VI PROJECT OUTPUT

This research project results in two already published in an international journal and one to be submitted, as follows;

- Yukoltorn Opornsawad, Bussarin Ksapabutr, Sujitra Wongkasemjit and Richard Laine, "Formation and Structure of Tris(alumatranyloxy-I-propyl)amine Directly from Alumina and Triiospropanolamine", Eur. Polym. J., 37/9, 1877-1885 (2001).
- Wissanee Charoenpinikarn, Mathavee Suwankuruhasn, Bussarin Kesapabutr, Sujitra Wongkasemjit, and Alex. M. Jamieson, "Sol-gel processing of silatranes", European Polymer Journal, 37/7, 1441-8 (2001).
- 3. Bussarin Kesapabutr, Erdogan Gulari and Sujitra Wongkasemjit, "Sol-Gel Transition Study and Pyrolysis of Alumina Based Gels Prepared from Alumatrane Precursor", To be submitted.

APPENDIX A

Formation and Structure of Tris(alumatranyloxy-i-propyl)amine

Directly from Alumina and Triiospropanolamine



European Polymer Journal 37 (2001) 1877-1885



Formation and structure of tris(alumatranyloxy-i-propyl)amine directly from Al(OH)₃ and triisopropanolamine

Yukoltorn Opornsawad ^a, Bussarin Ksapabutr ^a, Sujitra Wongkasemjit ^{a,•}, Richard M. Laine ^b

The Petroleum and Petrochemical College, Chulalongkorn University, Bangkok 10330, Thailand
 The Department of Materials Science and Engineering, University of Michigan, Ann Arbor, MI 48109-2136, USA
 Received 24 March 2000; received in revised form 31 August 2000; accepted 15 February 2001

Abstract

Recently, a new one step method was developed for synthesizing a methyl substituted alumatrane directly from aluminum hydroxide [Al(OH)₃] and triisopropanolamine (TIS). The structure of TIS-Al was characterized using DSC, TGA, FAB⁺-MS, NMR (1 H-, 13 C-, 27 Al-), and FTIR. Triethylenetetramine (TETA), a stronger base than TIS, was found to act as a catalyst to accelerate the Al(OH)₃ dissolution rate. The kinetics of TIS-Al formation were studied as a function of different conditions. The activation energy of reaction was 24 ± 2 kJ mol⁻¹. © 2001 Elsevier Science Ltd. All rights reserved.

Keywords: Tris(alumatranyloxy-i-propyl)amine; Aluminum hydroxide; Triisopropanolamine; Kinetics

1. Introduction

Atranes, I, with M = B, Al, Si, Ge, Sn, Pb, P, Ti, V. Mo, etc. have been synthesized and studied extensively over the last three decades [1-5]. These compounds are of interest owing to their cage structure and physical/chemical properties. The behavior of alumatrane, where M = Al, 2,8,9-trioxa-5-aza-1-alumatricyclo [3.3.3.0^{1.5}] undecane, and oligomeric alumatrane has been described previously [6-9]. In benzene, cryoscopy and ebullioscopy indicate tetrahedral and octahedral behavior. A mass spectroscopic (EI 70 eV) study showed the stability of the dimer I' in the gas phase.

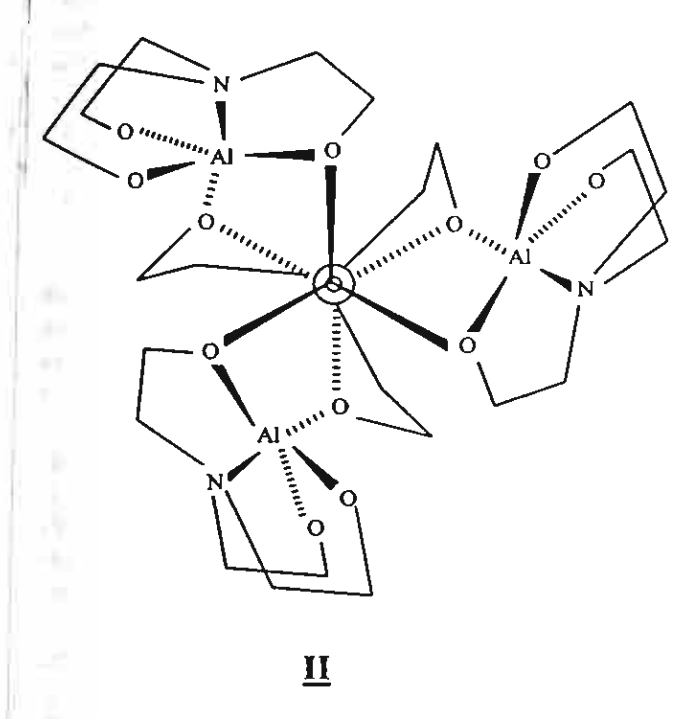
There are several methods of preparing alumatranes. Alumatrane is prepared readily in high yield by reaction of aluminum alkoxides with triethanolamine in an aromatic solvents [10,11] or with no solvent [12-14]. Triethylaluminum also reacts with triethanolamine in toluene or hexane at -78°C to form alumatrane [15]. Verkade [16] prepared alumatrane by the alcoholysis of tris-(dimethylamido) aluminum with triethanolamine

E-mail address. dsujitra'a chula ac th (S. Wongkasemjit)

^{*}Corresponding author. Tel: +66-662-218-4133; fax +66-662-215-4459.

and also by transligation of monomeric and dimeric

According to ²⁷Al-, ¹H-, and ¹³C-NMR data, they found tetramers, II, in solution and dimeric I' by mass spectra in the gas phase. Alumatrane precursors, aluminum alkoxides [Al(OR)₃] or aluminum alkyl [Al(R)₃] are expensive and the syntheses are multistep. Laine et al. have developed an inexpensive way to convert metal oxides or hydroxides, namely, Al(OH)₃ and silica, into novel materials ranging from ion conducting [17], liquid crystalline polymers [18], to oligomeric and polymeric precursors [19].



Laine also found that higher boiling point amine bases (b.p. >200°C), such as triethanolamine and triethylenetetramine (TETA) can be used either in catalytic or stoichiometric quantities to dissolve SiO₂. Moreover, they also found that approximately stoichiometric quantities of triethanolamine will effectively dissolve Al(OH)₃. The "oxide one pot synthesis process (OOPS)" for alkoxyalanes was developed after it was discovered that stoichiometric amounts of triethanolamine would dissolve Al(OH)₃, the source material for most pure alumina.

The purpose of this work is to extend previous efforts to reactions of Al(OH)₃ and triisopropanolamine (TIS), and study the kinetics of the product formation, which includes the reaction order, rate constant, and activation energy. Along with this, the effect of TETA on the reaction was also studied to improve the solubility of this novel aluminum alkoxide in non-polar solvents for use as a catalytic intermediate in the sol-gel processing.

2. Experimental

2.1. Materials

The starting materials and products are slightly moisture and air sensitive. Therefore, all operations were carried out with careful exclusion of air by purging with nitrogen gas.

UHP grade nitrogen; 99.99% purity was obtained from Thai Industrial Gases Public Company Limited (TIG). Aluminum hydroxide hydrate [Al(OH)₃·xH₂O] containing 57.5% Al₂O₃ as determined by TGA was purchased from Aldrich Chemical Co. Inc. (USA) and used as received. Ethylene glycol (EG), used as solvent in the reaction, was purchased from Farmitalia Carlo Erba (Barcelona) and purified by fractional distillation at 200°C, under N₂ before use. TIS was obtained from Fluka Chemika-BioChemika (Switzerland) and used as received. TETA was obtained from Union Carbide Thailand Limited (Bangkok, Thailand) and distilled under vacuum (10⁻² Torr) at 120°C. Acetonitrile and methanol were purchased from J.T. Baker Inc. (Phillipburg, USA) and purified by standard techniques.

2.2. Instrumentation

Mass spectra were obtained on a 707E-Fison Instrument (VG-Autospec, Manchester, England) with a VG data system, used in the positive fast atomic bombardment (FAB+) mode. Thermal analysis was carried out on a Netzsch DSC 200 (Germany) and a Netzsch Gerätebue BmbH Thermal analysis TG 209 (Germany). ¹H- and ¹³C-NMR spectra were obtained using a 500 MHz JEOL (JNM-A500) spectrometer at the Scientific and Instrumental Research Equipment Center, Chulalongkorn University, using deuterated methanol (CD₃ OD) and tetramethylsilane (TMS) as the solvent and internal reference, respectively. 27Al-NMR spectra were recorded on Bruker 360 MHz at the University of Michigan. Fourier transform infrared (FTIR) spectra were recorded on a Bio-Rad FT-45A FTIR spectrometer with a resolution of ± 4 cm⁻¹.

2.3. Procedure

General procedures to obtain tris(alumatranyloxyi-propyl)amine are as follows; Al(OH)₃, 50 ml of EG, and TIS were added to a 250 ml two-necked round bottomed flask. The reaction mixture was stirred and heated under N₂ in a thermostatted oil bath. When the oil bath temperature reached 200°C, the reaction was considered to have commenced. Fresh EG in the same amount as the distillate was added to maintain the total reaction volume until the reaction mixture turned clear, indicating reaction completion. After letting the reaction

mixture stand without stirring overnight, white product precipitated out. After filtering, the product was stirred with dried acetonitrile overnight to remove excess TIS. The solid product was then filtered off and dried under high vacuum (10⁻² Torr) at 120°C for 5 h. Dried products were then characterized by DSC, TGA, FTIR, FAB*-MS and NMR.

Unreacted alumina recovered from a reaction was purified as follows: after the reaction mixture was cooled, unreacted Al(OH)₃ was filtered off, and stirred with dried methanol overnight to extract remaining product from unreacted Al(OH)₃. The unreacted Al(OH)₃ was filtered off, washed with 2 × 20 ml of dried methanol, and then oven dried at 120°C for 10 h. Finally, the dried Al(OH)₃ was calcined in the TGA to obtain the alumina content. The total unreacted Al(OH)₃ was recalculated to obtain reacted alumina.

2.4. Kinetic studies

The kinetic studies were conducted primarily on the dissolution of Al(OH)₃ as a function of changes in the reaction conditions, namely, the amount of TIS, the amount of Al(OH)₃, reaction temperature, and time. Each condition was repeated three times.

The optimum ratio of TIS was first studied by fixing the amount of Al(OH)₃ (57.5% Al₂O₃ content by TGA) at 22.7-10 mmol equivalent of Al₂O₃. The amount of TIS was varied from 0 to 50 mmol. The reaction time and temperature were fixed at 3 h and 200°C, respectively.

2.4.1. Dissolution rate as a function of Al(OH);

The amount of TIS was fixed at 3.83 g (20 mmol) and the amount of Al(OH)₃ was varied from 0.89 to 8.87 g (5-40 mmol). EG was added to make the total volume of the reaction mixture 50 ml. The reaction time and temperature were set at 1 h and 200°C, respectively. The relationship between mmol of unreacted alumina and mmol of alumina added was plotted.

2.4.2. Dissolution rate as a function of TETA concentra-

To study the effect of TETA concentration on the rate of reaction, Al(OH)₃ and TlS quantities were fixed at 1.77 g (22.7 mmol) and 0.96 g (5 mmol), respectively. The concentration of TETA was varied from 0.00 to 4.39 g (0-30 mmol). The reaction time and temperature were fixed at 3 h and 200°C. The relationship between mmol dissolved alumina and mmol TETA added was then plotted.

2.4.3. Determination of the reaction rate constant and activation energy

Amounts of Al(OH)₃ and TIS were fixed at 1.77 g (22.7 mmol) and 0.96 g (5 mmol), respectively. The re-

action time was varied from 15 to 120 min with increments of 15 min at 150°C, 170°C, 190°C, and 200°C. The relationship between mmol of unreacted alumina versus reaction time at each reaction temperature was then plotted to obtain the reaction rate constant (k). The activation energy was then calculated by plotting $\ln(k)$ versus 1/T $(1/K^{-1})$.

2.4.4. Dissolution rate as a function of time in the presence of TETA as a catalyst

The effect of time on the reaction of Al(OH)₃ and T1S with TETA as a catalyst was studied by fixing the amounts of Al(OH)₃, TIS, and TETA at 1.77 g (22.7 mmol), 0.96 g (5 mmol), and 0.18 g (1.25 mmol), respectively. The reaction temperature was fixed at 200°C and the reaction time was varied from 15 to 120 min. The mmol of unreacted alumina for each run were then plotted versus time.

3. Results and discussion

In this study, recovered Al(OH)₃ was thermally converted to α -alumina to determine the actual amount dissolved. Al(OH)₃ used at the beginning and left after the reaction was measured as Al₂O₃ using TGA ceramic yields.

As seen in Fig. 1, with a fixed amount of aluminum hydroxide hydrate at a reaction time and temperature of 3 h and 200°C, respectively, the reaction went very slowly for TIS quantities less than 20 mmol. However, it went to completion when 35 mmol of TIS was used. The addition of 10 mmol of TETA with 22.7 mmol of Al(OH)₃ and 35 mmol of TIS led to complete reaction within 2 h (see Fig. 6).

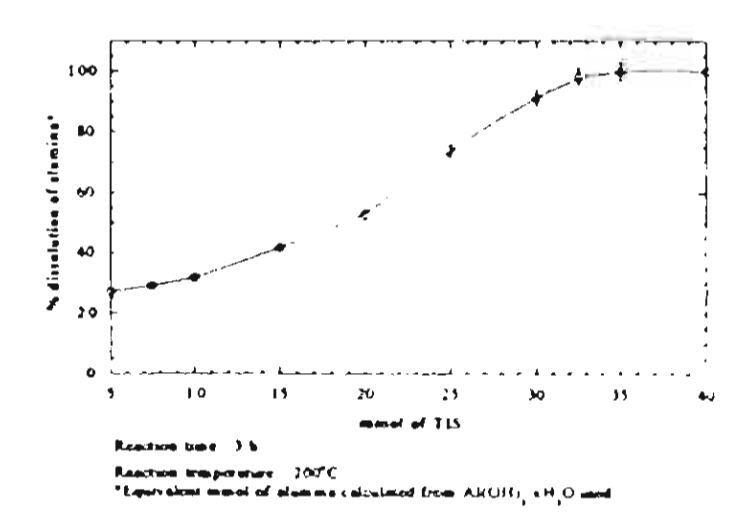


Fig. 1. Optimization of $Al(OH)_{\rm t}$ TIS ratio for complete $Al(OH)_{\rm t}$ dissolution

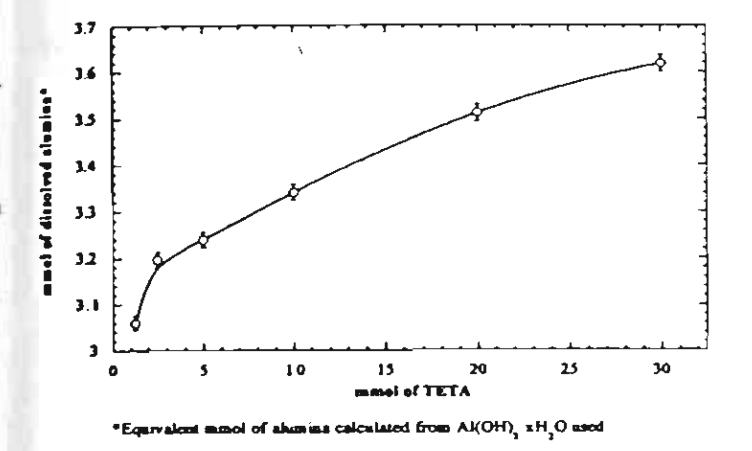


Fig. 5. Effect of the TETA concentration.

and without TETA. The dissolution reaction rate with TETA was faster than that without TETA because TETA increased solubility of Al(OH)₃, resulting in increasing its surface area which caused the reaction to go faster, as discussed previously.

3.5. Characterization

3.5.1. Thermogravimetric analysis

The TGA data for the product from the reaction without TETA shows two major regions of mass loss (see Fig. 7(a)). The first region between 180–260°C indicated the decomposition of TIS ligand while the second region occurred at about 260–550°C corresponding to the oxidative decomposition of carbon residues. The % ceramic yield of the product was 27.6%, which was higher than the theoretical ceramic yield (23.7%) owing to the incomplete combustion of the sample since the final ash was still gray in color.

Similarly, the TGA of the product synthesized in the presence of TETA (Fig. 7(b)) also showed two major mass losses at 180-250°C and 250-500°C corresponding

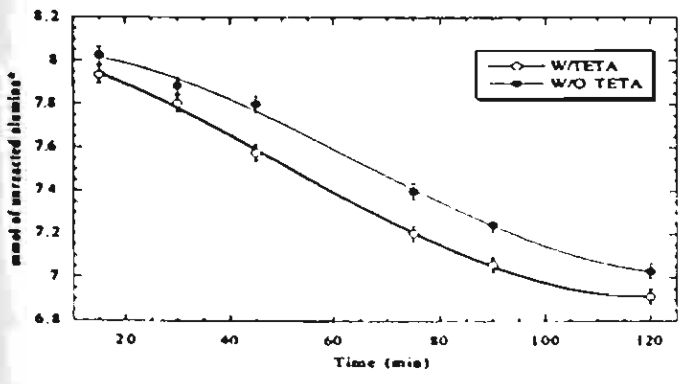
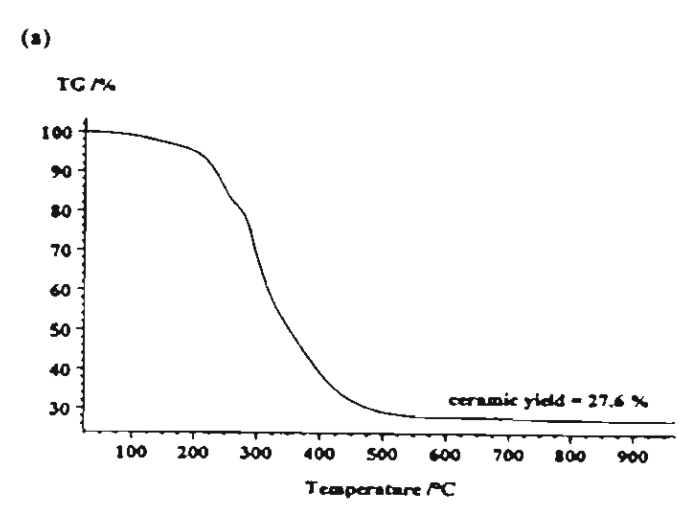


Fig. 6. Effect of TETA concentration with time.





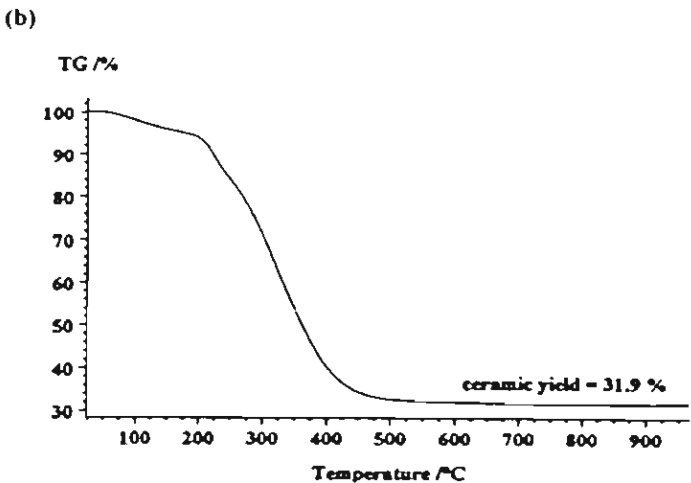


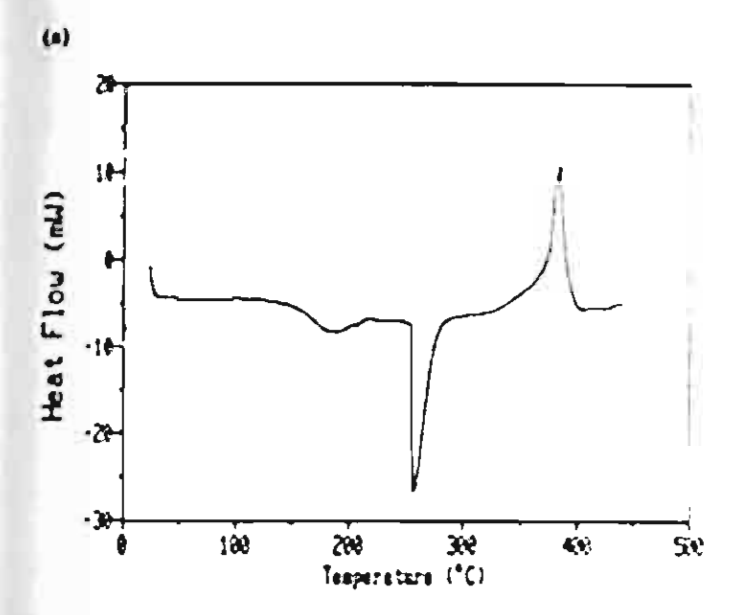
Fig. 7. TGA data of the products obtained from the reactions: (a) with and (b) without TETA.

to the decomposition of TIS ligand and the oxidative decomposition of carbon residues, respectively. The % ceramic yield of product was 31.9%, which was much higher than the theoretical yield. This can be explained along with the mass spectrum which indicated that the product synthesized from the batch containing TETA using as catalyst gave more smaller units, dimer (m/e 431), than the one without TETA. The more smaller unit, the higher ceramic yield. Moreover, the final ash was darker in color.

3.5.2. Differential scanning calorimetry

The DSC of the product from the reaction without TETA, see Fig. 8(a), showed an exotherm at 250-280°C corresponding to the melting point immediately followed by the decomposition temperature of the product, the endotherm at 280-400°C. It is coincident with the result of its TGA. The $T_{\rm g}$ was observed at about 167°C.

Similarly, the DSC data of the product from the reaction with TETA, as shown in Fig. 8(b), indicated the



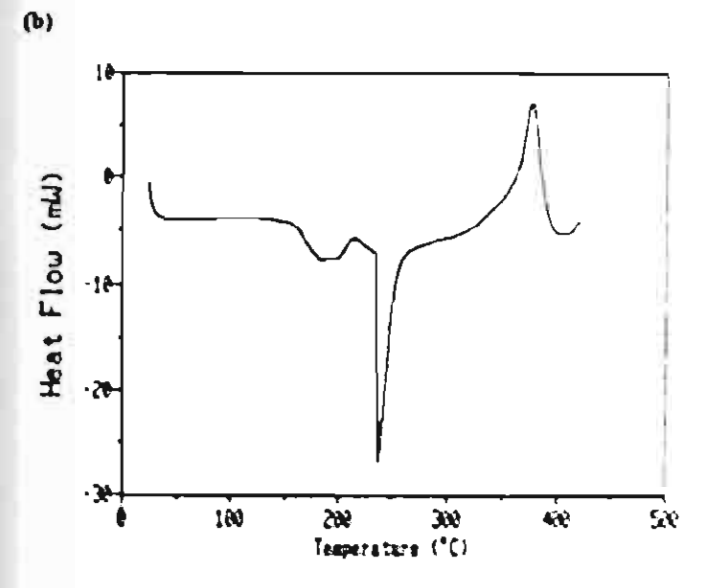


Fig. 8. DSC thermograms of the products obtained from the reactions (a) with and (b) without TETA

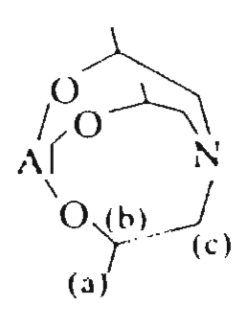
exotherm at about 220-260°C corresponding to the melting point followed by the decomposition of the product, the endotherm at about 260-380°C. It is worth noticing that the both temperatures are lower than those in Fig. 8(a). This is due to the more smaller units containing in the products obtained from the reaction with catalyst TETA. The I_4 of this product occurred at about 166°C.

3.5.3. Positive fast atomic bombardment mass spectroscopy

Mass spectral analysis suggests that there are four different alumatrane complexes, hexamer (m/e 1292), the highest intensity pentamer plus one morpholine (m/e 1250) resulted from losing a molecule of water in TIS, trimer plus one ethylene glycol (m/e 707), and monomer plus one TIS (m/e 409) and the intensities of all proposed structures was shown in Table 1

The fragmentation pattern of the product from the reaction with TETA gave higher intensities of the lower unit peaks at m/e 216 and 409, and lower intensity of the peak at m/e 1250. This result can obviously confirm that the reaction carried out without TETA gives the product containing higher molecular weight unit than the one run with TETA owing to the acceleration of TETA resulting in faster completion of the reaction.

3.5.4. Nuclear magnetic resonance spectroscopy



The NMR results showed that the products certainly contained several kinds of oligomers, such as monomer, dimer, etc., which are coincided with the mass spectroscopy results. The ¹H-NMR spectrum of the product from the reaction without TETA showed three multiple characteristics of quadrapolar coupling peaks indicating the presence of a few species in the product. The peaks at 1.1–1.4 ppm correspond to the -CH₃ group of TIS, position (a). The peaks at 2.4–3.1 ppm are assigned to the methylene group adjacent to the N-atom of TIS (-N-CH₃) at position (c). The peaks at 3.6–4.2 ppm are assigned to the tertiary carbon adjacent to the O-atom of TIS, position (b). The ¹H-NMR spectrum of the product from the reaction with TETA gave a similar one.

Similarly, the "C-NMR spectrum of the product from the reaction showed a multiple peak at 22.0 ppm corresponding to -CH₁ groups at position (a) coupled to itself and proton of the tertiary carbon. The sharp peak at 64.3 ppm belongs to the carbon adjacent to N-atom of TIS (-N CH₂) at position (c). The multiple peak at 79.0 ppm is associated with the carbon adjacent to O-atom of TIS (position (b)) due to the coupling with -N-CH₂ and -CH₃. The spectrum of both reactions, with and without TETA, showed the unitlar positions.

The ²⁷Al-NMR spectra of the products from the reaction with and without TETA coincidentally showed three different peaks, as shown in Table 2, at around 65, 49 and 7 ppm at the ratio of 1.1.1. Again, these three peaks indicated the presence of both hexa-(at 7 ppm) and tetracoordinated (at 65 and 49 ppm) aluminum compounds.

Table 1
The proposed structures and fragmentation pattern of products

=/e	Intensities	Proposed structure
216	50	O'H.
		AIN(CH-CH-CH-O),H
409	17.5	H ² OH OH OH
		AIN(CH-CH-CH-O),N(CH-CH-CH-O) (CH-CH-CH-OH),H
492	38.7	0 1 -0 0 - 1 0 0 0 0 0 0 0 0 0 0 0 0 0 0
		Al ₂ [N(CH ₂ CH ₂ CH ₃ O) ₃] ₃ (OCH ₂ CH ₂ O) H ₂ *
7 07	35.4	AL-NICH CHOREMOCHEMI.
959	7.9	ALIN CHEH CHOLLARING HEH CHEH CHOLL
1076	15	ALINCH CHOILEN

frontinued on next paper

Table 1 (continued)

Intensities	Proposed structure
46.3	
	VICHICHICHICHICHICHICHICHICHICHICHICHICHI
100	
	wite content on production content.
7.8	
	ALINICH,CH,CH,O), LH
	46.3

Table 2
Peak positions of ¹H₂, ¹³C₂, and ²⁷Al-NMR of products

Compounds	¹ H-NMR (ppm)	"C-NMR (ppm)	TAI-NMR (ppm)
Product w/o TETA	1.1-1.4 (a)	22 O (a)	7.5, 49.6 and 66.0
	2 4-3.1 (c)	64 J (c)	
	36-42(b)	79 0 (b)	
Product w/o TETA	1.1-1 9 (a)	21 O (a)	7.4, 48.8 and 64.9
	2.2-2 8 (c)	65 O (c)	
	37-41 (b)	79 O (b)	

Table 3
Peak position and assignments of FTIR spectra of products with without TETA

Pruk positions (cm ⁻¹)		Assignments	
Al-TIS	TIS-AI-TETA		
3300-3700	3300-3700	.O.H	
27.50-3000	2750 3000	w C B	
1650	1830	O H overtone, C H bending	
1450	1430	A C B	
1000-1200	1006-1250	w.C. N. O. H. bending	
\$00-800	500 800	≽ Al ·O	

3.5.5. Fourier transform infrared spectroscopy

The FTIR spectra of the products from the reactions with and without TETA show similar functional groups (Table 3). Due to the moisture sensitivity of the products, the v_{O-H} appears at 3300–3700 cm⁻¹, and the wave number at 2750–3000 cm⁻¹ corresponds to v_{C-H} . The single peak at about 1650 cm⁻¹ is O-H overtone and C-H bending. The strong peak at 1000–1250 cm⁻¹ results from the v_{C-N} and/or O-H bending. The broad peak at 500–800 cm⁻¹ represents the v_{Al-O} of the product.

4. Conclusions

In this work, alumatrane complexes were synthesized directly from inexpensive starting material, Al(OH)₃, and TIS, via the one step process, called "OOPS" process. Mass spectra revealed that products were oligomers. The main product was pentamer bonded with TIS that lost one H₂O molecule. From TGA data, the % ceramic yields of the product from the reactions without and with TETA were 27.6 and 31.9%, respectively, which are higher value than the theoretical yield (23.7%). The higher percent ceramic yields were due to the small unit of oligomers in the product and the small amount of unreacted Al(OH)₃ remaining in the product.

The reaction order was second order overall, first order with respect to Al(OH)₃ and first order with respect to TIS. The dissolution rate increased when the reaction temperature increased. The activation energy of this reaction was about 24 ± 2 kJ mol⁻¹.

Acknowledgements

This study was funded by the National Research Council of Thailand and Thailand Research Fund.

References

- [1] Voronkov MG, Seltschan GI, Lapsina A, Pestunovitsch VA. Metal atranes [cyclic metal alcoholates of triethanolamine]. Z Chem 1968;8:214.
- [2] Voronkov MG. Metal atranes, a new class of physiologically active substances. Vestnik Akad Nauk SSSR 1968;38:48.

- [3] Voronkov MG, Zelchan GI. Preparation of organoxy (2,2',2"-nitrilotriethoxy) silanes. Khim Geterotsikl Soed 1965:51.
- [4] Bradley DC, Mehrotra RC, Gaur DP. Metal alkoxides. New York: Academic Press; 1978. p. 266.
- [5] Pinkas J, Verkade G. Alumatrane, Al(OCH₂CH₂)₃N:A reinvestigation of its oligomeric behavior. Inorg Chem 1993;32:2711.
- [6] Hein F, Albert PWZ. Aluminium triethanolaminate and its coordination relations. Anorg Allg Chem 1952;269:67.
- [7] Mehrontra RC, Mehrotra RK. Reactions of aluminium alkoxides with acetyl chloride. J Indian Chem Soc 1962;39:677.
- [8] Mehrotra RC, Rai AK. A convenient route to lead (II) alkoxides. Polyhedron 1991;10:1967.
- [9] Shklover VE, Struchkov YuT, Voronkov MG, Ovchinnikova ZA, Baryshok VP. Crystal and molecular structure of the unusual alumatrane complex [Al(OCH₂CH₂)N]₄ 3HOCH(CH₃)₂. 0.5C₆H₆. Dokl Akas Nauk (Engl. Transl.) 1984;227:723.
- [10] Voronkov MG, Baryshok VP. Metallatranes. Organomet Chem 1982;239:199.
- [11] Thomas WM, Groszos SJ, Day NE. Alkanolamine aluminates as ester redistribution catalysts. US Patent 2, 1961, 985,685; Chem Abstr 1961;55:20966.
- [12] Icken JM, Jahren EJ. Aluminium tris(alkoxyalkoxides) and nitrilotrialkoxides. Belg Patent 619, 1963, 940; Chem Abstr 1963;60:2768.
- [13] Stanley RH. Water-based paints containing alkanolamine aluminate gelling agents. British Patent 1, 1968, 123,559; Chem Abstr 1968;69:78532.
- [14] Elbing IN, Finestone AB. Insulation for electrical machinery, building elements or apparatus with hardened epoxy resin. German Offen 1. 1,162439; Chem Abstr 1964;60:17/ 4705.
- [15] Higashi H, Namikawa S. Studies on organometallic compound, ethanolamine catalyst (V):polymerization of acetaldehyde by Al foil treated with HgCl₂. Kogyo Kagaku Zasshi 1967;70:97.
- [16] Verkade JK. Atranes: new examples with unexpected properties. Acc Chem Res 1993;26:483.
- [17] Blohowiak K, Tradewell D, Mueller R, Hoppe M, Jouppi S, Kansal P, Chew KW, Scotto C, Babonneau F, Kampf J, Laine RM. SiO₂ as a starting material for the synthesis of pentacoordinate silicon complexes. 1. Chem Mater 1994; 6:2177-92.
- [18] Ray DG, Laine RM, Robinson TR, Viney C. Thermotropic and lyotropic copolymers of bis(dioxyphenyl)silanes. Mol Crys Liq Crystal 1993;225:153.
- [19] Laobuthee A, Wongkasemjit S, Traversa E, Laine RM. MgAl₂O₄ spinel powders from oxide one pot synthesis (OOPS) process for ceramic humidity sensors. J Eur Ceram Soc 1999;20:91-7.

APPENDIX B

Sol-gel Processing of Silatrane



European Polymer Journal 37 (2001) 1441-1448

EUROPEAN POLYMER JOURNAL

www.elsevier.nl/locate/europolj

Sol-gel processing of silatranes

Wissanee Charoenpinijkarn a, Mathavee Suwankruhasn a, Bussarin Kesapabutr a, Sujitra Wongkasemjit a.*, Alex M. Jamieson b

* The Petroleum and Petrochemical College, Chulalongkorn University, Bangkok 10330, Thailand

b The Department of Macromolecular Science, Case Western Reserve University, Cleveland, OH 44106, USA

Received 16 June 2000; accepted 10 November 2000

Abstract

Silatrane complexes are organosilicon compounds synthesized by direct reaction of SiO₂ and trialkanolamines. Here, we explore their potential as ceramic precursors via the hydrolytic sol-gel processing method. Viscoelastic analysis is used to characterize the gelation behavior of silatranes based on triisopropanolamine, under different hydrolysis conditions. Pyrolyzed ceramic products are characterized in terms of surface area and morphology and found to have a homogeneous microporous structure with high surface areas (313-417 m²/g). Faster hydrolysis rates lead to shorter gelation times, and smaller pore sizes in the derived ceramic. © 2001 Elsevier Science Ltd. All rights reserved.

Keywords: Silica; Silatranes; Morphology; Sol-gel

1. Introduction

Organosilicate polymers are of interest for their potential as precursors in sol-gel processing to form complex preceramic shapes and structures, not readily accessible by melt processing [1,2]. Due to widespread availability and low cost, silica, (SiO₂) is the ideal starting material to make organosilicon polymers. However, the Si-O bond is very strong and difficult to manipulate chemically [3]. As a corollary, organosilicate polymers, once formed, are very easy to hydrolyze back to SiO₂. Such high reactivity can create problems in chemical processing, therefore it is advantageous to be able to create precursors with reduced hydrolytic activity.

Silatrane complexes are a family of organosilicate compounds derived from reaction of SiO₂ with trialkanolamines such as triethanolamine or triisopropanolamine [4-6]. These materials are hydrolytically stable in air for periods up to several weeks. For this reason, they are candidates for use as precursors in ceramic pro-

cessing via the sol-gel technique. Here, we report some preliminary viscoelastic studies of sol-gel processing of silatranes under different hydrolysis conditions, and investigate the characteristics of glasses formed by pyrolysis of the products.

2. Methods

2.1. Synthesis of silatrane complex

2.1.1. Materials

Fumed silica (surface area 280 m²/g, average particle size of 0.007 μm) was purchased from Aldrich Chemical Co., and dried in an oven at 90°C for 10 h. Ethylene glycol (EG), purchased from Labscan, was used as reaction solvent, and purified by fractional distillation at 200°C under N₂ atmosphere. Triisopropanolamine (T1S, N(CH₂CHCH₃OH)₃) was obtained from Fluka Chemical Co., and dried in a desiccator. Commercial grade triethylenetetramine (TETA, H₂NCH₂(CH₂NHCH₂)₂-CH₂NH₂), supplied by Union Carbide Thailand, Limited, was purified by vacuum distillation at 120°C (1 mm Hg).

E-mail address: dsujitra@chula.ac.th (S. Wongkasemjit).

0014-3057/01/S - see front matter © 2001 Elsevier Science Ltd. All rights reserved. PII: S0014-3057(00)00255-X

^{*}Corresponding author, Tel.: +66-662-218-4100-6, ext. 4133; fax: +62-662-215-4459.

Anhydrous diethyl ether and dichloromethane, used as precipitants, were purchased from Baker Analytical Co. Dichloromethane was distilled over anhydrous calcium chloride under N₂ atmosphere. Anhydrous diethyl ether was dried by adding anhydrous calcium chloride, let stand for 24 h with occasional shaking, and then filtered into a clean dry bottle. HPLC grade tetrahydrofuran, used as solvent for molecular weight determination by gel permeation chromatography (GPC), was purchased from J.T. Baker Inc., and used as received.

2.1.2. Reaction conditions

As discovered by Piboonchaisit et al. [6], silatrane complexes were formed by mixing fumed silica with TIS (and TETA as catalyst) in EG as solvent. The reaction temperature was set at the distillation point of EG (200°C). Water formed during the reaction, and EG were continuously removed and replaced by an equivalent amount of fresh EG distillate. After reaction, the residual EG was removed by vacuum distillation (1 mm Hg). Based on GPC analysis described below, four distinct chemical species may be formed during the reaction, with proposed structures shown in Fig. 1, whose relative abundance depends on the molar ratio of TIS:SiO₂, the amount of TETA catalyst present, the temperature at which the vacuum distillation of EG is carried out, and on the duration of this distillation procedure. Of the four structures shown, that with molecular weight 407 is particularly undesirable, because the silicon content is low, and hence the % ceramic yield is poor, which makes the product unsuitable as a ceramic precursor. The optimal reaction condition, at which minimal formation of this species occurs, was found to be at a 1:1 molar ratio of TIS:SiO₂, (with TETA in the amount of 5 mol% of silica [6]). As the vacuum distillation temperature increases, the amount of high molecular weight species increases up to 180°C, after which it decreases again, as shown in Fig. 2. The

(a)
$$O - Si - OH$$

(b) $O - Si - OH$

(a) $O - Si - OH$

(b) $O - Si - OH$

(c) $O - Si - OH$

(d) $O - Si - OH$

(e) $O - Si - OH$

(ii) $O - Si - OH$

(iii) $O - Si - OH$

(iv) $O - S$

Fig. 1. The proposed structures of silatrane complexes using 1:1 ratio of [TIS]:[SiO₂].

optimum temperature for high ceramic yield is therefore 180°C.

2.2. Characterisation of silatrane complexes

2.2.1. FTIR spectroscopy

FTIR spectroscopic analysis was performed using a Bruker instrument with a resolution of 4 cm⁻¹. Powdered specimens containing 1.0% sample mixed with 99% crystalline KBr were compressed into pellets. The pellets were placed in the sample chamber purged with N₂ for 20 min to remove CO₂.

2.2.2. NMR spectroscopy

¹³C- and ¹H-NMR spectra of silatrane complexes were obtained using a 500 MHz JEOL spectrometer. Samples were dissolved in deuterated DMSO. Tetramethylsilane was used as the internal reference for both proton and carbon NMR.

2.2.3. Gel permeation chromatography

GPC chromatograms were performed using a Waters 600E Instrument equipped with UV and RI detectors (Waters 486 and 410, respectively). The column used

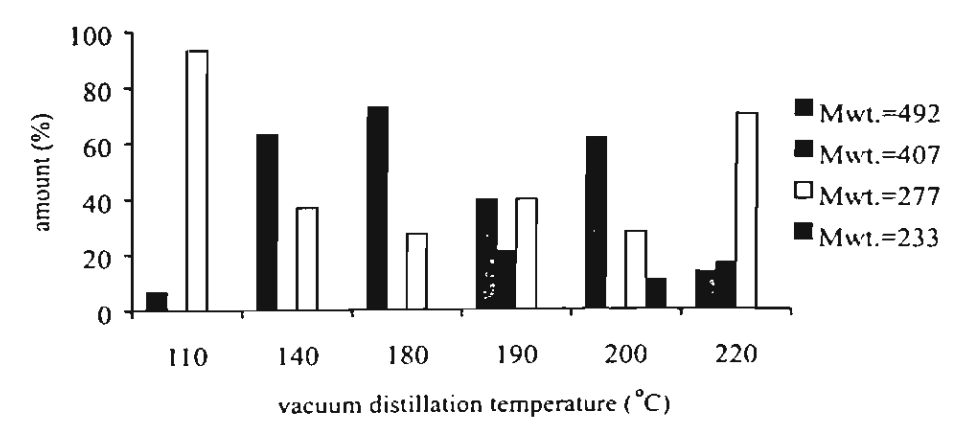


Fig. 2. Silatrane complexes obtained at 1:1 [TIS]:[SiO₂] and various vacuum distillation temperature.

was Styragel of pore size suitable to separate molecular weights in the range 0 to 1,000. Calibration was performed using polystyrene standards of narrow molecular weight distribution. THF was the solvent at ambient temperature. The silatrane samples were dissolved in THF at concentration below 0.3% weight, and filtered through 0.45 µm membrane filters prior to GPC analysis.

2.2.4. Rheological determination of the sol-gel transition

The transformation from a sol to a gel can be monitored rheologically by following the change in viscoelastic properties. The silatrane reaction product, after removal of residual EG, has the appearance of a hard plastic, and was used without further purification. The material was dissolved in the hydrolysis solvent at a concentration of 150% w/v. The hydrolysis temperature was selected to be 40°C, 50°C, or 60°C. The solution was stirred until homogeneous and preheated in a water bath at the hydrolysis temperature, until the solution was viscous enough to be transferred to the rheometer. The cone and plate attachment of the rheometer was preheated to the hydrolysis temperature. The gelation time was determined from the point during preheating at which the solution reached the hydrolysis temperature in the water bath. Measurements of storage $(G(\omega))$ and loss $(G'(\omega))$ moduli were made in a Rheometrics ARES rheometer with a 10 g cm transducer, in cone and plate geometry (cone radius 50 mm, cone angle 0.04 rad). Measurement of $G'(\omega)$ and $G''(\omega)$ was performed at 10 frequencies ω ranging from 0.1 to 1.6 rad/s. Each frequency scan required 10 s.

The precise location of the gel point as determined from viscoelastic measurements has been discussed in the previous literature [7]. Initially, the material in the sol state is a viscous fluid such that $\tan \delta =$ $G''(\omega)/G'(\omega) \gg 1$. As gelation proceeds, G' and G'' increase and, ultimately, the material becomes an elastic gel, $\tan \delta \ll 1$. Frequently, it is assumed that the gel point occurs at the location of the cross-over of the loss (G" and storage (G') moduli (i.e. where $\tan \delta = 1$). However, experimentally, this cross-over point is often found to depend on the deformation frequency, ω . A more definitive analysis is now possible following more recent experimental and theoretical work [7,8]. At the gel point, power-law behavior is observed in the frequency dependence of dynamic mechanical experiments. Specifically, the storage and loss moduli follow the relationships [7,8]:

$$G'(\omega) = G''(\omega)/\tan(n\pi/2) = \Gamma(1-n)\cos(n\pi/2)S\omega^*$$
(1)

where $\Gamma(1-n)$ refers to the gamma function of argument (1-n). The phase angle δ between stress and

strain is independent of frequency and proportional to the relaxation exponent, n:

$$\delta = n\pi/2 \tag{2}$$

A variety of experimental studies have been reported [7,9-12], which support the validity of this viscoelastic definition of the gel point, including both chemically and physically cross-linked systems. Experimental values of the relaxation exponent n vary from $n \ge 0.2$ to $n \ge 0.8$. For certain chemically cross-linked systems, n depends on stoichiometry. Theoretical predictions, which support various values of the dynamical exponent, n, have been reported [7,13,14]. Physically, the power-law dependence of the moduli originates in the fact that the gel point occurs when the first sample-spanning gel cluster forms. Hence, the magnitude of the dynamical exponent is determined by the structure and hydrodynamic properties of the critical cluster. The power-law behavior originates in the fact that the structure of the critical gel has a fractal character [14].

2.2.5. Characterization of pyrolysis products

2.2.5.1. BET surface area measurement. The surface area of pyrolyzed polysilatrane gels was determined using an Autosorb-1 gas sorption system (Quantachrome Corporation) via the Brunauer-Emmett-Teller (BET) method. A gaseous mixture of nitrogen and helium was allowed to flow through the analyzer at a constant rate of 30 cc/min. Nitrogen was used to calibrate the analyzer, and was also used as the adsorbate at liquid nitrogen temperature. Each sample was degassed at 300° C for 2 h before analysis. The surface area was obtained from a five-point isotherm at P/P_0 ratio less than 0.3. The results were computed based on the desorption surface area and the dried weight of the sample after analysis.

2.2.5.2. Scanning electron microscopy. SEM micrographs were obtained using a JEOL 5200-2AE(MP 15152001) scanning electron microscope. Samples were prepared for SEM analysis by attachment to aluminum stubs, after pyrolysis at 800°C. Prior to analysis, the specimens were dried in a vacuum oven at 70°C for 5 h, and then coated with gold by vapor deposition. Micrographs of the pyrolyzed sample surfaces were obtained at 2000 and 7500 magnification.

3. Results and discussion

3.1 Structural characterization of silatrane complex

Silatrane complexes produced by the synthetic method described above are a mixture of four molecular species, based on GPC analysis. Proposed structures of

. Table 1
Assignments of infrared spectra of the products

	20.6		
	Characterization	Silatrane complexes	
i	Si-N stretching	560-590 cm ⁻¹	
1	Si-O-CHb	970,883 cm ⁻¹	
	C-O4	1013-1070 cm ⁻¹	
	Si-O-CH ^b	1015-1085 cm ⁻¹	
	C-N°	1270 cm ⁻¹	
	C-H bending	1380-1460 cm ⁻¹	
	C-H stretching ^a	2800–29760 cm ⁻¹	

^{*}Silverstein et al., 1991 [17].

each species are shown in Fig. 1. Evidence for the formation of silatrane complexes includes observation of characteristic absorption bands in FTIR analysis (Table 1) and resonance frequencies in ¹³C- and ¹H-NMR spectroscopy (Table 2).

Table 2 ¹H- and ¹³C-NMR chemical shifts of silatrane complexes

Position	Groups	¹ H-NMR (ppm)	¹³ C-NMR (ppm)
(a)	N-CH,	2.86-2.91	57.7
(b)	$CH-CH_1$	4.0	23
(c)	C <u>H</u> -CH,	0.96-1.12	20-21
(d)	CH_2-O	3.3	59.2
(e)	С <u>н</u> ОН	3.4-3.5	62.5-65

3.2. Rheological analysis of sol-gel transition of silatranes

Silatrane complex formed after vacuum distillation of EG was dissolved in one of three hydrolysis solvents at a concentration of 150% w/v. The hydrolysis solvents were: distilled de-ionized water with measured pH = 6.7; MgO solution prepared by dissolving 0.5 g MgO in 1 l distilled de-ionized water with measured pH = 11.3; and

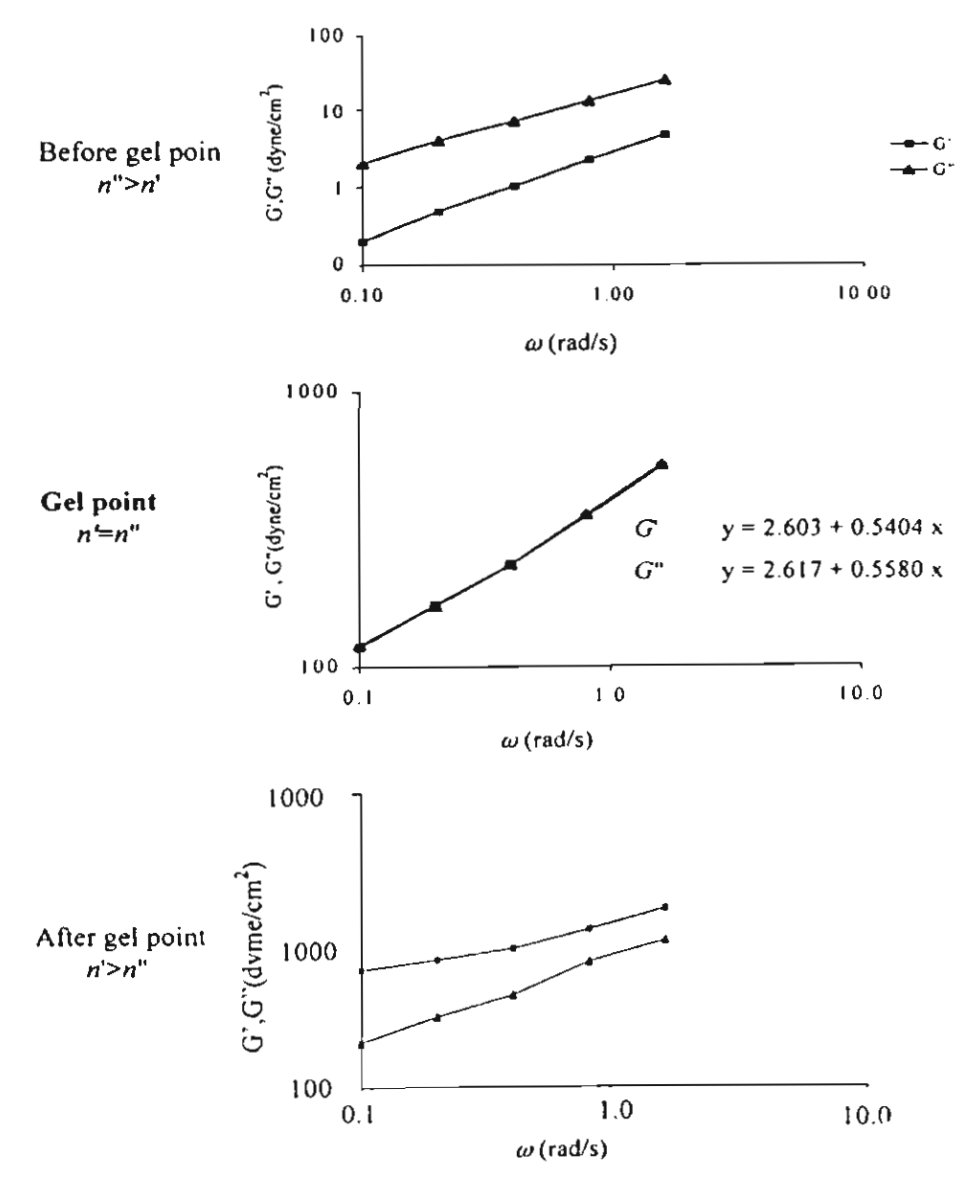


Fig. 3. The relationship of $\log G'$ and $\log G''$ vs. \log frequency of 150% w/v silatrane complex hydrolyzed in water at T = 40°C.

^b Anderson D.R., 1974 [18].

a solution of methanol in distilled de-ionized water at a ratio 1:1 (pH = 8.1). The change in G' and G'' was observed following procedures described above. In Fig. 3, we show frequency scans of G' and G'' during hydrolysis in water at 40°C at three times, viz. before the gel point, at the gel point, and after the gel point. The location of the gel point was identified following the discussion of Chambon and Winter [7], summarized above in Eqs. (2) and (3), as the point where G' and G'' follow the same power law with exponent n, i.e. a frequency-independent $\tan \delta$. As evident in Fig. 4, this occurs at gel time $t = 15600 \pm 1100$ s, when $n \sim 1.0$ and $\tan \delta \sim 1.0$. The corresponding variation of $\tan \delta$, the apparent frequency

exponents of G' and G'', and the change in magnitude of the dynamic viscosity, $\eta^*(\omega)$, during hydrolysis are shown in Figs. 4-6, respectively. As evident in Figs. 4 and 5, there is considerable uncertainty ($\sim i T_{ij}$) in deciding the location of the gel point based on the frequency-independence of $\tan \delta$, and, therefore, a corresponding uncertainty in the precise values of the dynamic exponent $n=0.55\pm0.15$. Fig. 6 confirms that, as expected, the dynamic viscosity increases dramatically at the gel point and, after gelation, exhibits a strong dependence on deformation frequency.

Hydrolysis experiments were carried out at three temperatures, and the gel times determined are tabulated

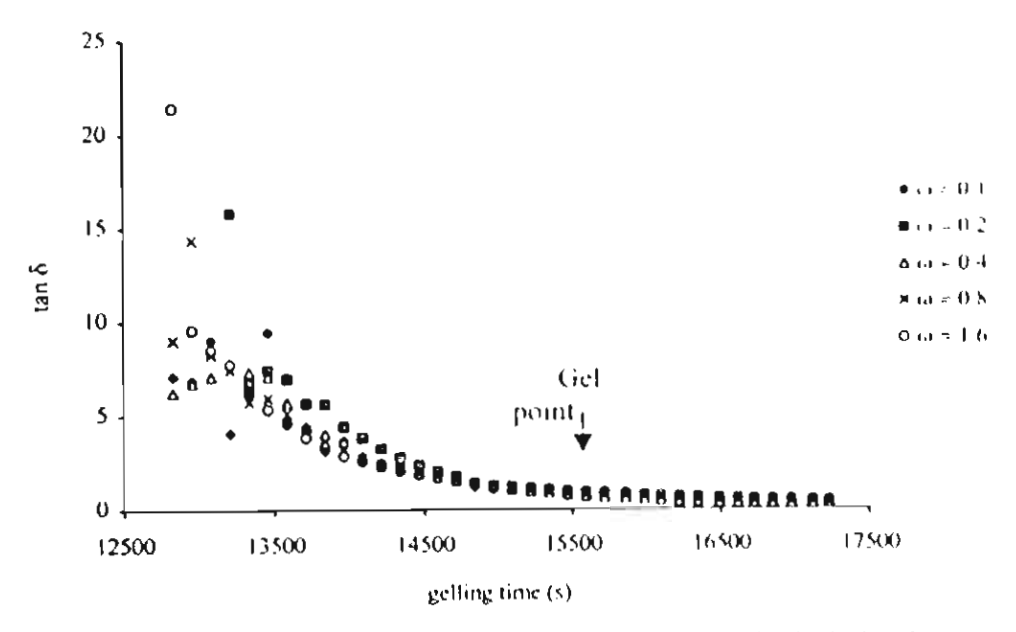


Fig. 4. Multi-frequency plot of $\tan \delta$ vs. gelling time of 150% w/v silatrane complex hydrolyzed in water at T = 40°C

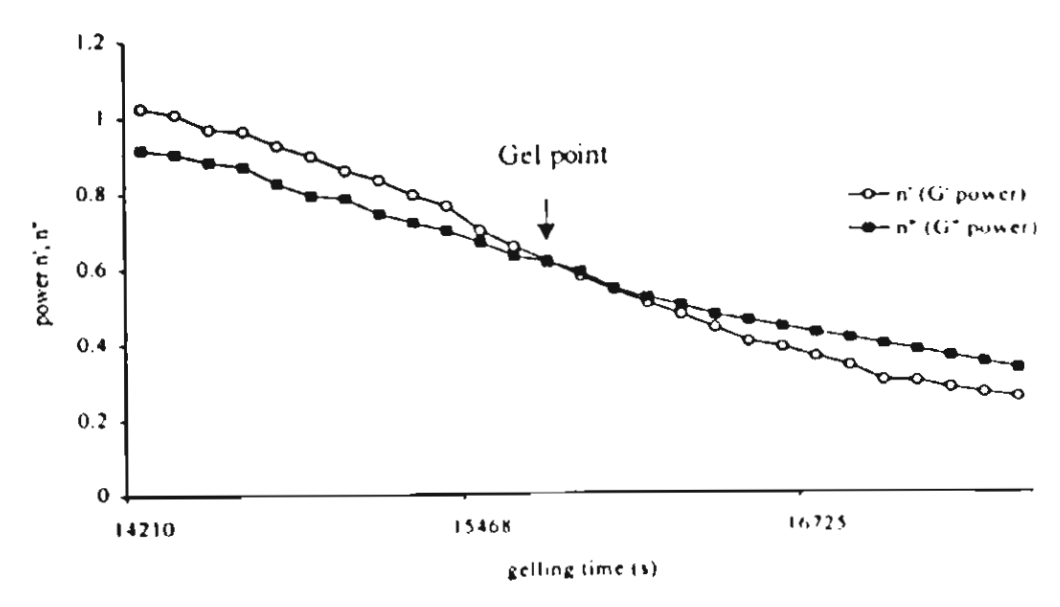


Fig. 3. The plot of power-law exponent n' and n'' vs. gelling time of 150% w/s silatrane complex hydrolyzed in water at T=40 (

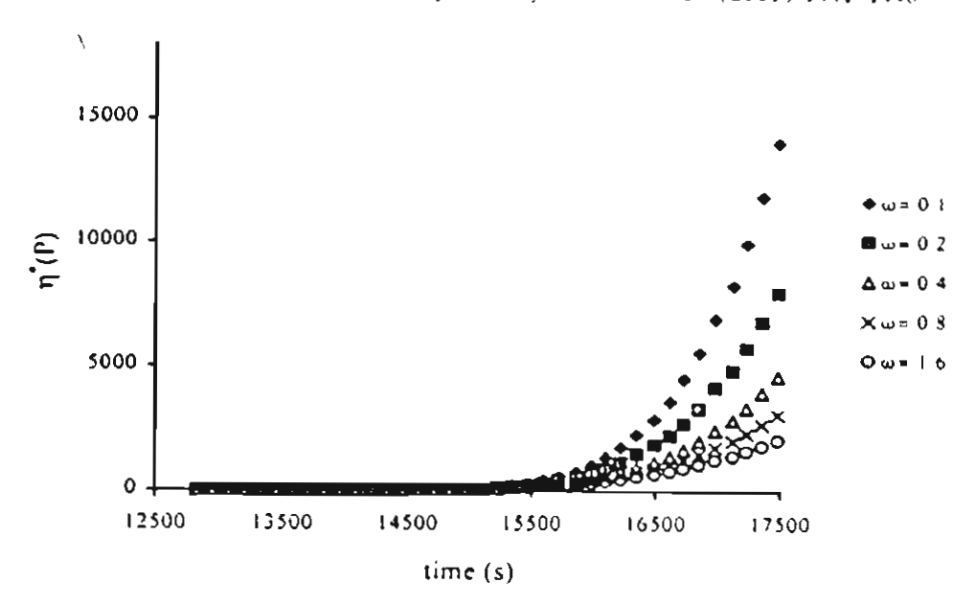


Fig. 6. Complex viscosity (η^*) at different frequency plotted vs. gelling time of 150% w/v silatrane complex hydrolyzed in water at $T = 40^{\circ}$ C.

Table 3
Viscoelastic properties at the sol-gel transition of polysilatrane

Solvent	Temperature (°C)	Gelling time (s)	tan δ	n
MgO + H ₂ O	60	4500	1.31	0,55
H ₂ O	60	6620	1.62	0.75
MeOH + H ₂ O	60	8260	1.20	0.61
$MgO + H_2O$	50	8950	3.02	0.85
H ₂ O	50	9350	2.24	0.79
MeOH + H ₂ O	50	9560	0.98	0.49
MgO + H ₂ O	40	14 567	1.20	0.62
H ₂ O	40	16 200	1.06	0.53
MeOH + H ₂ O	40	18 892	1.42	0.67

in Table 3. At each temperature, as illustrated by Roy [15] and McCarthy and Roy [16], the shortest gel times are observed in the most ionic MgO solvent, where the hydrolysis rate is fastest, and the longest gel times are in the least ionic MeOH solvent, which has the slowest hydrolysis rate. Also increase of temperature increases the rate of hydrolysis and thus decreases the gel times.

3.3. Characterization of pyrolyzed ceramics

Polysilatrane gels produced via hydrolysis in the three solvents at 40°C were pyrolyzed at various temperatures in the range 200-800°C. FTIR spectra are shown in Fig. 7 and indicate increasing conversion to silica, with increasing temperature such that at 800°C, essentially pure SiO₂ is obtained. Thus pure ceramic product can be generated in high yield, using processing temperatures as low as 800°C. The surface areas of ceramics produced by pyrolysis at 800°C of gels formed in

each of the hydrolysis solvents at 40°C were determined by the BET method. The results are listed in Table 4, and indicate a trend of decreasing surface area with decreasing gel times. At high rates of gelation, it is likely that smaller gel particles are formed, which might lead to smaller pore sizes, and hence higher surface areas in the pyrolyzed products. In Fig. 8, we show SEM micrographs, taken at a magnification of ×7500, of the surfaces of the three pyrolyzed ceramics together with that of the fumed silica starting material. Clearly, sol-gel processing via formation of silatrane complexes has converted the silica from a granular porous solid into a homogeneous microporous glass, with a corresponding increase in surface area from 280 to ~410 m²/g. From the micrographs, there appears to be a tendency towards smaller pore sizes with shorter gel times. In particular the ceramic from the MgO hydrolysis solvent has the most finely divided morphology, but shows evidence of contamination by small amounts of precipitated MgO on the surface.

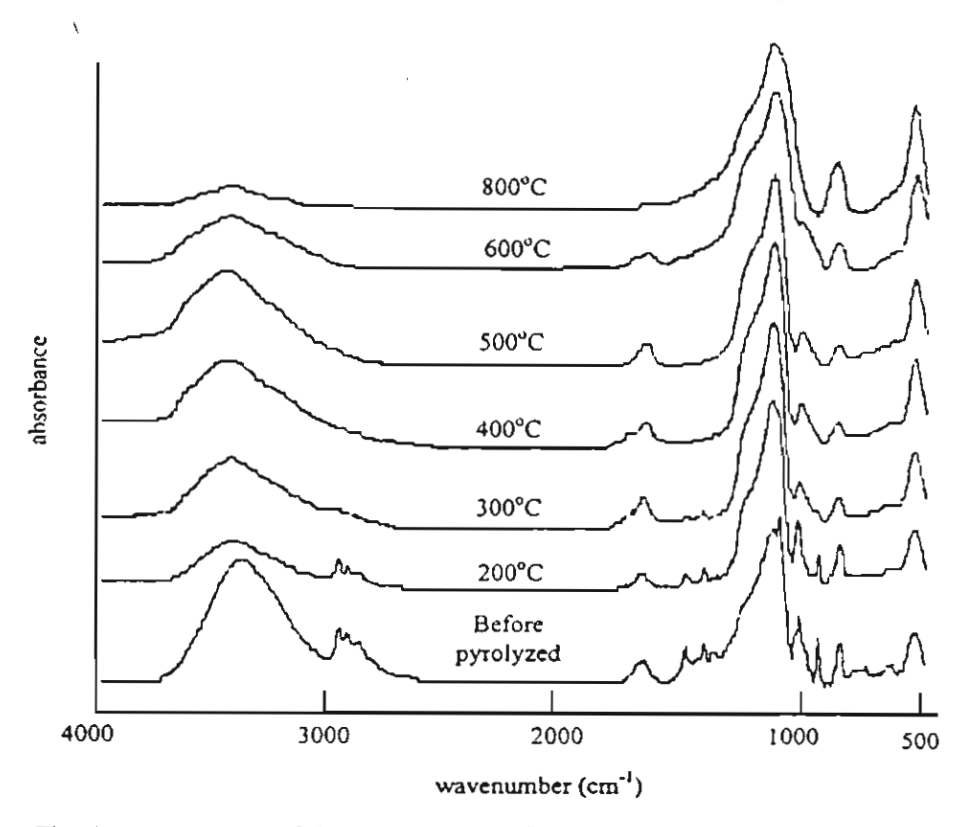


Fig. 7. FTIR spectra of the pyrolyzed polysilatrane gel at different temperatures.

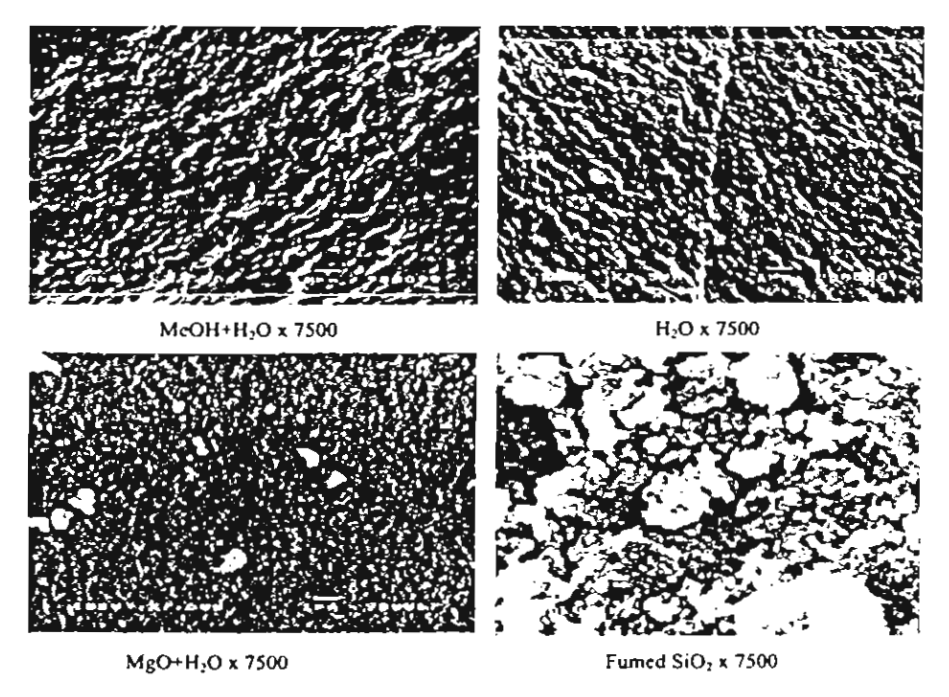


Fig. 8. SEM micrographs of pyrolyzed polysilatrane hydrolyzed with various solvents, at 800°C, and heating rate of 10°C/min as compared with fumed SiO₂ with magnification of 7500.

4. Conclusions

The optimal reaction mixture for silatrane synthesis is one with equimolar amounts of TIS and SiO₂ in the

presence of 5 mol% of silica. The optimum vacuum distillation temperature is 180°C. After 12 h under these conditions, most of the solvent is removed, and the monomer (M = 277) is largely converted to the dimer

Table 4
Surface area of polysilatrane gel pyrolyzed at 800°C

Gel	Surface area (m ² /g)
Hydrolyzed MgO + H ₂ O	417
Hydrolyzed H ₂ O	401
Hydrolyzed MeOH + H2O	313
Pyrolyzed start from 500°C	414
Pyrolyzed start from room temperature	388

with M=492. Gelation of the silatrane complex formed under these conditions is achieved by hydrolysis under ionic conditions. Pyrolysis of the gels at 800° C produces a homogeneous microporous glass. Glass formed under more ionic conditions (MgO/H₂O) has the smallest pores and largest surface area, but suffers from contamination by precipitated MgO.

Acknowledgements

This research was supported by the Thailand Research Fund.

References

- [1] Saegusa T, Chujo Y. Organic polymer hybrids with silica gel formed by means of the sol-gel method. Adv Polym Sci 1992;100:11.
- [2] Varshneya A. Fundamentals of inorganic glassmaking. Boston: Academic Press; 1994.
- [3] Iler R. The chemistry of silica. NewYork: Wiley; 1979.
- [4] Hencsei P, Parkanyi L. The molecular structure of silatranes. Rev Silicon Germanium, Tin Lead Compound 1985;8(2):191.

- [5] Bickmore C, Hoppe M, Laine R. Processable oligomeric and polymeric precursors to silicate prepared directly from SiO₂, ethylene glycol and base. Mater Res Soc Symp Proc 1992;249:81.
- [6] Piboonchaisit P, Wongkasemjit S, Laine R. A novel route to tris(silatranyloxy-i-propyl)amine directly from silica and triisopropanolamine. SciAsia J Sci Soc Thailand 1999:25:113.
- [7] Winter H, Chambon F. Analysis of linear viscoelasticity of a crosslinking polymer at the gel point. J Rheol 1986; 30:367.
- [8] Muthukumar M, Winter H. Fractal dimension of a crosslinking polymer at the gel point. Macromolecules 1986;19:1284.
- [9] Hodgson D, Qun Y, Amis E. Dynamic viscoelasticity during thermoreversible gelatin gelation. J Non-Cryst Solids 1991;131-133:913.
- [10] Muller R, Gerard E, Dugand P, Rempp P, Gnanou Y. Rheological characterization of the gel point: a new interpretation. Macromolecules 1991;21:532.
- [11] Izuka A, Winter H, Hashimoto T. Molecular weight dependence of viscoelasticity of polycaprolactone critical gels. Macromolecules 1992;25:2422.
- [12] Hsu S, Jamieson A. Viscoelastic behavior at the thermal sol-gel transition of gelatin. Polymer 1993;34:2601.
- [13] Lin Y, Mallin D, Chien J, Winter H. Dynamic mechanical measurement of crystallization-induced gelation in thermoplastic elastomeric poly(propylene). Macromolecules 1991;24:850.
- [14] Muthukumar M. Screening effect on viscoelasticity near the gel point. Macromolecules 1989;22:4656.
- [15] Roy R. Gel route to homogeneous glass preparation. J Am Ceram Soc 1969:344.
- [16] McCarthy G, Roy R. Gel route to homogeneous glass preparation II, gelling and desiccation. J Am Ceram Soc 1971:639.
- [17] Silverstein, et al. Spectrometric identification of organic compound, 5th ed. New York: John Wiley & Sons, Inc.; 1991.
- [18] Anderson DR. In: Lee S, editor. Analysis of silicones. New York: John Wiley & Sons, Inc.; 1974.

APPENDIX C

Sol-Gel Transition Study and Pyrolysis of Alumina Based Gels

Prepared from Alumatrane Precursor

Sol-Gel Transition Study and Pyrolysis of Alumina Based Gels Prepared from

Alumatrane Precursor

Bussarin Ksapabutra, Erdogan Gularib and Sujitra Wongkasemjitab

- a. The Petroleum and Petrochemical College, Chulalongkorn University, Bangkok 10330, Thailand
- b. Department of Chemical Engineering, University of Michigan, Ann Arbor, MI 48109-2136, USA.

Abstract

Alumina gels were prepared by the sol-gel method using alumatrane or tris (alumatranyloxy-i-propyl)amine as precursor. Alumatrane are aminoalkoxide derivatives of aluminium synthesized directly from the reaction of inexpensive and readily available compounds, aluminium hydroxide and triisopropanolamine, via the one step process. Sol-gel process parameters, such as gelation time, were correlated to variables of the initial stage of the process, such as pH, temperature of hydrolysis and water/alkoxide ratio. The sol-gel transition of alcoholic alumatrane solutions was monitored by multiple waveform rheological measurements. The gelation time could be determined from the evolution of the storage (G') and loss (G") moduli versus time at different frequencies using the Winter Chambon criterion (convergence of the loss tangents at the gel point). Increasing pH values, hydrolysis ratio and/or temperature accelerates the kinetics of hydrolysis-condensation reactions and thus reduced the gelation time. The gelation times at various temperatures were used to calculate apparent activation energy of the cross-linking leading to the gelation, which was found to be approximately 139 kJ mol-1 and independent of hydrolysis ratio. Alumina materials prepared from the heat treatment of obtained gel at temperature 500°C, were analyzed using X-ray diffraction and the BET method.

Keywords: Sol-gel transition, Alumatrane precursor, Alumina, Rheology, Gelation time

Tel.66-2-218-4133; Fax.66-2-215-4459; E-mail address: dsujitra@chula.ac.th

^{*}To whom correspondence should be addressed:

1. Introduction

Alumina materials have a wide range of applications in a great number of industrial areas, particularly in catalysis, membrane separation processes, catalytic membrane reactors, adsorbent, composite, coating, fiber, electronic and optic fields. 1-7 Alumina prepared by sol-gel process is frequently used in such areas. In the development of soft chemistry, the sol-gel process is considered to be the most practical method for the synthesis of inorganic oxides. This process usually involves the hydrolysis and condensation of various metal alkoxide molecules under controlled conditions to form metal-oxygen-metal bridging units. In many cases the metal alkoxide precursors are very sensitive to water and, therefore, cannot control the hydrolysis reaction. 8-9 Generally, the aluminium alkoxides, such as aluminium sec-butoxide and aluminium iso-propoxide, are used to prepare alumina by sol-gel method. 10-12 However, these usual precursors are expensive and aluminium sec-butoxide can be rapidly hydrolyzed to give the hydrolysis products dispersed in 2-butanol. 13-17

Alumatrane is aminoalkoxide derivatives of aluminium synthesized directly from the reaction of inexpensive and readily available compounds, aluminium hydroxide and triisopropanolamine, via the one step process. It containing trialkanoamine ligands is hydrolytically stable, thus yielding more controllably chemistry and minimizing special handling requirement. Therefore it should be used as precursors in ceramics processing by sol-gel route. In this work, we investigate the dynamic viscoelastic properties and FTIR studies on sol-gel process of alumatrane under different conditions. This observation is mainly focused on the influence of pH, hydrolysis ratio and temperature on the crosslinking process. In addition, some preliminary thermal studies of an alumina obtained by the sol-gel technique were also observed.

2. Experimental

2.1 Preparation and Heat Treatment of Alumina Gels

Alumatrane or tris(alumatranyloxy-*i*-propyl)amine was used as an alumina source or the precursor of the sol-gel derived system under investigation with various pH values, temperature and hydrolysis ratio. The preparation of alumatrane has already been reported in a previous paper.¹⁸ To begin with it was dissolved with dried methanol for a period. This methanolic alumatrane solution was checked using FT-IR spectroscopy and TGA in order to confirm the absence of alcohol interchange reactions. Then water was added together with catalyst, except in case of pH = 9 where no catalyst was added. For acid conditions, pH = 3 and pH = 5, HNO₃ was used and for neutral condition, pH = 7, HNO₃ was also used to adjust pH value of alcoholic alumatrane solution (pH = 9). To attain basic conditions, pH = 10 and 11, NH₄OH was added. Two hydrolysis ratios of 9 and 27 and six pH values ranging from 3 to 11 were investigated while the mole ratio of methanol to [Al] was kept equal to 60. The solution was mixed with a vigorous stirring at the range of temperature varied from 20°C to 36°C.

Alumina powders were produced by heat treatment the resulting gels at various pH values in a furnace at 500°C and held at the final temperature for 7 hours.

2.2 Measurements

2.2.1 Sol-gel process

2.2.1.1 Rheological characterizations

The rheological measurements, which were performed to determine sol-gel transition and dynamic viscoelastic properties, were carried out using a Rheometric Scientific Inc. (Model ARES) with a cone-plate configuration covered with the humidity chamber. The humidity chamber filled with methanol to obtain a saturated atmosphere was used to prevent evaporation of solvent during measurement. The dimensions

corresponding to the geometry were 25 mm for the diameter and 0.04° for the angle. The minimum distance between plate and truncated cone was 0.051 mm. The temperature control was achieved with a thermostated-circulating bath. The sample was stirred until homogeneous and loaded in the rheometer. The time for loading the sample was kept to a minimum so as to reduce the solvent evaporation. The experimental conditions (applied strain amplitude and frequency sweep range) were fixed after preliminary experiments. The amplitude was fixed within the linear viscoelastic range. The multiwave experiments were run with eight frequencies ranging from 0.2 to 1.6 rad s⁻¹ and the strains (γ) were kept at 3% at each harmonic. A narrow frequency range was employed because their properties change markedly with time. In addition, no intersection of the tan δ curves at a certain point identified as gel point was observed at higher frequencies.

Although the time requested for G' and G" to be equal is designated as the gel point by some authors¹⁹⁻²⁰, a more accurate investigation of the gel point has been given by Winter and co-workers as the point where $\tan \delta$ (=G"/G") is independent of frequency. The gel point can be precisely identified and located by the study of the evolution of G' and G" as a function of the frequency at various reaction times near the gel point. This criterion was firstly proposed for chemical gels but has also been applied to physical gels.²¹⁻²³ For such systems the linear viscoelastic behavior at gel point is described by the *gel equation*. ²¹⁻²²

$$\tau(t) = S \int_{-\infty}^{\infty} (t - t')^{-n} \dot{\gamma}(t') dt'; \ 0 \le n \le 1$$
 (1)

where τ is the stress tensor, $\dot{\gamma}$ is the rate of deformation tensor, S is the strength of the network at the gel point depending on the flexibility of molecular chains and crosslinks, and on the crosslink density. The value of relaxation exponent, n, varies over about the

entire possible range between 0 and 1 indicating a strongly elastic gel (n=0) or a more viscous gel (n=1).²⁵ The dynamic mechanical behavior at the gel point is given by a power law relation between moduli (G' and G'') and the angular frequency (ω)

$$G'(\omega) \sim G''(\omega) \sim \omega''$$
 (2)

i.e., storage (G') and loss moduli (G") are parallel in a log-log plot. Consequently the loss angle (δ) is independent of frequency at the gel point but proportional to the relaxation exponent:

$$\delta_c = n\pi/2$$
 or $\tan \delta_c = G''/G' = \tan (n\pi/2)$ (3)

Therefore the gel point can be conveniently determined by the evolution of $\tan \delta$ at different frequencies as a function of reaction time. The various curves intersect at one critical point, at which $\tan \delta$ becomes independent of frequency. The time at which this occurs is the gel time.²⁵

In very recent years, some studies have also been used to determine the gel time based on a modification of self-similarity method. It is useful for systems exhibiting no intersection of the curves but is also applicable to systems whose curves coincide at a specific point. The gel point is associated with the occurrence of statistical loss factor self-similarity. In this way, the gel time is obtained by the minimum of the curve log $(s/(\tan \delta))$ as a function of reaction time where s is the standard deviation of $\tan \delta$ in a frequency sweep.²⁶

2.2.1.2 FT-IR spectroscopic characterizations

The hydrolysis and condensation of alumatrane as a function of the reaction time were followed by Fourier-transform IR spectroscopy. An FT-IR spectrophotometer (Nicolet, NEXUS 670) with 16 scans at a resolution of 4 cm⁻¹ was used in this study.

2.2.3 Characterization of pyrolyzed gels

Alumina supports obtained from annealing the gel at 500°C were characterized using BET method and X-ray diffraction techniques. BET surface area and pore size distribution were measured by using nitrogen at 77 K in Autosorb-1 gas sorption system (Quantasorb JR.). Samples were degassed at 200°C under a reduced pressure prior to each measurement. The structure of the phases in the samples, annealed at various temperatures, was obtained at room temperature by using X-ray powder diffraction. XRD spectra were recorded on D/MAX 2000 series (Rigaku Co.) using Cu K α radiation (λ =0.154 nm).

3. Results and Discussion

3.1 Sol-gel process

3.1.2 Gelation times and dynamic viscoelastic properties by rheological measurements

The evolution of gelation process with time was investigated in eight different frequencies ranging from 0.2 to 1.6 rad s⁻¹. Figure 1a and 1b show measured values of loss G" and storage G' moduli, respectively, as a function of reaction time for the system with pH = 7 and h = 9 at 25°C. In the initial part of the reaction, G" is greater than G', which is a characteristic feature of liquids. With continuing gelation reaction, both the moduli increased with time. However, G' rises more sharply than G" indicating a gradual formation of gel network with a predominantly elastic character. In Figure 1c the complex dynamic viscosity (η^*) was plotted as a function of time at different frequencies. The viscosity increases as the gelation grows, because more work must be done to produce flow of the sol. In addition, the complex dynamic viscosity η^* increased

as frequency decreased. These observations are more significant when reaction time increased indicating an evolution from liquid-like to solid-like state.

According to eq 3 the critical gel is identified by a loss tangent, $\tan \delta = G^{**}/G^{*}$, which is independent of frequency. Therefore, $\tan \delta$ was investigated as a function of time at different frequencies. For the system with pH = 7 and h = 9 at 25°C, the various curves intersect at one point, at which tan becomes independent of frequency (Figure 2). The time at which this occurs is the gel time (8114 s) as depicted in Section 2.2. Before the gel point, $\tan \delta$ decreased with increasing frequency, which is typical for a viscoelastic liquid. After the gel point, $\tan \delta$ increased with frequency, as is characteristic of a viscoelastic solid. Apparently, the sample had changed from a viscoelastic liquid to a viscoelastic solid. Equivalently, the gel time can be calculated by the method of statistical loss factor self similarity as noted above by observation of the minimum of the curve $\log (s/(\tan \delta))$ against reaction time. Figure 3 illustrates that the time at the minimum point compared very well with the experimental value observed for the frequency independence of loss tangent.

The frequency dependence of G' and G" for several measurement times with pH = 7 and h = 9 at 25° C was exhibited in Figure 4. Early in the reaction G' is smaller than G". As gelation proceeds at the instant, the traces of G' and G" became parallel to each other showing power law behavior. Such a condition corresponds to a sol-gel transition according to the criterion suggested by Winter and Chambon. As noted in Section 2.2. values of n near the gelation critical point can be identified from power law character. The slopes of these lines gave n, the viscoelastic exponent in eq.2, for the frequency dependence of the moduli. The changes of n with extent of reaction were shown in Figure 5 where n' and n" for storage and loss moduli, respectively, were plotted against

time. Both decreased and then merged to 0.36 at 8114 s. These values of n component were in good agreement with the values obtained from Figure 2 and eq.3 At the gel point, $\tan \delta$ equals 0.56, which corresponds to a relaxation exponent of n = 0.33.

Many studies of critical gel rheological properties were found that most results show $n \ge 0.5$. Values of n below 0.5 have also been found.^{23, 27-30} Winter reported that if n > 0.5, the gel point preceded the intersection of G' and G". In contrast, if n < 0.5, the intersection occurs before the gelation. This is coincident with the results from our system.

The value obtained in our system was very close to the one found for polycaprolactone. Izuka et al. suggested that a low n value implies that the material at the gel point is a mostly elastic body with the limit of G'' = 0 at n = 0 and vice versa. The low value of n found for our case is probably due to the presence of physical crosslinks with a finite lifetime, in addition to the permanent chemical crosslinks leading to a denser network with elastic behavior.

3.1.2.1 Effect of pH

The systems with the pH ranging from 3 to 11 at h = 9 and temperature of 25°C were also studied. The values of rheological properties at the gel point were provided in Table 1. The gel time at each pH was obtained from plots of tan δ against time in the same manner as Figure 2. The relaxation exponent n was calculated from eq.3 at 0.8 rad s^{-1} . The maximum gelation rate was observed near pH 11, with the rate decreasing significantly at lower pH. As is investigated, the value of t_{gel} at higher pH is less than at lower pH. The maximum at around pH 9 corresponds to the isoelectric point of alumina. However, it is also evident, Table 1, that the strength of the gel network formed at lower pH (determined from the value of G'/G" at t_{gel}) is substantially higher than that obtained at higher pH. This is consistent with a decrease of n values with decreasing pH. As

pointed out above, a lower value of n is related to higher elastic body implying that intermolecular crosslinks were stronger.

3.1.2.2 Effect of hydrolysis ratio

The dynamic viscoelastic properties at the gel point were demonstrated in Table 2 for each set of reaction conditions at 25°C. The increase of hydrolysis ratio reduces the times required for gelation. Also, G' outweighs G" for all systems showing that the elastic component appreciably predominates over the viscous one at the gel point. Furthermore, G' and η^* decrease with increase of hydrolysis ratio while the relaxation exponent increases with increase of hydrolysis ratio. It could be justified that when the hydrolysis ratio is greater, gel formation evolving quickly through the reaction of hydrolysis and condensation contain low interconnected networks. Consequently, the network is looser with lower value of G'. On the other hand, a system with a lower hydrolysis ratio grows slowly resulting in a denser network with higher G'. Correspondingly, a higher value of n is related to a lower elastic system indicating that intermolecular crosslinks are weaker.

3.1.2.3 Effect of temperature

The temperature at which the measurement is performed is one of the most important factors influencing the gel time. The results for the systems varying between 20° C and 36° C were reported in Table 3. At higher temperatures gelation occurs faster, resulting in a shorter time to gel. The values of the dynamic moduli at the gel point decreased with increasing temperature. The trend of these results is analogous to that of other studies. ^{25,31} In addition, the temperature dependence of the complex dynamic viscosity η^* was also similar to that of the dynamic moduli. In contrast, the n values obtained for all systems increase with temperature. These observations indicate that the network formation proceeded faster with increasing temperature, whereas the gel texture

is rather loose. There exhibits some discussion in the literature regarding an apparent activation energy for the gelation reaction calculated from the gel time at different temperatures. Because gelation represents a specific extent of reaction, the temperature dependence of the time to gel should be described by the Arrhenius equation

$$ln(tgel) = A + E_a/RT$$
 (4)

where A is a constant, R is the ideal gas constant, and T is temperature. The activation energy Ea of the gelation can be calculated from the slope of a plot of log t_{gel} against 1/T. The Arrgenius plots for our system are shown in Figure 6. The values of Ea were estimated to be approximately the same in each case, varying slightly around 139 kJ mol⁻¹. This implies that E_a of the gelation does not depend on hydrolysis ratio.

3.1.3 FT-IR analysis

The FTIR spectra of the gel as a function of time were compared to elucidate the study of the hydrolyzed alumatrane in sol-gel process. As the reaction precedes, a decrease in the intensity of the Al-O-C vibration of alumatrane at 1087 cm⁻¹ was observed. Some peaks present in the 900 – 500 cm⁻¹ region disappear, while the width and intensity of this spectral range increase. This result corresponds to the formation of Al-O-Al bonds according to the condensation reaction. Figure 7 depicts the FTIR spectra of hydrolyzed systems at different hydrolysis ratio. The intensity of Al-O-Al is maximized at h = 27 with the intensity decreasing at lower hydrolysis ratio. The decrease in intensity of Al-O-C band is accompanied with the increase of Al-O-Al band as hydrolysis ratio increases. This implies that the gelation can be accelerated with increasing hydrolysis ratio leading to the reduction of the gel time.

In order to confirm the above conclusion, a careful deconvolution of the IR profiles using a computer program was also investigated. The results of the analysis are shown in the relationship between the peak ratio of Al-O-C band (1087 cm⁻¹) and Al-O-Al band (683 cm⁻¹) and time (Figure 8). This is only a semiquantitative picture of the gelation of alumatrane molecule. Generally, the gel time is decreased by factors that increase the condensation rate. It is obvious that values of pH, hydrolysis ratio and temperature are the important factors affecting the gel time. The results obtained here compared favorably with earlier study by qualitative FTIR. Furthermore, it was found that these FTIR observations are consistent with the rheological results.

3.2 Characterization of pyrolyzed gel

Some preliminary studies of pyrolyzed gel were performed to examine the influence of pyrolysis temperature on the properties of alumina obtained from the heat treatment of alumatrane gels. XRD patterns of pyrolyzed gel at different temperatures ranging between 400 and 1100°C showed amorphous nature at 300°C in Figures 9. The sample treated at 500°C presents three γ -alumina peaks (ICDD, File 29-63). At 900°C, the XRD pattern of γ -alumina is better defined, however, characteristic peaks of δ -alumina are not well resolved (ICDD, File 16-394). After heating at 1000°C, two phases of δ -alumina and α -alumina were detected. When the sample was heated from 1000 to 1100°C, the δ -alumina was totally transformed into α -alumina.

The sample treated at 500°C shows the monomodal pore size distribution in the mesopore range having a maximum center around a pore diameter of 70 Å (Figure 10a). Also, the resulting powder shows the nitrogen adsorption/desorption isotherms of type IV (IUPAC classification) which exhibit hysteresis loops mostly of type H2 (Figure 10b).³³ Further investigations on the pyrolysis of alumina gel obtained various reaction conditions are in progress and will be reported later.

4. Conclusions

Alumatrane can be used as metal alkoxide precursor for preparing high surface alumina powders via sol-gel route. The multiple-waveform rheological technique and FTIR were found to be effective for studying the gelation of alumatrane. The operation variables, viz. pH, hydrolysis ratio and temperature, affect dramatically the gel time. An increase of these parameters leads to the reduction of gel time. However, the strength of the gel network formed more quickly is lower than that obtained gradually. The value of n for our systems was found to be fairly low indicating high elastic gel. The apparent activation energy of the gelation reaction determined directly from gel time measurement at different temperatures was around 139 kJ mol⁻¹. Heat treatment of the resulting alumatrane gels at 500°C produces a homogeneous mesopore alumina having high surface area.

Acknowledgments

This work was supported by the Thailand Research Fund and PPT consortium (ADB).

References

- 1. Guizard, C.G.; Julbe, A. C.; Ayral, A. J. Mat. Chem. 1999, 9, 55.
- 2. Quanttrini, D.; Serrano, D.; Perez Catán, S. Granular Matter 2001, 3, 125.
- 3. Livage, J. Solid State Ionics 1996, 86-88, 935.
- 4. Suda, S.; Yamashita, K.; Umegaki, T. Solid State Ionics 1996, 89, 75.
- Browne, C. A.; Tarrant, D. H.; Olteanu, M. S.; Mullens, J. W.; Chronister. E. L. Anal. Chem. 1996, 68, 2289.
- 6. Kuraoka, K.; Tanaka, H.; Yazawa, T. J. Mater. Sci. Lett. 1996, 15, 1.

- 7. Skapin, T.; Kemnitz, E. Catal. Lett. 1996, 40, 241.
- 8. Roger, A.A.; Bruce, D. K. J. Non-Cryst. Solids 1988, 99, 359
- 9. Blanchard, J.; Barboux-Doeuff, S.; Maquet, J.; Sanchez, C. New J. Chem. 1995, 19, 929.
- 10. Jarayaman, V.; Guanasekaran, T.; Periaswami, G. Mater. Lett. 1997, 30, 157.
- 11. Yoldas, B. E. J. Non-Cryst. Solids 1992, 147/148. 614.
- 12. Uchilhashi, H.; Tohge, N.; Minami, T.; J. Ceram. Soc. Jpn. Int. 1989, 97, 389.
- 13. Yoldas, B. E. J. Appl. Chem. Biotechnol. 1973, 23, 803.
- 14. Yoldas, B. E. Ceram. Bull. 1975, 54, 286.
- 15. Yoldas, B. E. Ceram. Bull. 1975, 54, 289.
- 16. Pierre, A. C.; Uhlmann, D. R. J. Am. Ceram. Soc. 1987, 70, 28.
- Ogihara, T.; Nakajima, H.; Yanagawa, T.; Ogata, N.; Yoshida, K. J. Am. Ceram.
 Soc. 1991, 74, 2263.
- 18. Opornsawad, Y.; Ksapabutr, B.; Wongkasemjit, S.; Laine, R. M. European Polymer Journal. 2001, 37, 1877.
- 19. Djabourov, M., Leblond, J. and Papon, P. J. Phys. France 1988, 49, 333
- 20. Tung, C. M. and Dynes, J. J. Appl. Polym. Sci. 1982, 27, 569
- 21. Winter, H. H.; Chambon, F. J. Rheol. 1987, 31, 683.
- 22. Winter, H. H.; Chambon, F. J. Rheol. 1986, 30, 367.
- 23. Lin, Y. G.; Mallin, D. T.; Chien, J. C. W.; Winter, H. H. Macromolecules, 1991, 24, 850.
- 24. Yu, J. M.; Jerome, R.; Teyssie, P. Polymer, 1997, 38, 347.
- 25. Izuka, A.; Winter, H. H.; Hashimoto, T. Macromolecules 1992, 25, 2422.
- 26. Rude, E.; Llorens, J.; Mans, C. Progress and Trends in Rheology, 1998, 613.
- 27. Scanlan, J.; Winter, H. H. Macromolecules, 1991, 24, 47.

- 28. Hodgson, D. F.; Amis, E. J. Macromolecules, 1990, 23, 2512.
- 29. Raghavan, S. R.; Chen, L. A.; Mc Dowell, C.; Khan, S. A. Polymer, 1996, 37, 5869.
- 30. Ponton, A.; Barboux-Doeuff, S.; Sanchez, C. Colloids and Surface A: 1999, 162, 177.
- 31. Srinivasa, R.R.; Li Ang Chen.; Christopher, M.; Saad, A. K. *Polymer*, 1996, 37, 5869.
- 32. Gough, L. J.; Smith, I. T. J. Appl. Polym. Sci., 1960, 3, 362.
- 33. Leofanti, G.; Padovan, M.; Tozzola, G.; Venturelli, B. Catal. Today 1998, 41, 207.

Figure 9. XRD patterns of hydrolyzed alumatrane at various pyrolysis temperatures. (a) 400°C; (b) 500°C; (c) 700°C; (d) 900°C; (e) 1000°C; (f) 1100°C.

Figure 10. Plots showing (a) Pore size distribution; (b) Nitrogen adsorption/desorption isotherms of the alumatrane gel pyrolyzed at 500°C for 7 h.

Table Captions

Table 1. pH effect on the gel time, and dynamic properties for h = 9 at 25° C

Table 2. Hydrolysis ratio effect on the gel time, and dynamic properties for pH = 9 at 25° C.

Table 3. Temperature effect on the gel time, and dynamic properties for pH = 9 and h = 9, 18 and 27.

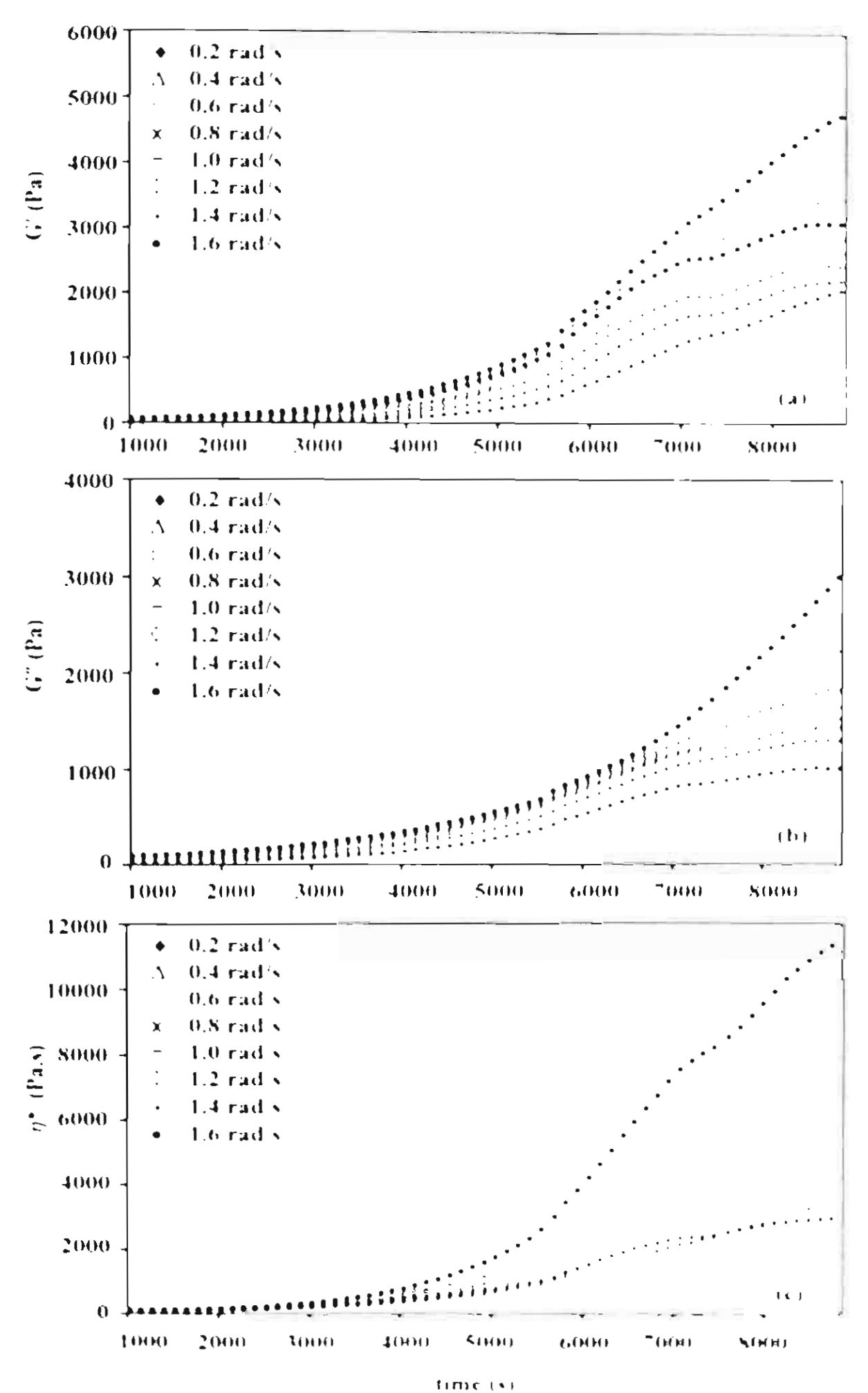


Figure I. (Ksapabutr et al.)

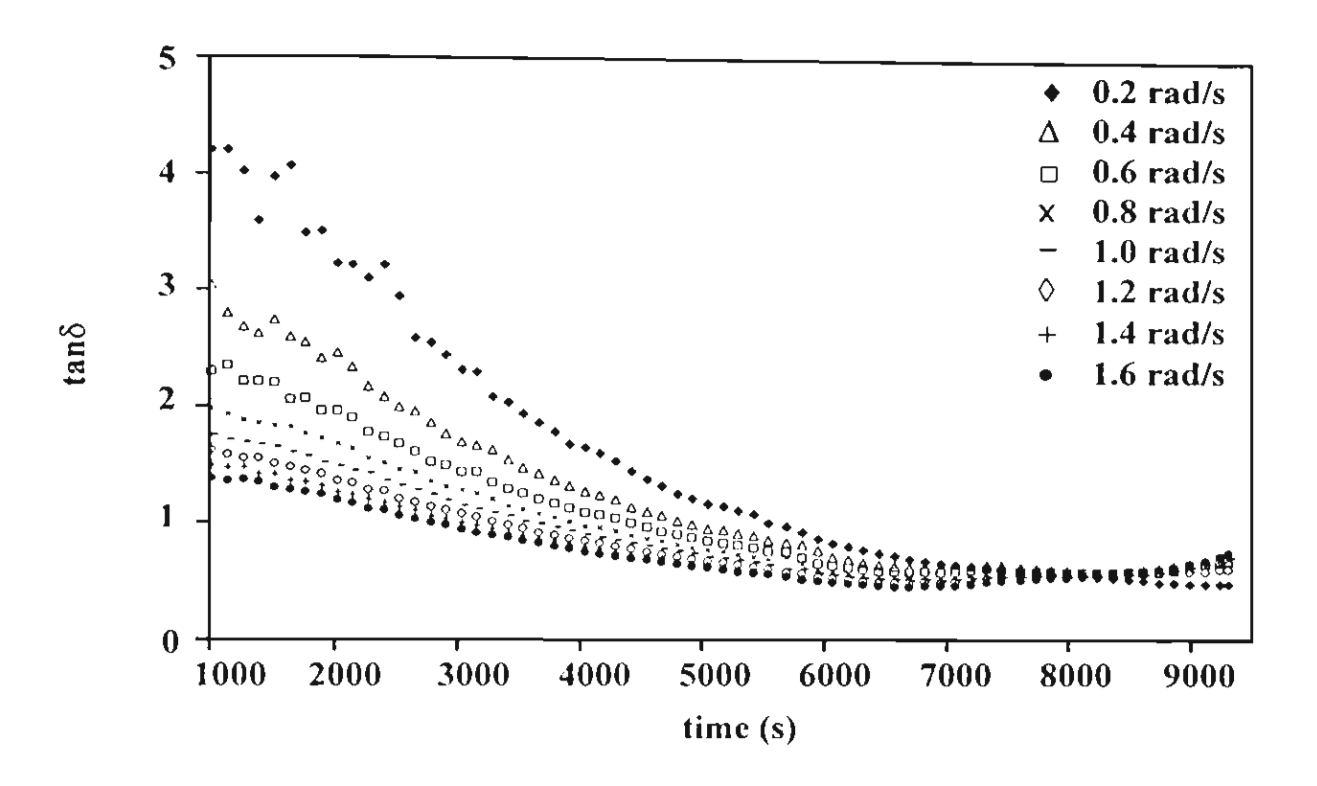


Figure 2. (Ksapabutr et al.)

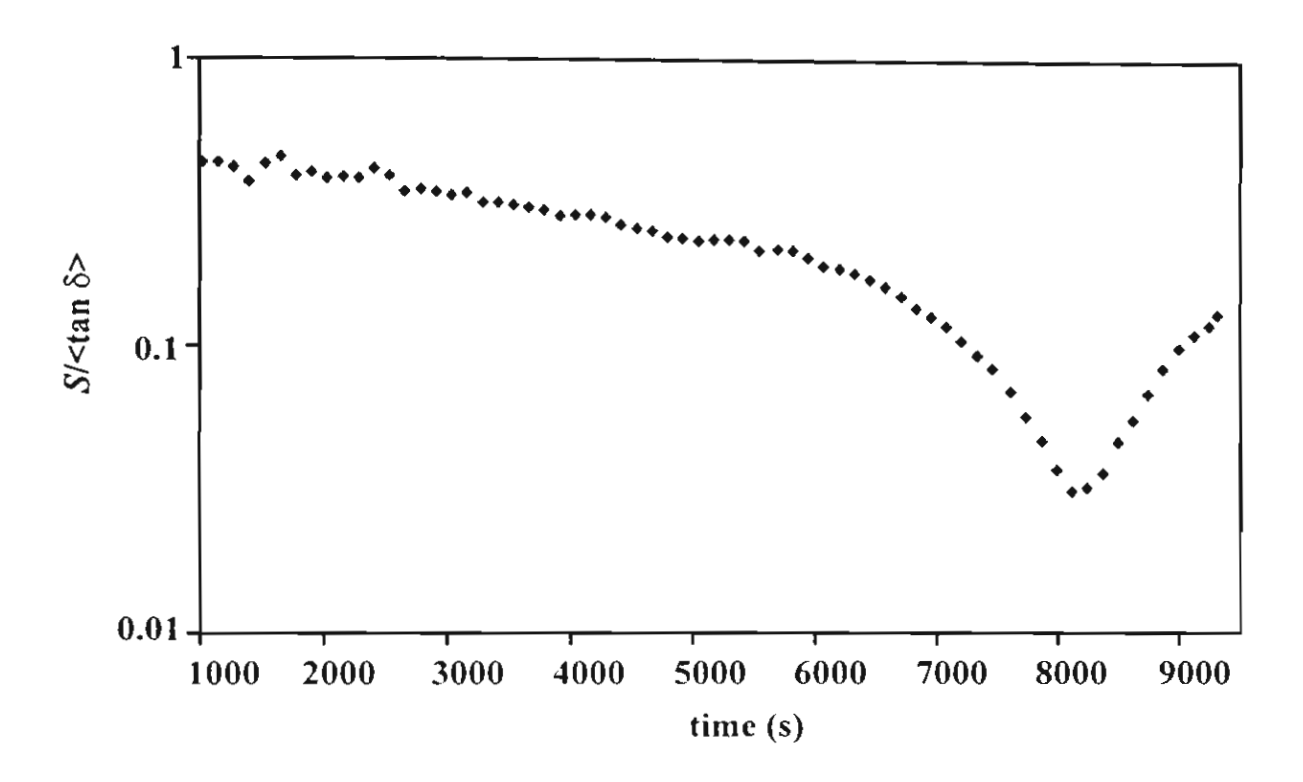


Figure 3. (Ksapabutr et al.)

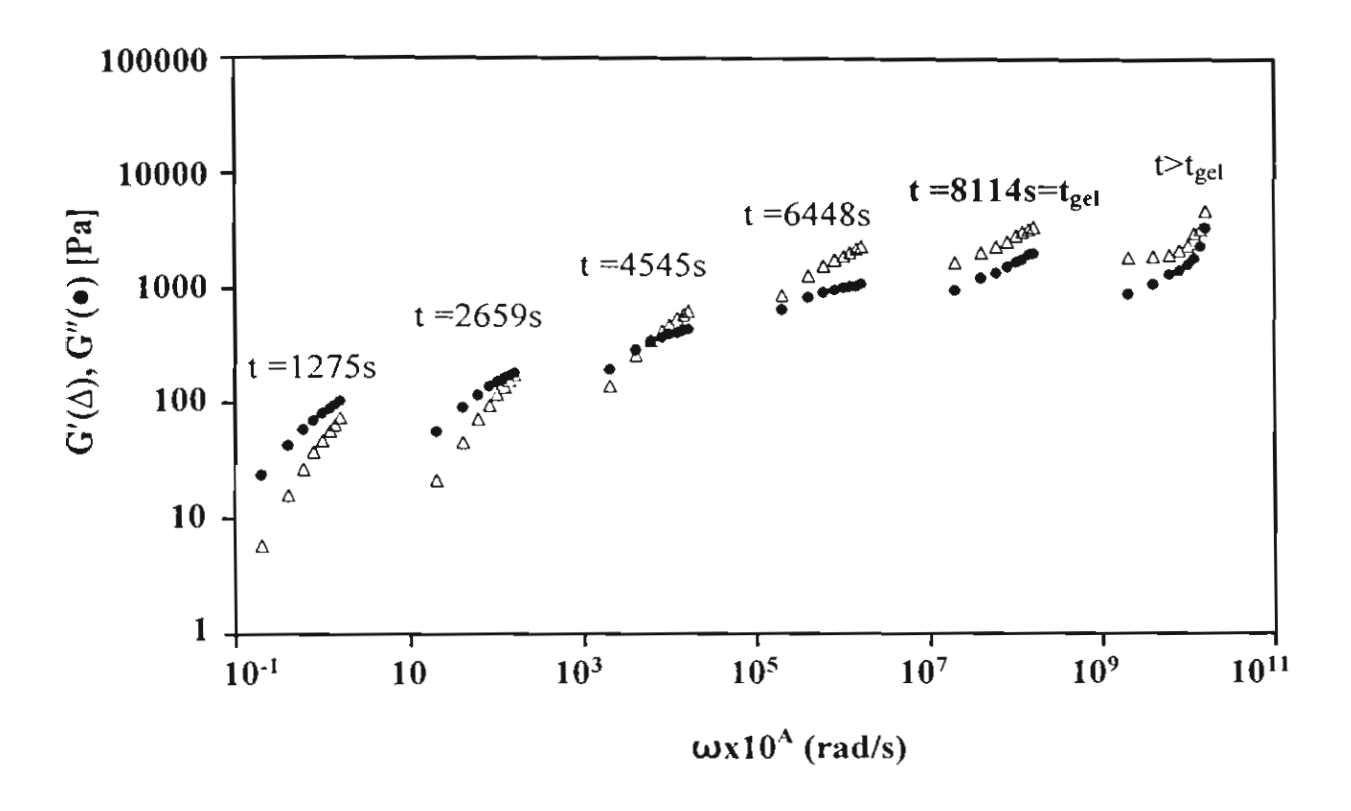


Figure 4. (Ksapabutr et al.)

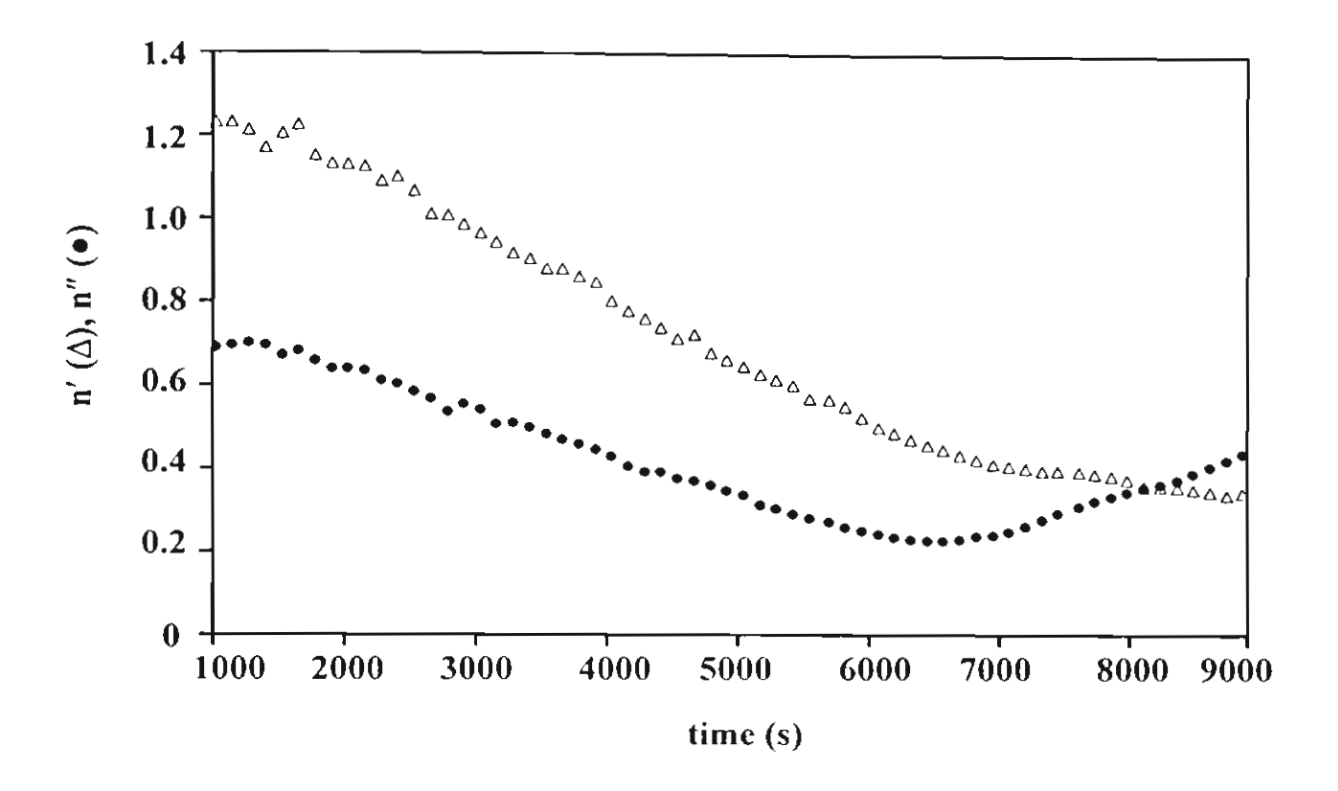


Figure 5. (Ksapabutr et al)

рН	t _{gel} (s)	G' (Pa)	G" (Pa)	η* (Pa.s)	G'/ G"	n
3	16891	4800.45	1105.54	6157.63	4.34	0.14
5	13109	2875.11	1293.79	3941.00	2.22	0.27
7	8114	2556.35	1424.30	3657.94	1.79	0.33
9	17798	5802.23	1200.03	7406.28	4.83	0.13
10	5548	1500.92	989.11	2246.91	1.52	0.37
11	3076	1003.24	750.18	1565.88	1.34	0.41

Table 1. (Ksapabutr et al)

h	t _{gel} (s)	G' (Pa)	G" (Pa)	η* (Pa.s)	G'/ G"	n
9	17798	5802.23	1200.03	7406.28	4.83	0.13
18	9575	3003.25	1351.46	4116.65	2.22	0.27
27	3642	2116.89	1206.62	3045.79	1.75	0.33

Table 2. (Ksapabutr et al)

	t _{gel} (s)	G' (Pa)	G" (Pa)	η* (Pa.s)	G'/ G"	n
20°C						
h = 9	34987	7645.23	1287.78	9691.16	5.94	0.11
h = 18	21875	5134.42	2053.77	6912.43	2.50	0.24
h = 27	11265	4211.56	2190.56	5933.99	1.92	0.31
23°C						
h = 9	23142	6178.21	1173.85	7860.92	5.26	0.12
h = 18	12017	4214.25	1727.84	5693.38	2.44	0.25
h = 27	5987	3165.51	1709.37	4496.94	1.85	0.32
25°C						
h = 9	17798	5802.23	1200.03	7406.28	4.83	0.13
h = 18	9575	3003.25	1351.46	4116.65	2.22	0.27
h = 27	3642	2116.89	1206.62	3045.79	1.75	0.33
28°C						
h = 9	9878	5620.17	1348.8	7224.69	4.17	0.15
h = 18	5164	2534.43	1241.87	3527.92	2.04	0.29
h = 27	2132	1676.51	1022.67	2454.76	1.64	0.35
32°C						
h = 9	3985	4802.47	1392.72	6250.42	3.45	0.18
h = 18	2227	2138.73	1176.3	3051.09	1.82	0.32
h = 27	1135	1032.23	650.31	1525.00	1.59	0.36
36°C						
h = 9	2013	4059.12	1380.11	5359.16	2.94	0.21
h = 18	1198	1851.21	1166.26	2734.94	1.59	0.36
h = 27	582	823.17	617.38	1286.21	1.33	0.41

Table 3. (Ksapabutr et al)

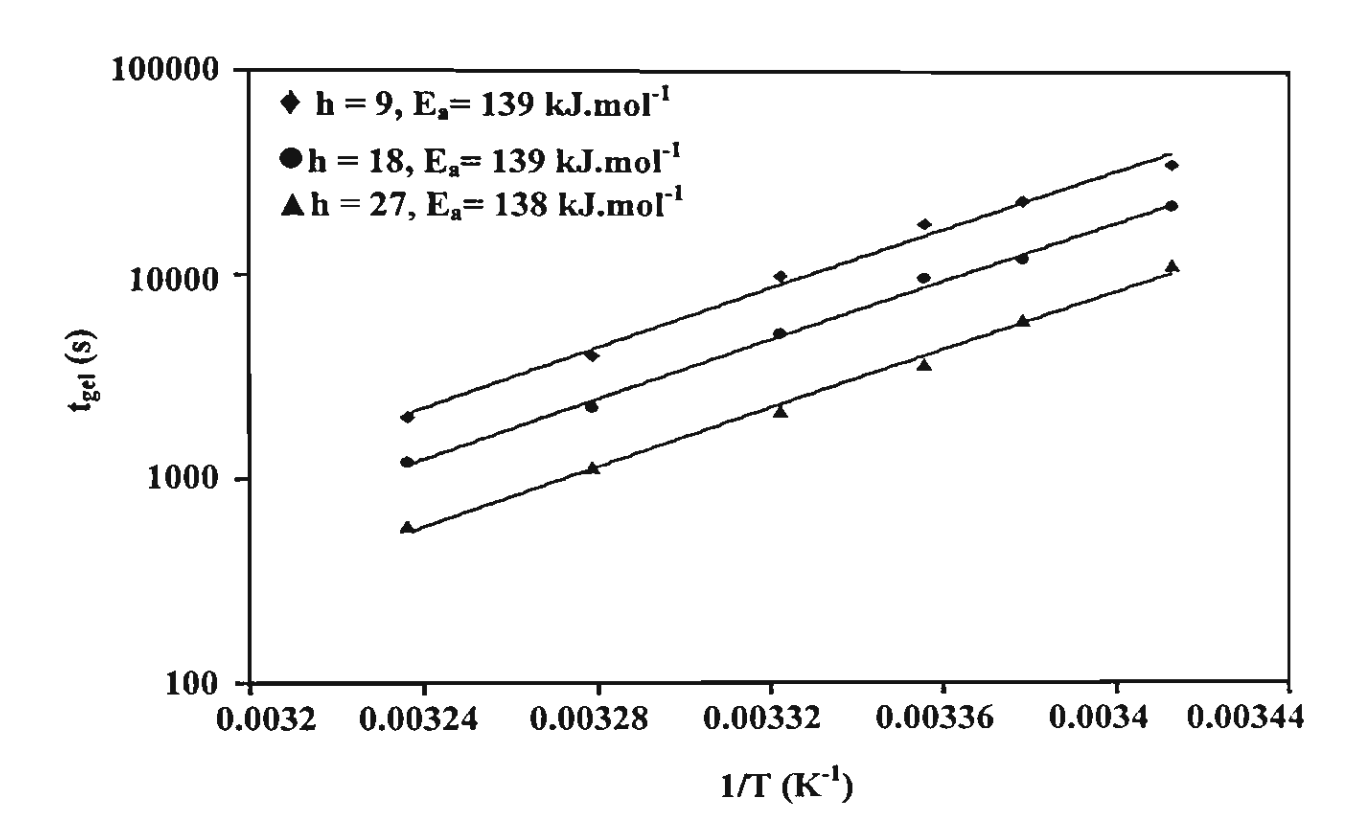


Figure 6. (Ksapabutr et al.)

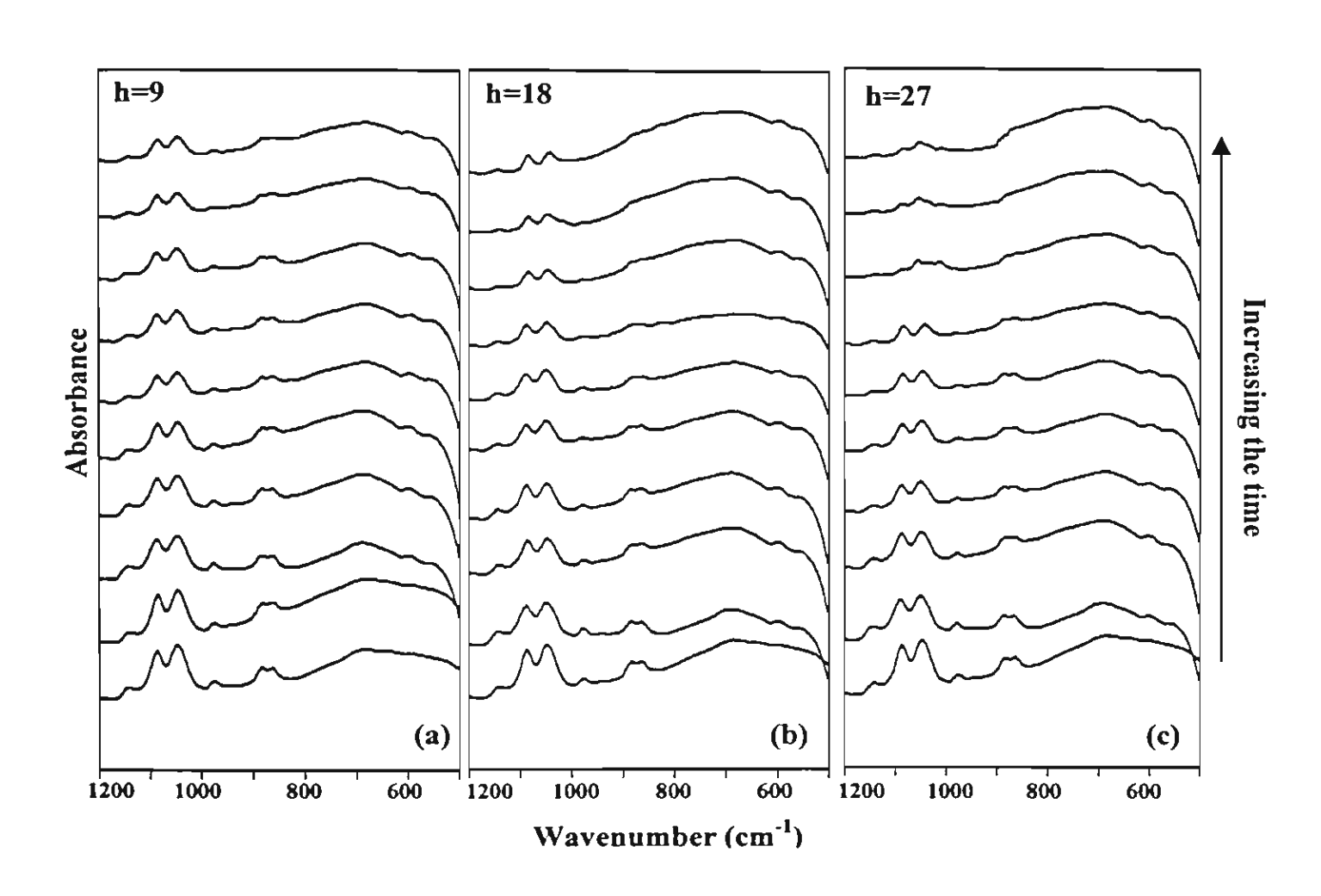


Figure 7. (Ksapabutr et al.)

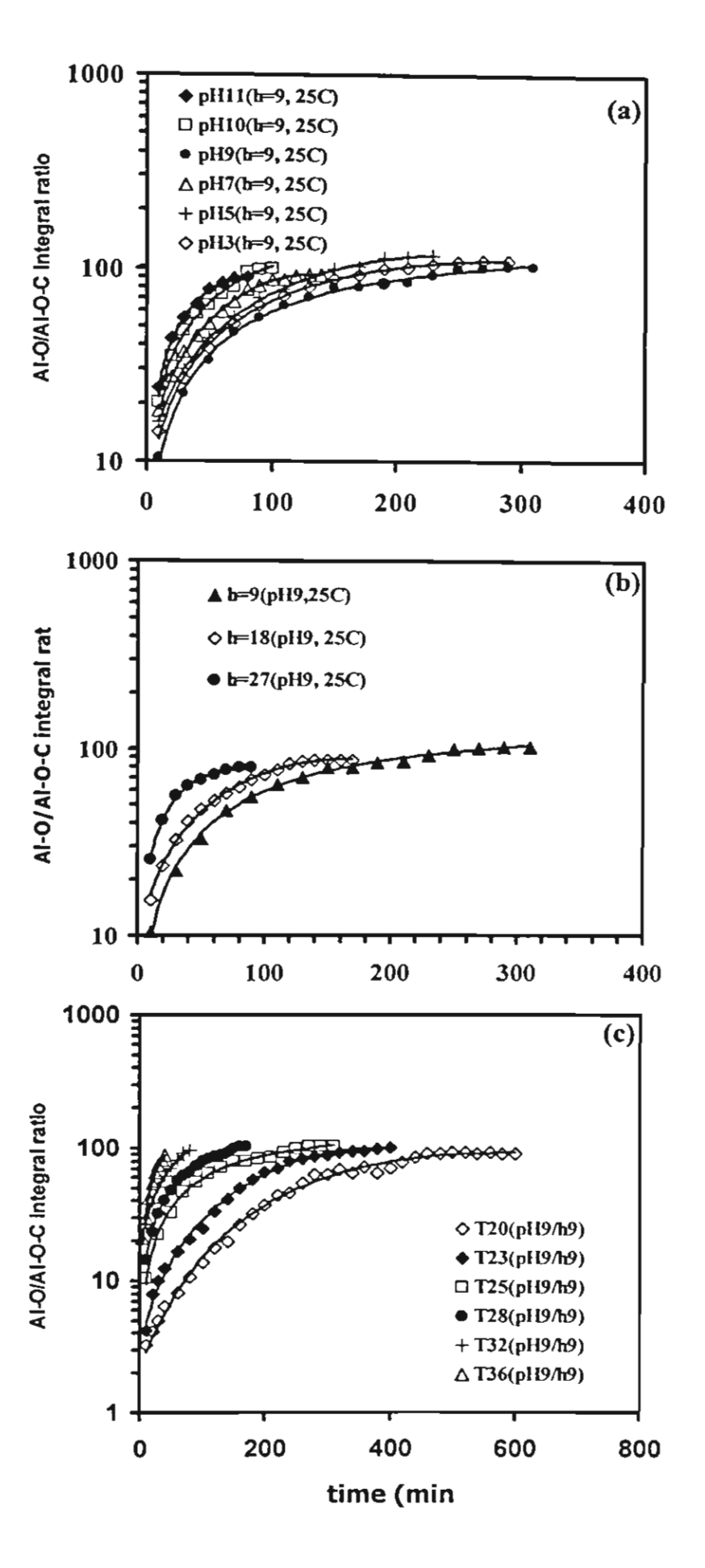


Figure 8. (Ksapabutr et al.)

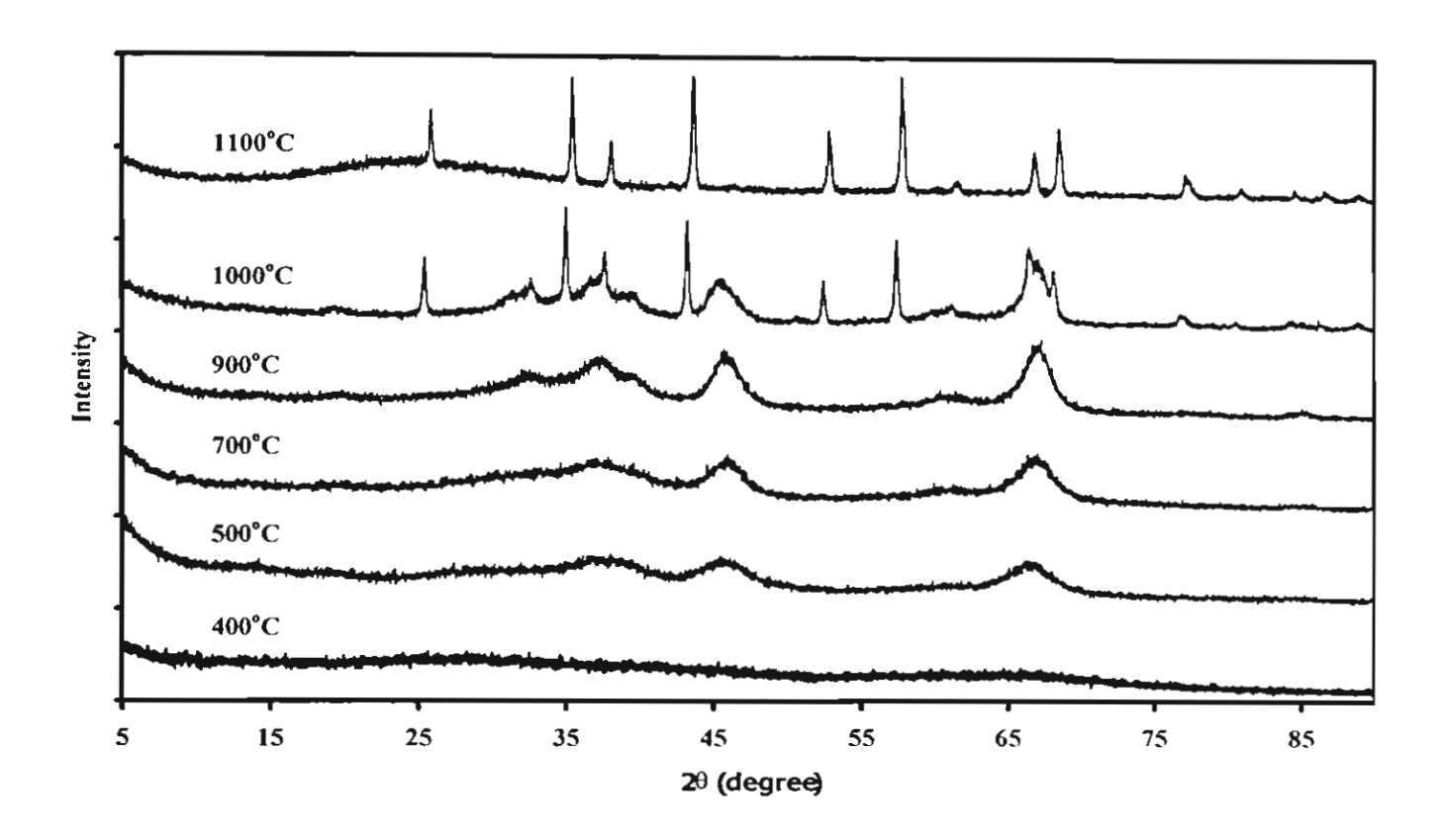


Figure 9. (Ksapabutr et al.)

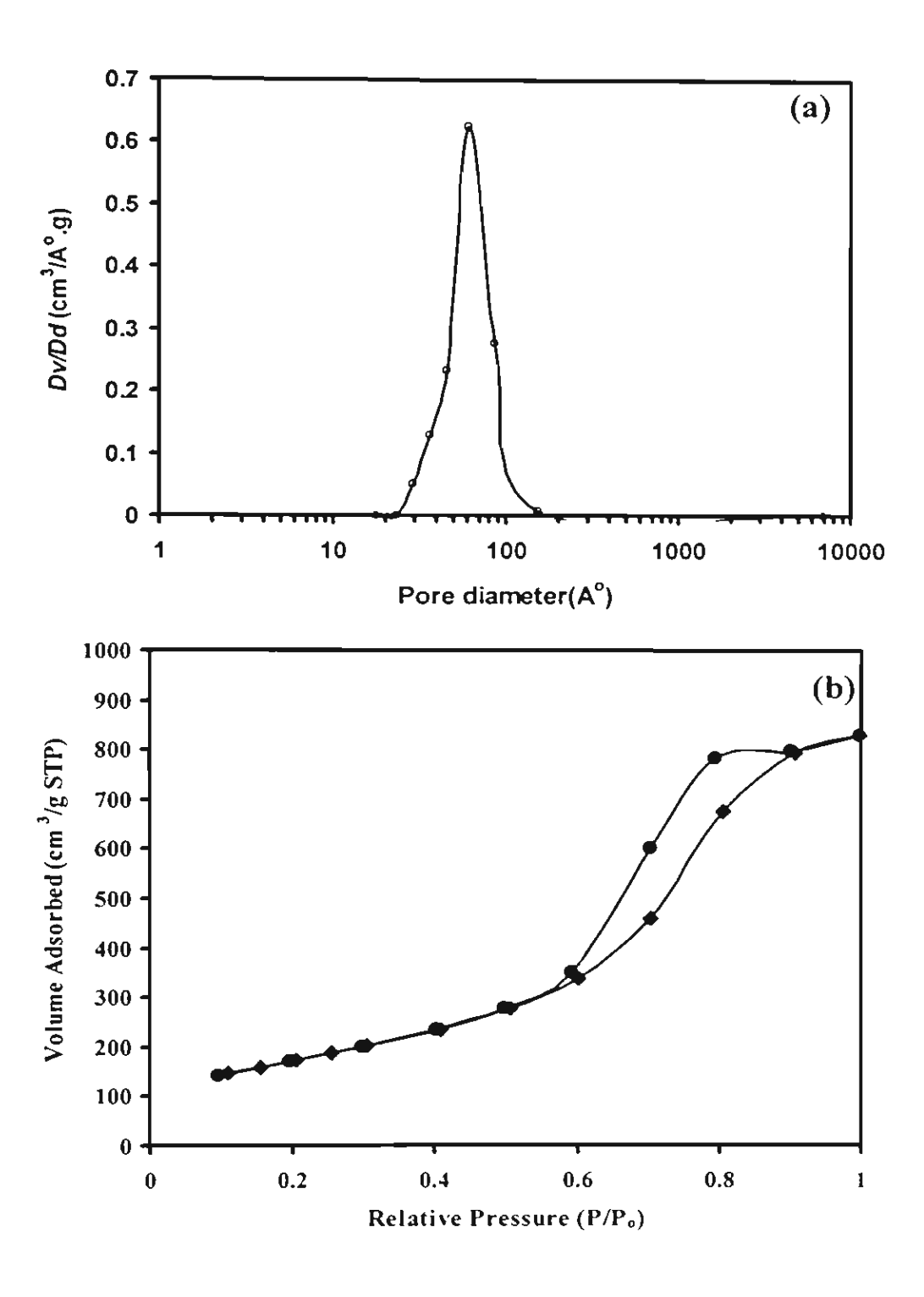


Figure 10. (Ksapabutr et al.)